Smartphone-based nitrate sensor

by

Joelcia M. da Franca Pereira Ingles

Thesis presented in partial fulfilment of the requirements for the degree of Master of Engineering (Electronic) in the Faculty of Engineering at Stellenbosch University

Supervisor: Prof. MJ. Booysen

Co-supervisor: Dr. TM. Louw

December 2019

Declaration

By submitting this thesis electronically, I declare that the entirety of the work contained therein is my own, original work, that I am the sole author thereof (save to the extent explicitly otherwise stated), that reproduction and publication thereof by Stellenbosch University will not infringe any third party rights and that I have not previously in its entirety or in part submitted it for obtaining any qualification.

Date: December 2019

Abstract

Smartphone-based nitrate sensor

JMD. Pereira Ingles

Department of Electrical and Electronic Engineering,
University of Stellenbosch,
Private Bag X1, Matieland 7602, South Africa.

Thesis: MEng (Electronic Engineering)

December 2019

The scarcity of sanitary water is a well-known issue that prevails in Africa, and nitrates are one of the most concerning water quality parameters. Nitrates can easily contaminate water sources through human-made or natural processes, and cause the degradation of aquatic ecosystems and health complications to humans.

In light of this matter, the purpose of this thesis was to develop a "lab-in-a-suitcase" smartphone-based nitrate sensor, that was portable and more affordable to rural communities in comparison to traditional counterparts, specifically spectrophotometers. For this application, the smartphone-based nitrate sensor performed spectrophotometric analysis, specifically UV spectroscopy, to quantify the concentration of nitrates in a water sample. Spectrophotometry is a methodology that quantifies the amount of light a sample absorbs and relates it to the concentration of the sample.

Spectrophotometry utilises a few optic components that can be costly, complex to implement and increase the size of the overall device. Some of these components, such as the diffraction grating, are essential to allow spectrophotometers to analyse various chemicals. Since this application was specific to nitrates, it did not require all these components. Hence, this thesis explored the possibility of excluding some commonly used optic components to minimise the cost, size and complexity of the smartphone-based nitrate sensor. This was achieved by investigating whether a diffraction grating and a bandpass filter were indispensable for the smartphone-based nitrate sensor to operate ideally. The investigation consisted of the design of three scenarios, where all three scenarios consisted of the same elemental components, but each scenario differed by a component. One scenario contained just the elemental components, another scenario included an extra diffraction grating, while the last scenario

included an extra bandpass filter. The performance of each scenario was compared against one another and with that of a laboratory spectrophotometer. Through the assessment of the three scenarios, it was deduced that the addition of the diffraction grating did not make a significant difference to the detection ability of the smartphone-based nitrate sensor. However, the inclusion of the bandpass filter increased the sensitivity of the smartphone-based nitrate sensor, allowing it to perform more on par with the laboratory spectrophotometer. The variance between the performance of the scenario with the bandpass filter and the laboratory spectrophotometer was less than 27%. Contrary, the variance between the other two scenarios and the laboratory spectrophotometer, was over 80%. Therefore, the adopted final design of the smartphone-based nitrate sensor consisted of the elemental components and a bandpass filter.

Thereafter, a comparison was made between the ability of the final smartphone-based nitrate sensor and the laboratory spectrophotometer to determine the nitrate concentration of an environmental sample. This comparison served as the final evaluation of the execution and accuracy of the smartphone-based nitrate sensor. It was learnt that the performance of the smartphone-based nitrate sensor was comparable to the performance of the laboratory spectrophotometer. The smartphone-based nitrate sensor was able to measure the concentration of the environmental sample with an accuracy of 19% and 7% less than that of the laboratory spectrophotometer, for a first and second set of tests, respectively. Additionally, the smartphone-based nitrate sensor was successfully able to measure the concentration of the environmental sample, within the reported range of the actual concentration of the environmental sample.

The smartphone-based nitrate sensor achieved a measurement sensitivity of 1.402×10^7P.U/ppm, a resolution of 0.2014 ppm, and a detection limit of 1 to 5 ppm. Therefore, the smartphone-based nitrate sensor displayed a prospective ability to be employed as a more economical and compact means of analysing nitrates in water sources, particularly for rural areas.

Uittreksel

Slimfone-gebaseerde nitraat-sensor

JMD. Pereira Ingles
Departement Electrical en Electronic Ingenieurswese,
Universiteit van Stellenbosch,
Privaatsak X1, Matieland 7602, Suid Afrika.
Tesis: MIng (Elektroniese Ingenieurswese)
Desember 2019

Die skaarste aan sanitêre water is 'n bekende probleem wat tans in Afrika heers, en nitrate is een van die belangrikste parameters wat waterkwaliteit betref. Nitrate kan maklik waterbronne besoedel deur mensgemaakte of natuurlike prosesse, en die agteruitgang van akwatiese ekosisteme veroorsaak gesondheidskomplikasies vir mense.

In die lig van hierdie saak was die doel van hierdie tesis om 'n "lab-in-a-suitcase"slimfoon-gebaseerde nitraat-sensor te ontwikkel wat draagbaar en meer bekostigbaar is vir gemeenskappe in landelike gebiede in vergelyking met tradisionele toerusting. Vir hierdie toepassing het die slimfoon-gebaseerde nitraat-sensor spektrofotometriese analise uitgevoer, meer spesifiek U V-spektroskopie, o m d ie n itraat k onsentrasie t e k wantifiseer in 'n watermonster. Spektrofotometrie is 'n metodologie wat die verband tussen die hoeveelheid lig geabsorbeer en die konsentrasie van die monster verkry.

Spektrofotometrie gebruik 'n paar optiese komponente wat duur kan wees, kompleks kan wees om te implementeer en die grootte van die toestel kan vergroot. Sommige van hierdie komponente, soos die diffraksierooster, is noodsaaklik om spektrofotometers in staat te stel om verskillende chemikalieë te ontleed. Aangesien hierdie toediening spesifiek o p n itrate van t oepassing was, het dit nie al hierdie komponente nodig nie. Hierdie tesis ondersoek dus die moontlikheid om sekere optiese komponente uit te sluit om die koste, grootte en kompleksiteit te verminder van die slimfoon-gebaseerde nitraat-sensor. Dit was bereik deur te ondersoek of 'n diffraksierooster en 'n banddeurlaatfilter onontbeerlik was vir die slimfoon-gebaseerde nitraat-sensor om ideaal te werk. Die ondersoek het bestaan uit die ontwerp van drie ontwerpscenario's, waar al drie scenario's uit dieselfde elementêre komponente bestaan het, maar elke scenario

het verskil met 'n komponent. Een scenario het slegs bestaan uit die elementêre komponente terwyl die ander scenario's onderskeidelik uit 'n banddeurlaatfilter en 'n diffraksierooster bestaan het. Die prestasie van elke scenario was in vergelyking met mekaar en met 'n laboratorium-spektrofotometer gestel. Deur die beoordeling van die drie scenario's was afgelei dat die toevoeging van die diffraksierooster geen noemenswaardige verskil aan die opspoorvermoë van die slimfoon-gebaseerde nitraat-sensor het nie. Die insluiting van die banddeurlaatfilter het egter die opsporingsvermoë van die slimfoon-gebaseerde nitraat-sensor verhoog om meer gelyk met die laboratorium-spektrofotometer te presteer. Die afwyking tussen die prestasie van die scenario met die banddeurlaatfilter en die laboratorium-spektrofotometer was minder as 27%. In teenstelling, die variansie tussen die ander twee scenarios en die laboratorium-spektrofotometer was meer as 80%. Daarom bestaan die finale ontwerp van die slimfoon-gebaseerde nitraat-sensor uit die elementêre komponente asook 'n banddeurlaatfilter.

Daarna was daar 'n vergelyking ingestel tussen die vermoë van die finale slimfoon-gebaseerde nitraat-sensor en die laboratorium-spektrofotometer om die nitraatkonsentrasie van 'n omgewingsmonster te bepaal. Hierdie vergelyking het gedien as die uiteindelike evaluering van die uitvoering en akkuraatheid van die slimfoon-gebaseerde nitraat-sensor. Dit is bepaal dat die slimfoon-gebaseerde nitraat-sensor se prestasie vergelykbaar is met die laboratorium-spektrofotometer. Die slimfoon-gebaseerde nitraat-sensor kon die konsentrasie van die omgewingsmonster met 'n akkuraatheid van 19% en 7% minder as die van die laboratorium-spektrofotometer opspoor vir onderskeidelik 'n eerste en tweede stel toetse. Boonop kon die slimfoon-gebaseerde nitraat-sensor die konsentrasie van 'n nitraatmonster binne die gerapporteerde omvang van die werklike konsentrasie van die omgewingsmonster meet.

Die slimfoon-gebaseerde nitraat-sensor het 'n meetings sensitiviteit van 1.402×10^7P.U/ppm, 'n resolusie van 0.2014 ppm en 'n opsporingslimiet van $1 - 5$ ppm. Daarom het die slimfoon-gebaseerde nitraat-sensor die moontlike vermoë om gebruik te kan word as 'n meer ekonomiese en kompakte manier om nitrate in waterbronne te ontleed, veral vir landelike gebiede.

Acknowledgements

I would like to express my sincere gratitude to the following people and organisations:

- Prof. MJ Booysen for providing this opportunity to me, and guiding and advising me throughout my postgraduate journey.
- Dr TM Louw for guiding and assisting me, particularly with ensuring that I understood the chemical aspects of my thesis.
- MTN for funding my master's studies.
- Ms H. Botha and Mr J. Van Rooyen, from the process engineering analytical laboratory, for assisting and allowing me to make use of their resources.
- Mr B. Botha and Ms A. Mogolegeng, from the Stellenbosch Wastewater Treatment Plant, for assisting me with the environmental sample collection and for sharing their concentration reports with me.
- Ms H. Lambrechts, for assisting me with my thesis.
- Mr W. Croukamp and Mr LG Lecholo for assisting me with the structural design and fabrication of this project.
- My family and friends for emotional support and encouragement.

Contents

List of Figures

List of Tables

Nomenclature

Definitions

Analyte A substance whose chemical constituents are being identified and measured

Reagent A substance or mixture for use in chemical analysis or other reactions

λ_{max} Wavelength at which a molecules experiences its absorbance peak.

Variables

NO_3- Nitrate ion

$NaNO_3$ Sodium Nitrates

Eu_+ Europium ion

mg/L Milligrams per litre

ppm parts per million

M Molarity

Fe^{2+} Iron ion

MP Megapixels

P.U pixel intentsity unit

Acronyms

WHO World Health Organisations

UV Ultraviolet

Vis Visible

POC Point of Connection

mHealth Mobile Health

ALS Ambient Light Sensor

LED Light Emitting Diode

RGB Red Blue Green

CMOS Complementary Metal-Oxide-Semiconductor

NMR Nuclear Magnetic Resonance

DVDR

SNS Smartphone-based nitrate sensor

LS Laboratory Spectrophotometer

DOC Dissolved organic carbon

WWTP Wastewater treatment

Chapter 1

INTRODUCTION

Eighty percent of all diseases in Africa derive from waterborne diseases such as Cholera, Malaria and Typhoid [1]. This comes to no surprise since Africa has over 300 million people living in conditions where there is only access to contaminated, hazardous water that has not been minimally treated to remove contaminants and pollutants [1]. Agriculture, along with other human-made activities and some natural processes are the main contributors to the discharge of pollutants and contaminants into regional water sources [2, 3]. Most pollutants and contaminants are imperceptible and require specialised equipment to be detected [2]. One of the most concerning pollutants is nitrogen; specifically, a nitrogen derivate denoted as nitrates [2, 3].

When excess quantities of nitrates pollute a water source, the aquatic ecosystem and all human life that depends on the water source, become at risk of complications [2, 3]. These complications include eutrophication and anoxia, which are phenomenons that can cause both the aquatic environment and life to gradually perish, by limiting the oxygen present, producing an unpleasant green colour, which eventually results in the death of aquatic animals that require oxygen to survive [2, 3]. With the perishing of the aquatic ecosystem, an accommodating site for waterborne disease-causing bacterias is created [2].

According to the World Health Organisation (WHO), concentrations of nitrate exceeding 26.56 ppm can be a health hazard to humans who consume it [4]. If digested by a human in such concentrations or more, nitrates can become toxic, and carcinogenic [2, 3]. More specifically, the consumption of high quantities can lead to a respiratory disease called methaemoglobinaemia, also known as "blue baby syndrome". Although all humans are also susceptible to methaemoglobinaemia, fetuses, infants and adults with certain health predispositions are more prone to this disease. In cases of fetuses or infants being affected by this disease, the disease may cause grave health issues or even become fatal [2, 3, 8].

However, people who are dependent on local water sources, and reside in areas where agriculture is extensively practised, are most prone to the issues

associated with the presence of high amounts of nitrates in water [4]. This is because the discharge of chemical fertilisers, through agricultural practices, are amongst the common causes of nitrate contamination in water sources [2, 3]. The threat becomes more critical for regions where the water treatment and sanitation are insufficient or non-existent, mainly rural areas. Therefore, research that focuses on finding solutions for detecting the levels of nitrates in water sources is critical. Especially solutions that are affordable to rural communities.

Some water contaminants and pollutants can be detected by humans, through sight, taste, or smell [2]. Nevertheless, like most chemicals, nitrates are challenging to detect, by a human alone [2]. The detection of nitrates requires specific methods and analytical equipment [2]. However, the existing approaches make use of sophisticated, expensive equipment and a complicated methodology. Additionally, such methods require instruments restricted to processing laboratories and that cannot be operated on the field. Since nitrates can only be detected with the help of specific equipment, the detection of nitrates is most likely not accessible to most rural communities. Consequently, if a local water source, in a rural area, is contaminated with nitrates, then it is presumable that the residents will be oblivious to the contamination.

Recently, the development of simplified and miniature versions of such analytical equipment has expanded, to reduce the complexity and expense while increasing their accessibility [5]. Many of these devices have been integrated with smartphones. A contributing factor to this rapid advancement of smartphone-based devices is that smartphones have become increasingly pervasive, especially so in developing countries, and their technologies have and continue to improve [5, 6, 7].

Therefore, this project will focus on developing an inexpensive and portable smartphone-based device that can sense nitrates in water.

1.1 Problem statement

Water that is contaminated with nitrates in high quantities can be very harmful to the aquatic environment, aquatic life and ultimately, humans. Residents of rural areas, particularly the ones who practice agriculture, can be at risk of nitrate contamination for three main reasons: agriculture is a common means of survival, and agricultural activities degenerate the water quality and contribute nitrate contamination, there is a lack of or no water treatment and sanitation facilities, and there is no access to nitrate detection resources.

One of the most commonly used methods to detect chemicals such as nitrates in water is spectrophotometry. Spectrophotometry is a chemical analytical method that analyses the interaction of a chemical with an incident light emitted at a specific wavelength, and through that analyses, the concentration of the chemical may be determined [2, 8, 9, 10]. The wavelength of the incident

light can be within the ultraviolet (UV) or visible range; however, it is chosen based on the chemical's characteristics [9, 10, 11]. Nitrates, in particular, can be quantified through the use of UV light, typically at 205 nm [12, 13]. Nevertheless, the challenge lies in developing a smartphone-based sensor that can analyse nitrates at 205 nm. The concern is that smartphone cameras are primarily designed to detect visible light and not UV light [14, 15]. Currently, most smartphone-based sensors that implement spectrophotometry have been limited to detecting within the visible range.

Therefore, this project aims to design a "lab-in-a-suitcase" water quality sensor that can detect the presence and concentration of nitrates, in a water sample, that is based on the principles of spectrophotometry, and uses a smartphone camera as the detection medium. The smartphone-based nitrate sensor should be less expensive than traditional laboratory equipment or machines. Additionally, the system should be portable and usable beyond the confines of a laboratory.

1.2 Objectives

To obtain the solution of the proposed problem statement, the following objectives were set out:

1. Objective 1: Assess the suitability of spectrophotometry as the means of measuring nitrates for this smartphone-based nitrate sensor.
    a) Assess spectrophotometry against other chemical analytical methods, commonly used to detect nitrates - based on the literature.
    b) Assess and choose appropriate light source - based on the literature.
    c) Assess and choose appropriate sample holder - based on experiments.
    d) Assess methods of shifting UV light into visible light.
2. Objective 2: Design and build a prototype of the smartphone-based nitrate sensor that uses spectrophotometry to detect nitrates.
    a) Preform a spectral shift of UV light into visible light.
    b) Evaluate the necessity of typical components used in spectrophotometers.
    c) Implement an algorithm to determine the concentration of nitrates in a water sample, based on the information captured by the smartphone.

d) Calibrate the smartphone-based nitrate detector, using known nitrate samples.

3. Objective 3: Assess the validity of the designed smartphone-based nitrate sensor.

1.3 Contributions

This research presented a "lab-in-a-suitcase" smartphone-based nitrate sensor that implements the principles of spectrophotometry. Furthermore, this research introduced the use of a smartphone camera as a detecting component specifically for UV spectrophotometric analysis of nitrate, at a wavelength of 205 nm, through the use of a fluorescent material (scintillator). More specifically, this research demonstrated the ability of a smartphone camera to indirectly detect UV light by using a scintillator that can shift UV light into visible light. This thesis presented an algorithm that can determine the concentration of a nitrate sample of unknown concentration, based on the information captured with a smartphone camera. This research developed a smartphone-based nitrate sensor that is a miniaturised and modified version of a typical spectrophotometer. However, even though the smartphone-based nitrate sensor did not implement all of the conventional components used in spectrophotometers, the smartphone-based nitrate sensor was still able to function comparably well to typical spectrophotometers. This research developed a smartphone-based nitrate sensor that is more affordable and portable in comparison to its commercial counterpart. This research presented a smartphone-based nitrate sensor that determines the absorbance of the nitrate sample similar to a typical spectrophotometer, thereby determining the concentrations of the nitrate sample.

1.4 Scope

The thesis intended to design a smartphone-based sensor that implements spectrophotometry, as the analytical method, and that is specific for the detection of nitrates in water samples. The smartphone-based nitrate sensor made use of the iPhone Xs Max (Apple Inc) to analyse the nitrate samples. Therefore, this application was only implemented with an iPhone Xs Max and thus was limited to the software and hardware capabilities of the iPhone Xs Max. This thesis consisted of the use of a fluorescence glass (scintillator) to permit the smartphone camera to detect the UV light indirectly. The size and power requirements of the chosen light source limited the overall size, weight and cost of the smartphone-based nitrate sensor. Nonetheless, the smartphone-based nitrate sensor was designed to be affordable to a community of people, potentially a rural community or a small institution. The smartphone-based nitrate

sensor was assessed using one environmental sample, collected from the local municipal Wastewater Treatment Plant. The performance of the smartphone-based nitrate sensor was evaluated against the UV Vis Spectrophotometer (AE-S60), manufactured by A & E Lab. For the assessment of the sample holders, one type of glass, plastic and quartz cuvettes were assessed, specifically the 100-OS glass cuvette (Hellma), the 100-QS10 quartz cuvette (Hellma) and the PS plastic cuvette (Lasec SA).

1.5 Layout of dissertation

This dissertation consists of another four sections that detail the process of implementing the smartphone-based nitrate sensor.

Chapter 2 describes the literature that was necessary to fulfil the objectives stated in Section 1.2. This chapter provides necessary background information on nitrates and the conventional analytical methods used for nitrate detection. Later, chapter 2 provides a study and comparison of the available methods of measure and the essential components needed to realise the smartphone-based nitrate sensor. The chapter finalises with a discussion on the current related works.

Thereafter, chapter 3 focuses on the methodology of the smartphone-based nitrate sensor. The chapter illustrates some of the preliminary experiments that were performed. Additionally, the chapter focuses on the setup and metrics of the smartphone-based nitrate sensor.

Chapter 4 documents the testing of the execution of the designed smartphone-based nitrate sensor, and it also presents and analyses the key results. Lastly, chapter 4 validates the results measured with the smartphone-based nitrate sensor to the results achieved with the laboratory equipment.

Finally, chapter, 5, provides the conclusion of the dissertation, by confirming whether the designed smartphone-based nitrate sensor adhered to the objectives mentioned in Section 1.2. Conclusively, a discussion, further work, as well as recommendations, are provided.

Chapter 2

LITERATURE REVIEW

It was crucial to perform a literature study to design a smartphone-based nitrate sensor. First and foremost, this chapter briefly describes water quality and its parameters. Proceeding that, basic background information of nitrates, as well as the implications of nitrate contamination in water sources, are outlined. Thereafter, an investigation and comparison of the available measuring methods for nitrates are presented in this chapter. Upon choosing the most suitable measuring method, the fundamental theory relative to the chosen measuring method is provided. Additionally, different setups and components, used to implement the desired methodology are discussed and compared. Finally, other works that are deemed relative to this thesis are considered and analysed. Ultimately, in this chapter objectives 1a, 1b and 1d are obtained.

2.1 Water quality

According to G.T Howard S. Peavy et al. water pollution can be defined as the quantity and nature of dissolved and suspended impurities present in the water that prevents the water from being used as intended. In general, water quality is categorised into three parameters: physical, chemical and biological [2].

The physical qualities of water parameters are water properties that can be detected by sense: taste, smell, sight and touch [2]. It includes suspended solids, turbidity, colour, taste and odour, as well as temperature. Physical parameters may impact on the water, such as decrease the aesthetic of the water and create sites for chemical and biological agents, but these parameters are easily monitored through simple methods or human senses [2].

Biological parameters refer to all organisms that spend part or all of their life cycle in water, from a single-cell microorganism to a killer whale [2]. However, the biological parameters that are usually monitored are pathogens, bacteria, viruses, protozoa, and helminths [2]. These parameters are responsible for infecting and transmitting waterborne diseases to humans, such as cholera,

typhoid and infectious hepatitis [2]. Monitoring these parameters is most challenging; therefore, while equipment has been developed to detect biological parameters, methods exist to prevent the repercussion of these parameters, such as immunisation of humans and disinfection of the water [2]. The techniques used to detect biological parameters can be expensive, time-consuming and require extensive laboratory equipment.

Chemical parameters are defined as the solvent capacity of water - mainly totally dissolved solids, alkalinity, hardness, fluoride, metals, biodegradable and non-biodegradable organics, as well as nutrients. Nitrogen and phosphorus are the most vital nutrients that are taken into consideration, in terms of water quality, as all living organisms require nitrogen and phosphorus to survive [2, 3]. Chemical parameters are more challenging to detect than physical parameters and can produce more significant consequences too. For example, certain chemical parameters help instigate the corrosion and deterioration of water pipes [2]. Additionally, high quantities of some dissolved chemicals and metals can be harmful to humans and both the aquatic life and environment, however, they are usually found in minute quantities [2]. An example of such a chemical is nitrogen.

2.2 Nitrogen

Proteins, chlorophyll, and many other biological compounds consist of nitrogen [2, 3]. When animals or plants die, they are eventually decomposed by bacteria into amino acids and then ammonia, which is then oxidised into nitrites and then nitrates [2, 3]. Wastewater, chemicals, especially chemical fertilisers, and animal waste discharges are other primary nitrogen sources found in water [2, 3]. Water can become contaminated by these sources through groundwater discharge, surface runoff or direct discharge into streams [2, 3]. The soil that is in contact with such water sources can oxidise the nitrogen into nitrates, enabling the nitrates to become free to flow and contaminate the water [2, 3].

Approximately 84% of Africans who do not have access to quality water or proper water sanitation rely on agriculture to survive [1]. Besides putting substantial strain on the water supply, agricultural activities also lower the quality of the water considerably [1]. Agricultural activities predominantly require the use of chemical fertilisers and manure, which are usually sources of nitrates [2]. Therefore, the practice of agriculture can jeopardise local water sources as it increases the potential for nitrate contamination in local water sources. Unfortunately, excessive amounts of nitrates in water can be a threat to the aquatic life, the aquatic system and also to human life [2].

Nitrates are commonly associated with eutrophication of aquatic environments [2, 8]. Aquatic plants and algae use nitrates as a food source. Consequently, high levels of nitrates can prompt the algae, aquatic plants and other microorganisms to grow uncontrollably [2, 3, 8]. As algae and aquatic plants,

use the oxygen available to them for photosynthesis, significant growth in algae can lead to the oxygen in the aquatic system to fluctuate and eventually become limited to the aquatic life [3]. Moreover, the excess amount of algae, plants and microorganisms can cause a layer of slime to form on the water's surface, which can then inhibit sunlight and the atmosphere's oxygen from entering the water [3, 8]. This circumstance conduces to the emergence of another phenomenon called anoxia [3, 8].

With the lack of light, the plants and algae located below the water's surface ultimately perish [8]. Subsequently, other microorganisms will decompose these dead plants and algae and further consume all the dissolved oxygen available in the aquatic system [8]. Inevitably, all the aerobic aquatic organisms - that is the organisms require oxygen to survive - die, while all anaerobic organisms - that is the organisms that do not require oxygen to survive - thrive [3, 8]. Consequently, an imbalance in the food chain is created [8]. Furthermore, the water develops an unattractive opaque green colour and smell [8]. With the decaying of the dead algae and plants, a favourable environment is created for the growth of disease-causing bacteria, such as Vibrio Comma and Salmonella [8]. Vibrio Comma and Salmonella Typhosa are responsible for transmitting Cholera and Typhoid respectively, and 80% of the diseases in developing countries around the world can be traced back to diseases like Cholera, Typhoid and other waterborne diseases [1].

Excessive nitrates in one's body can inhibit the capability of the red blood cells to carry oxygen around the body [3]. This condition is referred to as methaemoglobinaemia, commonly known as "blue baby syndrome" [2]. Since infants and fetuses are more fragile and are still developing, they are more susceptible to the complications of consuming water contaminated with excess nitrates [3, 16]. If an infant or a pregnant woman consumes an excess of nitrates, their red blood cells may fail to carry enough oxygen to their bodies. Consequently, the foetus or infant will struggle to breathe, causing their skin to develop a blue tint [16]. Moreover, the infant or fetus may develop long-term respiratory and digestive issues and, if not treated, methaemoglobinaemia may be fatal [16]. Similarly, older adults, adults with a hereditary predisposition, adults with peptic ulcers or chronic gastritis, as well as dialysis patients, are also more vulnerable to developing methaemoglobinaemia by consuming excessive nitrates [3]. Additionally, most people are also at risk of developing mucous membrane irritation should they consume a concentration of nitrate exceeding 88.54 ppm [4]. If a human or animal digests a concentration of nitrates exceeding 194.78 ppm, the presence of nitrates in the acidic stomach conditions can cause the body to produce substances such as nitrite, nitric oxide, and carcinogenic nitrosamines [8]. These substances are associated with gastric cancer and metabolic disorders [8, 17].

It is natural to observe the concentration of a few parts per million of nitrates in water [4]. However, anything above 26.56 ppm is already considered grave [4], as per Table 2.1, found in the South African Water Quality Guidelines

[18]. According to the World Health Organisation (WHO), intense agricultural activities may raise the level of nitrates to more than 221.34 ppm in the nearby water sources which, according to Table 2.1, is unacceptable [4].

Table 2.1: Effects of nitrate on human health. Adapted from the South African Water Quality Guidelines [18]

Nitrate (ppm)	**Effects**
0 - 26.56	No adverse health effects
26.56 - 44.27	Rare instances of methaemoglobinaemia in infants; no effects in adults. Concentrations in this range generally well tolerated
44.27 - 88.54	Methaemoglobinaemia may occur in infants. No effects in adults
$>$ 88.54	Methaemoglobinaemia occurs in infants. Occurrence of mucous membrane irritation in adults

Indeed, excess nitrates can create many complications for humans by impacting on the environment and the food chain - potentially limiting the availability of food to humans - generating disease-carrying bacteria, promoting health-threatening conditions and even cancer. These circumstances can make water inadequate for everyday use [8]. Hence the monitoring and treatment of nitrate are necessary to prevent and reduce the effects that it may cause, especially for the people who are living near and utilising water sources such as shallow wells near agricultural areas, as they are more susceptible to these risks.

2.3 Method of measurements

In the past two decades, many methods for the determination and monitoring of nitrates in various environmental matrices have been developed [8]. The most common approaches used for nitrate analysis in water are chromatographic, electrochemical and spectrophotometric methods [8, 17]. Therefore, this section will accomplish Objectives 1a by considering the three most common techniques and comparing them against one another.

2.3.1 Chromatographic methods

Chromatography involves the separation of a mixture of chemical substances into their individual elements, sequenced by the analysis of each individual ele-

ment [19]. This method allows for the separation of closely related components in complex mixtures [8, 19]. For some mixtures of chemical substances, the separation is only achievable through chromatography and not through other means [8, 19]. There is a variety of different types of chromatography, where the most common methods used for nitrate detection are gas chromatography and ion chromatography [8, 19].

Figure 2.1 illustrates the process of chromatography, where the sample is loaded into the stationary phase, which is an immiscible substance that is fixed on a solid surface or in a column [10, 19]. Thereafter, a solvent is added and is allowed to move through the surface or column with the help of gravity or pressure [10, 19]. This solvent is referred to as the mobile phase [10, 19]. Both phases are chosen to enable the individual elements of the sample to be distributed between the two phases at varying degrees, since each element experiences different levels of adhesion to the stationary phase [10, 19]. Therefore, each component will travel through the stationary phase at their speed as the mobile phase flows through it [10, 19]. The components that adhere firmly to the stationary phase move slowly with the flow of the mobile phase [10, 19]. Contrarily, the components that adhere weakly to the stationary phase travel rapidly [10, 19]. As a consequence of these differences in mobility, the sample components separate into discrete bands or zones, as observed by Figure 2.1, that can be analysed quantitatively or qualitatively [10, 19].

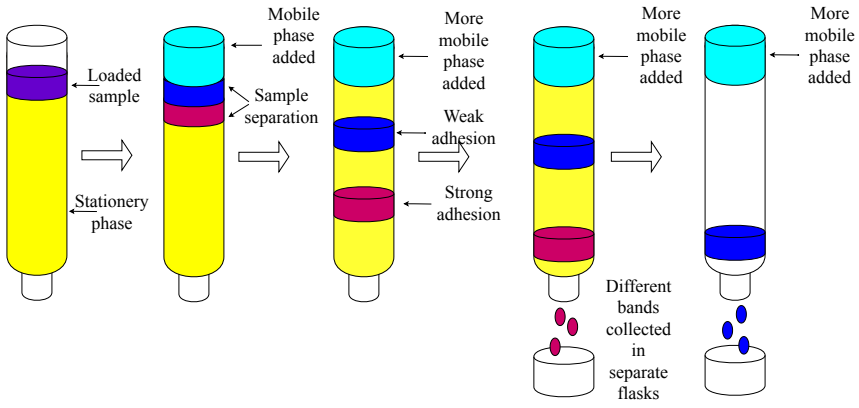

Figure 2.1: Chromatographic separation. The sample is loaded into the column filled with the stationary phase. The mobile phase is then added to the column, and immediately, the sample starts to separate into its elements. The elements with the strongest adhesion properties move slowly down the column, while the elements with the weakest adhesion properties move fast down the column. The difference in movement allows for each element to be collected separately.

This method is sensitive and can detect distinctly minute concentrations of nitrate. Nonetheless, ion chromatography requires specialised and expensive materials to prevent interference from other ions with similar retention times [8]. Gas chromatographic methods require sample pretreatment or derivatisation step, in order to make the nitrate a measurable entity [8, 17]. The most significant limitation of gas chromatography is that only skilled chemists can perform this method [17]. Additionally, complications can arise when trying to implement a portable device based on chromatography, as the accuracy of the mobile phase is affected by vibrations; however, it is almost inevitable that the portable device will experience movements and vibrations [20]. Miniaturisation can also be a challenge in some instances, since some types of chromatographic methods have specific requirements, such as the use of a long column of 200 mm or more [20].

2.3.2 Electrochemical methods

Electrochemistry includes a variety of analytical techniques that work by the electrical potential through electrical conductors to a sample solution, followed by the measurement of a current or voltage that is a consequence of the oxidation or reduction of the ions in the sample solution [9]. The resultant measured current or voltage provides information about the ions present in the sample.

Figure 2.2 shows an electrochemical cell, which consists of two electrical conductors, referred to as electrodes. In one of the half cells, the positive electrode (cathode) is contained, while in the other half cell, the negative electrode (anode) is contained. Each electrode is submerged in an appropriate electrolyte solution [10]. A metal conductor externally connects both electrodes to allow current to flow in the cell [10]. The salt bridge is a tube usually filled with potassium chloride solution, that joins the two electrolyte solutions [10]. The salt bridge allows electrical contact to be maintained between the two half cells while preventing the contents of either half cell from coming in contact with one another [10]. The electricity is maintained by allowing the potassium to travel to the left-hand half cell and the chloride to the right-hand half cell [10]. Porous plugs are placed on either side of the salt bridge to allow for the movement of ions while isolating the two half-cells [10]. In the right-hand cell, reduction occurs, that is the ions that are present in the anode pull away from the anode [10]. In the left-hand cell, oxidation takes place, and the ions present in the solution draw towards the cathode [10].

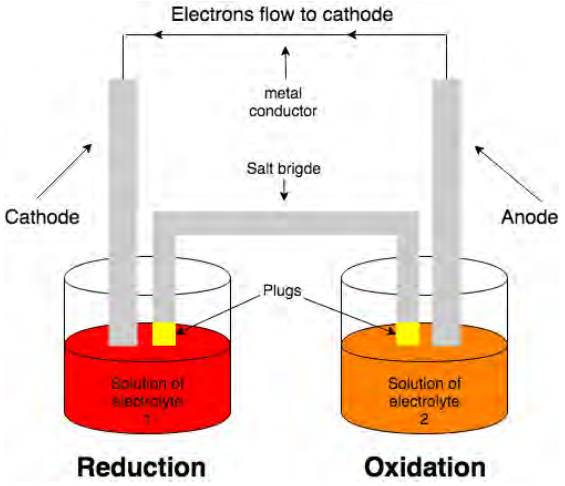

Figure 2.2: Layout of an electrochemical cell. An electrochemical cell allows for electricity to be generated through the flow of the electrons from the anode (positive electrode) to the cathode (negative electrode), resulting in the reduction and oxidation of the solutions found in the left cell and right cell, respectively. The salt bridge maintains the balance between the ions in each cell.

One of the most significant advantages of this method is that it is relatively inexpensive to implement, and it has the potential to be portable [10, 17]. Nevertheless, electrochemical analysis does not necessarily indicate the concentration of the chemical species, but rather provide information about the activities of the species present in the sample, and this could be an advantage or disadvantage, depending on the application [10]. Most water samples, from ground to surface waters, contain complex mixtures of different substances, and interferences can occur, mainly if oxygen or pollutants are present in the sample, or if the sample contains a variety of chemicals in it [8, 17]. These potential interferences are a barrier to electrochemistry since the sensitivity and accuracy of this method can be harmed [8, 17]. Another aspect that requires improvement is that the detection range of electrochemistry is limited to micro and milli-molarities (μM or mM) [17].

2.3.3 Spectrophotometric methods

Spectrophotometry is a technique that quantifies the interaction of matter with light [9, 10]. As light interacts with a sample, the light can either be reflected, absorbed or transmitted through the sample. The interaction of a sample with light can be analysed to provide information about the sample, including its concentration [9]. Beer-Lambert's law states that the concentration of a solution is proportional to the absorbance of the incident light on the solution [10]. As shown in Figure 2.3, the electromagnetic spectrum is divided into

different parts, starting with gamma-rays and ending with radio-waves [9]. All molecules are affected differently to the various parts of the spectrum. Likewise, humans can only see within the visible spectrum and experience the other spectrums as heat [9, 21]. Moreover, specific molecules readily absorb light within the visible spectrum, while others readily absorb light within the UV spectrum or the infrared spectrum [9, 10, 21]. Therefore, each analyte will have a better ability to absorb light at one specific wavelength, as compared to other wavelengths. There are various types of spectrophotometric techniques used to detect nitrates. However, the ones that are usually used for nitrate determination are colourimetry and ultraviolet-visible spectroscopy [8, 17].

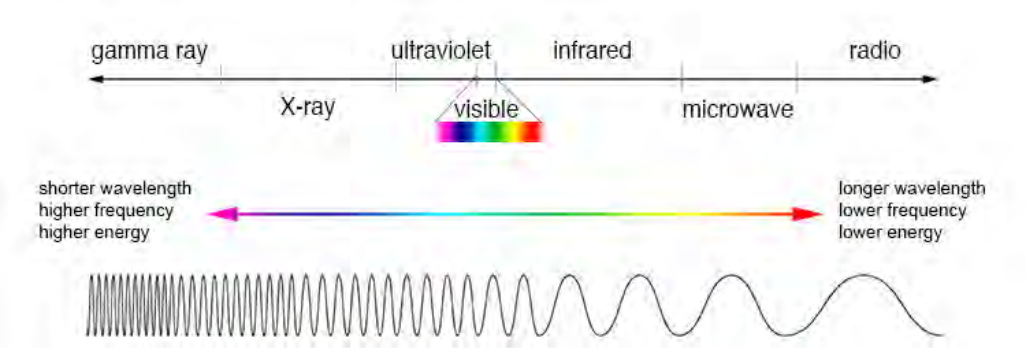

Figure 2.3: Electromagnetic light spectrum. The spectrum consists of gamma, ultraviolet, visible, infrared, microwave and radio ways. The spectrum ranges from shorter to longer wavelengths or waves [22].

2.3.3.1 Colourimetry

When a specific chemical is added to an analyte, it reacts with the analyte to produce a colour change [9]. The intensity of the colour produced indicates the concentration of the analyte, i.e. the colour intensity is directly proportional to the concentration of the analyte [9]. Therefore colourimetry is a method that measures the amount of colour change that takes place when a specific chemical is added to an analyte and relates it to the concentration of the analyte [9]. As shown in Figure 2.3, the electromagnetic spectrum has a narrow region, spanning from 400 to 700 nm, within which humans can detect (see) radiation, referred to as the visible spectrum [9]. Thus, any colour change that happens in this region can be observed by human eyes [9]. Nonetheless, sometimes these colour changes that take place in colourimetry, may not be noticeable or detectable by a human. Therefore, it is necessary to use instrumentation that measures the intensity of the colour of the sample, so that the concentration of the sample can be quantified.

The first step in colourimetry is to add a chemical to the analyte, that will produce a desired coloured solution. Thereafter, colourimetry uses the

principles of Beer-Lambert's law [10, 23]. The coloured solution will absorb light that is complementary to it, and the amount of absorbed complimentary light will be linear to the intensity of the colour of the analyte, thus linear to the concentration of the analyte [23, 24]. A basic colourimetric setup makes use of a light source, a sample and a detector, as depicted in Figure 2.4, however, colourimetry analysis is usually performed using spectrophotometers, which might consist of more components. The wavelength of light emitted onto the sample is selected so that it is the complementary colour of the sample's colour. When the complementary coloured light is emitted onto the coloured sample, the detector measures how much of the complementary colour is transmitted through the coloured sample [24]. In Figure 2.4, the light source emits onto the green coloured sample, and the filter between them converts the light from the source into a red light, which is the complement of green. The green solution absorbs some of the red light and transmits the rest onto the detector.

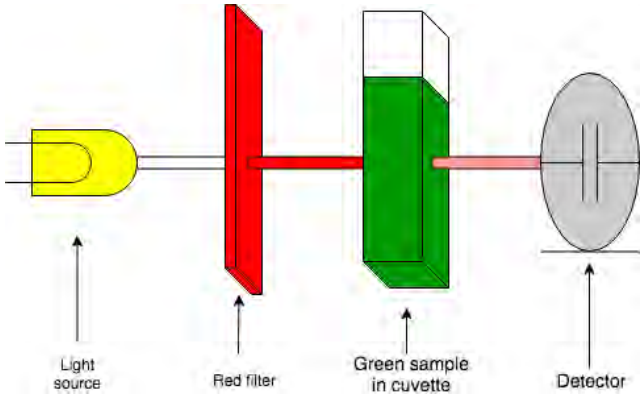

Figure 2.4: Configuration of a basic colourimetric scenario. The process of colourimetry consists of a light source, a filter that is complementary to the sample, a sample, and a detector. The detector measures the amount of light the is transmitted through the sample.

When used to detect nitrates, the colourimetry essay requires that the nitrate is reduced to nitrite, as a prerequisite [8]. To achieve this reduction of nitrates, it is necessary to use biological or chemical methods, which usually require some time to react [8]. The rest of the method consists of a reaction between the nitrite and a reagent to form a coloured solution [8, 17]. The solution will usually have a green colour, with a wavelength ranging between 495 nm and 570 nm [8, 17, 25]. However, this method can become tedious, as it requires quite a few steps, and can be time-consuming, as each step may require some time to implement and to develop [8]. In addition, it is subject to reduced sensitivity in comparison to other methods [8]. Groundwater and surface water contain many ions, and colourimeters are subject to interference

from other ions [8]. Therefore, if a colourimeter is used to test ground or surface water, it is likely to suffer from inaccuracies.

2.3.3.2 Ultraviolet-Visible spectroscopy

As previously mentioned, Beer-Lambert's law states that the light absorbed by a solution is linear to the concentration of the solution [9, 10]. Ultraviolet-visible spectroscopy (UV-Vis spectroscopy) measures the transmittance or the absorbance of incident light on a solution contained in a transparent cell [10]. Through the quantification of the transmittance and absorbance, the concentration of the sample can be estimated [10].

Similar to colourimetry, a spectrophotometer can also be used for UV-Vis spectroscopy. The setup of a typical spectrophotometer consists of a light source, a detector and a cuvette filled with an analyte solution, along with some optics, as observed in Figure 2.5. The light source directs light onto the solution. Depending on the concentration of the analyte, the analyte absorbs some of the incident light. Consequently, the rest of the incident light is transmitted through the sample and onto the detector. Thereafter, the detector measures how much light is transmitted through the sample [9, 10, 21]. If there is a low concentration of the analyte, then a small portion of the incident light will be absorbed by the solution, and most of the incident light will be transmitted to the detector. On the other hand, if there is a high concentration of the analyte, then a considerable amount of the incident light will be absorbed by the solution, and only a limited amount of the incident light will be transmitted to the detector.

Most spectrophotometers use an optical device called monochromator to increase the accuracy and resolution of the detector. With the use of the monochromator, the emission wavelength of the light source can be adjusted or selected to a specific wavelength [26]. A monochromator consists of a diffraction grating or a dispersive element and collimators [27]. The diffraction grating or the dispersive element helps separate the light into its various components or colours, with high resolution [27]. The one collimator helps control the light that is being diffracted or dispersed, by focusing and keeping the light beams aligned in different directions, reducing the cross-sections [28, 29]. The other collimator isolates the diffracted light at a specific wavelength or a narrow band of wavelengths, thus allowing only the isolated diffracted light to be an incident on the sample [28, 29].

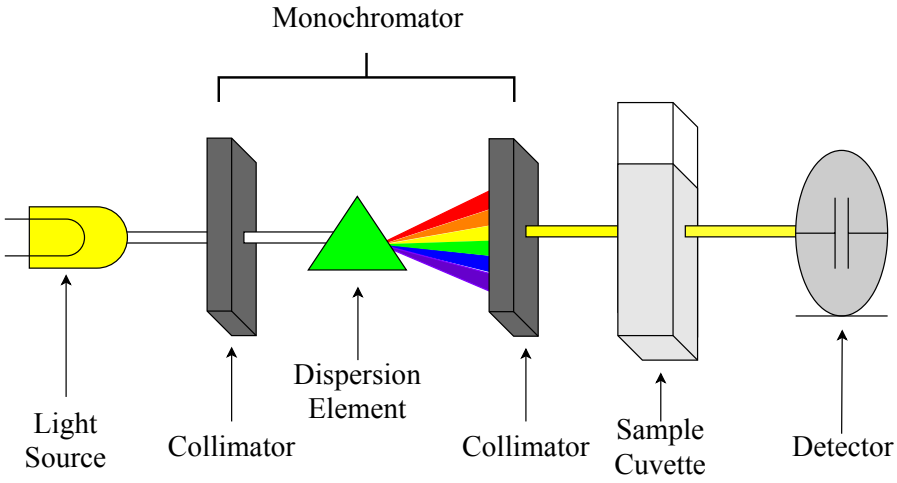

Figure 2.5: Arrangement of a typical spectrophotometer. In a spectrophotometric setup, the monochromator splits the light emitted from the source into its components. Thereafter, the monochromator selects and allows for light of one wavelength or a narrow band of wavelengths to be an incident on the cuvette. Where the cuvette is responsible for holding the sample. The detector then measures how much of the incident light is transmitted through the sample.

The wavelength of the isolated light is usually equivalent to a wavelength in which the analyte readily absorbs the most light in the electromagnetic spectrum. Nitrate ions display the strongest tendency to absorb light in the UV region, specifically at 205 nm [12, 13]. Therefore, to detect nitrates in a solution, it is essential to make use of a UV light source and a detector that can detect UV light.

UV-Vis spectroscopy is the most common technique used for nitrate analysis, as it provides prompt response, and lacks complexity in comparison to other methods [8, 17]. However, the potential for interference can arise in the detection of nitrates, if organic matter or ionic species that absorb light within the same region as nitrates are present in the sample [8]. Turbidity can also intervene with the results of this technique, as turbidity can cause the light transmitted onto the water to scatter, which can thus influence light absorbance [13]. Finally, this technique can be quite costly to implement, as it does require a few optics [30, 31].

2.3.4 Comparison of the methods

Table 2.2 compares the four methods proposed. The methods were compared by cost, feasibility, complexity, sensitivity and interferences.

Method	Interferences	Complexity	Feasibility	Sensitivity	Cost
Electro-chemistry	Oxygen, complex sample	Requires specialized materials and components	Easily feasible only requires sample to be collected	Poor	Low
Chroma-tography	Ions with similar retention times	Requires expensive, specialized materials and complex components	Prerequisite steps	High	High
Colorimetry	Ions	Low complexity, needs few equipment	Prerequisite steps	Poor	Low
UV-Vis spectroscopy	Organic matter and ions	Medium complexity, needs optics	Easily feasible only requires sample to be collected	High	Medium

Table 2.2: Table comparing typical methods used for the measuring of nitrates in water samples.

In conclusion, all methods are subject to interferences besides chromatography. While chromatography is highly sensitive, it is rather intricate as it requires preparation and derivatisation processes, and specialised components, and can only be realised by proficient individuals, making this method more expensive and complicated than spectrophotometric and electrochemical methods [8, 17].

Electrochemistry has excellent potential, but it can suffer from reduced sensitivity and accuracy as it is subject to interferences from other ions, therefore not being suitable for nitrate detection in most water sources [8, 17]. Indeed, chromatography and electrochemistry are the least attractive for this application.

The spectrophotometric methods are less sophisticated to develop in comparison with the other methods. UV-Vis spectroscopy and colourimetry are very similar techniques, though colourimetry utilises the visible spectrum exclusively while the UV-Vis spectroscopy makes use of both the UV and Vis spectrum [32]. A commercial UV-Vis spectroscopy device, specifically a spectrophotometer, is usually more expensive to build, while a colourimetry can be implemented inexpensively, as it requires simple components [32]. However, the derivatisation step and the colour reaction step are prerequisite steps

that can make colourimetry more tedious [8, 17]. UV-Vis spectroscopy, on the contrary, is a prompt analytical method that entails no extra steps other than collecting the sample and is more sensitive than colourimetry [8, 17].

Unquestionably, all the methods proposed have their limitations; therefore, they could all do with some improvement. Nonetheless, UV-Vis spectroscopy is the most suitable for this application, as it appears to be the most feasible method to implement. Nonetheless, the project will aim to improve or eliminate the shortcomings of this method, specifically the cost and complexity.

2.4 Absorbance

Figure 2.6 demonstrates a scenario where an incident light beam with an intensity of I_0 is passed through a transparent cuvette [9]. The cuvette absorbs some of the light passed through it; consequently, a light beam of lower intensity, I, emerges from the cuvette [9]. Since light is energy, it is measured in joules (J) [9]. Therefore, the intensity of light beams is measured as the energy per unit of time, commonly known as power, measured in J/s or Watt

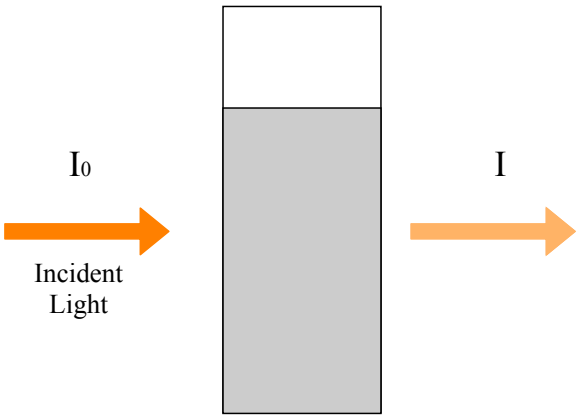

Figure 2.6: Transmittance of an incident light through a sample. The incident light has an initial intensity of I_0. The sample absorbs a specific amount of the incident light and transmits the rest, with a final intensity of I.

$$T = \frac{I}{I_0} \tag{2.4.1}$$

$$A = -\log T = \log_{10} \frac{I_0}{I} \tag{2.4.2}$$

When the intensity of the incident and transmitted light are the same in magnitude, the transmittance is equal to 1 [9]. Consequently, the absorbance will be equal to 0 [9]. If an absorbance of 1 is measured, the ratio of the intensity of the incident and the transmitted light ($\frac{I_0}{I}$) equals $\frac{10}{1}$, which means that 90% of the incident light was absorbed and 10% was transmitted [9]. With an absorbance of 2, $\frac{I_0}{I}$ is equal to 100; therefore, 99% of the incident light is absorbed while only 1% is transmitted [9]. An absorbance more significant than 2 suggests that only a minuscule amount of incident light is transmitted, which is usually immeasurable [9]. Thus, most instruments are likely only to measure absorbances from 0 to 2 accurately.

Nonetheless, the transmittance and absorbance cannot be accurately determined by directly measuring the incident light on and the transmitted light through an analyte solution [10]. The reason for this is that the analyte solution must be contained in a transparent cuvette [10]. Inevitably, some form of loss will occur when light is incident on a cuvette that contains an analyte solution. The likelihoods are that some of the incident light will be reflected away from the cuvette walls, dispersed by the larger molecules present in the analyte, or get absorbed by the cuvette walls [10]. To compensate for these losses, the intensity of the light beam transmitted through a cuvette containing the analyte solution is compared to a baseline. The baseline is the intensity of the light beam transmitted through a cuvette containing a solvent [10]. A solvent is defined as the liquid in which the analyte ions are dissolved into, to produce the analyte solution, commonly described as a blank or reference sample [33]. Therefore, for Equations 2.4.1 and 2.4.2 , I_0 can be redefined as the intensity of the light beam that emerges from the cuvette containing the reference sample, and I can be redefined as the intensity of the light that emerges from the cuvette containing the analyte sample, as seen in Equation 2.4.3 [10].

$$A = \log_{10} \frac{I_{solvent}}{I_{solution}} = \log_{10} \frac{I_0}{I} \tag{2.4.3}$$

Each chemical or element has a natural tendency to absorb light at a specific portion of the electromagnetic spectrum more so than in other parts of the electromagnetic spectrum. The portion of the electromagnetic spectrum where the chemical or element has a strong tendency to absorb light is known as the peak absorbance. The wavelength of the most substantial peak absorbance is referred to as λ_{max}. Equation 2.4.3 is only applicable if the incident light exists at wavelengths approximate or identical to the λ_{max} of the analyte chemical

[10]. As mentioned in Section 2.3.3.2, nitrates have a peak absorbance at 205 nm, that is to say, the λ_{max} of nitrates is equal to 205 nm. Therefore, for nitrates, equation 2.4.3 is only held for wavelengths close to or at λ_{max}.

2.5 Beer-Lambert's law

Beer-Lambert's law is the most well-known law applied for UV and VIS quantitative analyses, as it holds for most substances within a wide range of experimental conditions [9].

As previously discussed, the interaction of light of suitable energy with an appropriate molecule causes some light to be absorbed [9]. It so happens that when there is a large number of molecules present in the pathway of the light beam, the probability of the interaction between the light beam and the molecules increases, consequently so does the probability of absorbance [9]. This phenomenon can be observed in everyday life [9]. Take a glass of a colourful drink for an example; if the drink is diluted with water, then the intensity of the colour of the drink will decrease [9]. This decrease in intensity is a consequence of the reduction in the number of molecules that can absorb appropriate light. Moreover, the chances of the incident light interacting with light-absorbing molecules have diminished [9]. Therefore, if a light of an appropriate wavelength is incident on a cuvette that holds an analyte solution, the absorbance of the light will be proportional to the concentration of the absorbing analyte molecules and the path length [9, 10]. The path length is the distance the light has to travel, which is essentially the distance between the walls of the cuvettes [9]. Equation 2.5.1 is called Beer-Lambert's equation, as it describes the relationship between the absorbance of incident light on a molecule to the concentration of the absorbing molecules and the path length [9].

$$A = \varepsilon C l \tag{2.5.1}$$

ε is referred to as the extinction coefficient or molar absorptivity [9]. Each different molecule has its own unique molar absorptivity for a certain wavelength and path length since light absorbance is also dependent on wavelength [9]. The units for both the path length, l, and the extinction coefficient, ε, can be described in various ways [9]. ε and l can be expressed in $\mathrm{dm}^3/(\mathrm{mol\,cm})$ and cm respectively, which is most widely used [9]. Alternatively, ε and l can be expressed as $\mathrm{dm}^3/(\mathrm{mol\,m})$ and m respectively [9]. While the concentration, C, is commonly measured in $\frac{mol}{L}$ or M, also referred to as molarity [9]. Usually, the path length is selected as 1 cm to make it less complicated to calculate the molar absorptivity or the extinction coefficient [9]. If the absorbance is plotted against the concentration, a linear relationship, as illustrated in Figure 2.7a, is observed. Similar to the absorbance equation (Equation 2.4.2), Beer-

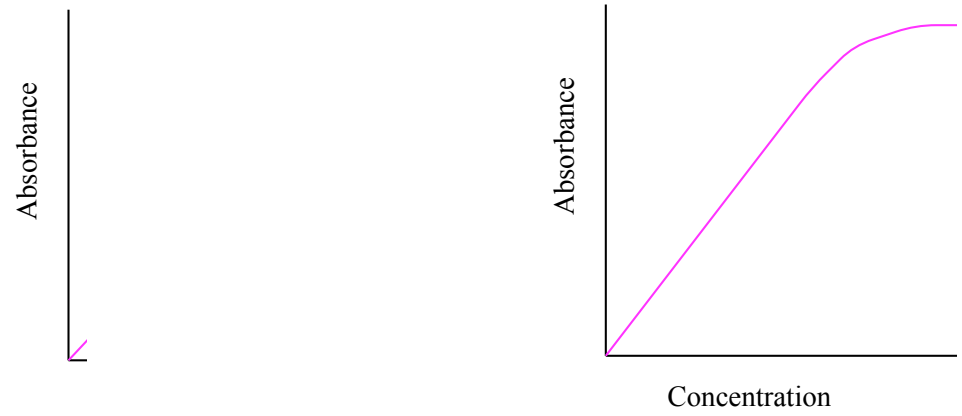

(a) Ideal
tion and ε

(b) Non-ideal relationship between concentration and absorbance.

Figure 2.7: Relationship between the concentration and absorbance of a sample - as per Beer-Lambert's law. (a) Beer-Lambert's law describes that the absorbance of an incident light through an analyte sample is linear to the concentration of the analyte. (b) However, particularly for higher analyte concentrations, the relationship between the concentration and the absorbance deviates from the linear region.

2.5.1 Beer-Lambert's law: limitations and deviations

Although it was discussed in the previous section that Beer Lambert's law states that the absorbance of a light emitted through an analyte sample is proportional to the concentration of the analyte, there are occasions where deviations occur, and the absorbance becomes disproportional [10, 11, 34]. There are various reasons why such deviations take place, and this section will discuss a few of them.

It is usually found that only smaller concentrations obey Beer-Lambert's law, while higher concentrations do not obey [10, 34]. At higher concentrations, the distance between the light-absorbing molecules is decreased to such an extent, that the charge distribution of the nearby molecules is disturbed [10]. As a result, the ability of the light-absorbing molecules to absorb the incident light can be changed, and non-linearities can be experienced between the concentration and the absorbance [10]. Refractive index is the ratio between the speed of light in a vacuum and the speed of light in a second medium of higher density. With highly concentrated analyte solutions, the refractive index can also be altered, and thus affect the capability of the analyte solu-

tions to absorb the incident light [10, 34, 35]. Additionally, the light-absorbing molecules of highly concentrated analytes can start to interact in a manner that modifies the absorbance characteristics of the analyte [10, 34]. Consequently, the absorbance will deviate from Beer-Lambert's law [10, 34]. Hence, the absorbance curve for an analyte solution will manifest a non-linear relationship, particularly at higher concentrations, as observed in Figure 2.7b [11].

At very low concentrations, the difference between the incident and the transmitted light is likely minimal, while the magnitude of the signals measured for both the incident and transmitted light is likey high [11]. Therefore, divergence from Beer Lambert's law may also happen at very low concentrations [11, 34].

Spectrophotometers may exhibit non-linear behaviour if there is a presence of stray-light or noise [34]. Additionally, the use of a light source that radiates multiple wavelengths (polychromatic source) can also produce undesirable results since Beer-Lambert's law is strictly obeyed for monochromatic sources, which are light sources that radiate at a single or very narrow band of wavelengths [10, 11, 34]. That is to say, Beer-Lambert's law is only applicable when the incident light exists at one wavelength, particularly a wavelength equal to or approximate to λ_{max} of the analyte of interest. Therefore, if a polychromatic light beam is an incident on an analyte, it is probable that the analyte will experience different molar absorptivities for each wavelength of the incident polychromatic light beam [10]. However, most spectrophotometers utilise polychromatic sources because spectrophotometers are used for a wide range of analysis, ranging from UV to visible analysis. For this reason, the majority of spectrophotometers use monochromators [10]. The use of monochromators ensure that incident light on the analyte solution has a wavelength identical or similar to λ_{max} of the analyte [10]. The monochromator selects between the available wavelengths of the polychromatic source and allows for a single or narrow band of wavelengths equivalent to λ_{max} of the analyte of interest to be an incident on the analyte solution [10]. In certain occasions, narrowband filters with a bandwidth that includes λ_{max} of the analyte of concern can be used [10]. Nevertheless, if during the analysis, the light is set to a wavelength that is not equivalent to λ_{max} of the analyte, then deviations can also exist [11, 34].

As previously mentioned in Section 2.3.3.2, spectrophotometry can experience interferences, if ions or organic substance are present in the analyte sample [10, 11]. Such ions and organic substance can cause the light to scatter in the cuvette. Alternatively, the ions or organic substance might have strong absorbances at λ_{max} of the analyte [10, 11]. Both of these situations can result in inaccuracies in the measurement of the absorbance.

2.5.2 Determining the concentration of an analyte

To measure the concentration of an analyte, first, it is necessary to know at which wavelength the analyte experiences its peak absorbance, i.e. the λ_{max} must be known [11]. There exist substantial literature that provides λ_{max} for chemicals that have been commonly studied. However, in cases where the chemical is not commonly studied, the peak absorbance can found by measuring and then plotting the absorbance of the chemical at various wavelength from UV light to VIS light [11]. Such a plot is commonly referred to as an absorption spectrum. As previously mentioned, the available literature advises that nitrates have a peak absorbance at approximately 205 nm, as seen in Figure 2.8 [12, 13, 36].

Secondly, the next step is to determine an absorbance, standard or calibration curve, by preparing a set of samples of varying concentrations, usually 3-5 samples containing different concentrations of the concerning analyte [11]. Additionally, a reference sample, that consists of the solvent of the analyte solution must also be prepared, as the absorbance of the reference will be calibrated to zero [11].

For standard spectrophotometers, the reference sample will be used to zero the device. In other words the measured intensity of the light transmitted through the reference sample is I_0 in Equation 2.4.3 (page 19) [11]. Once, the spectrophotometer has been zeroed with the reference sample, for each analyte sample, I in Equation 2.4.3 (page 19) can also be determined by measuring the intensity of the light transmitted through the analyte sample [11]. Then the absorbance of the samples can be solved by using Equation 2.4.3 (page 19) [11]. Following that, the absorbance of each sample can be plotted against the respective concentration, to produce the calibration curve or absorbance curve

Ideally, the absorbance or calibration curve should be linear, as observed in Figure 2.7a; therefore, a linear fit can be obtained. The linear fit should have an equation described in the same format as Equation 2.5.1 (page 20) [11].

Thereafter, the transmittance and absorbance of an unknown sample can be measured, using the derived equation. This is achieved by measuring the absorbance of the unknown sample, remembering to zero the spectrophotometer with a reference sample and by substituting the measured absorbance in the derived equation [11].

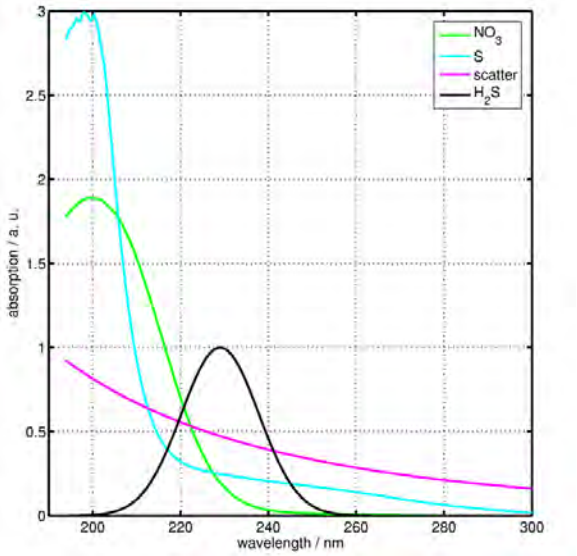

Figure 2.8: Absorbance spectrum of nitrates and other chemicals. Nitrates have a peak absorbance at 205 nm. Retrieved from https://www.cefns.nau.edu [36]

/

2.6 Types of spectrophotometers

This section discusses and compares the available types of spectrophotometer arrangements, namely single-beam and double-beam.

2.6.1 Single-beam

Single-beam spectrophotometers consist of a single light beam that is responsible for passing the radiation to the cuvette, as shown in Figure 2.5 (page 16) [9]. For this setup, one sensor is used to measure the intensity of the light that emerges from the cuvette [9]. As previously mentioned in Section 2.4, the light intensity may be reduced if the light is an incident on a cuvette containing an analyte solution [9]. Additionally, background disturbances may also arise, all of which can lead to inaccurate measurements of the absorbance [9]. For this reason, a reference sample is used to balance out the losses and potential background disturbances. For a single-beam spectrophotometer, the intensity of the light transmitted through the reference sample must be measured separately from the analyte sample, since there is only one light beam and one detector [9].

2.6.2 Double-beam

A double-beam spectrophotometer consists of two single beam setups, as seen in 2.9, that work simultaneously. Thus allowing for the immediate compensation of intensity losses and background interferences [9]. The one single beam setup is responsible for measuring the intensity of the light emerging from reference sample [9]. Meanwhile, the other single beam setup measures the

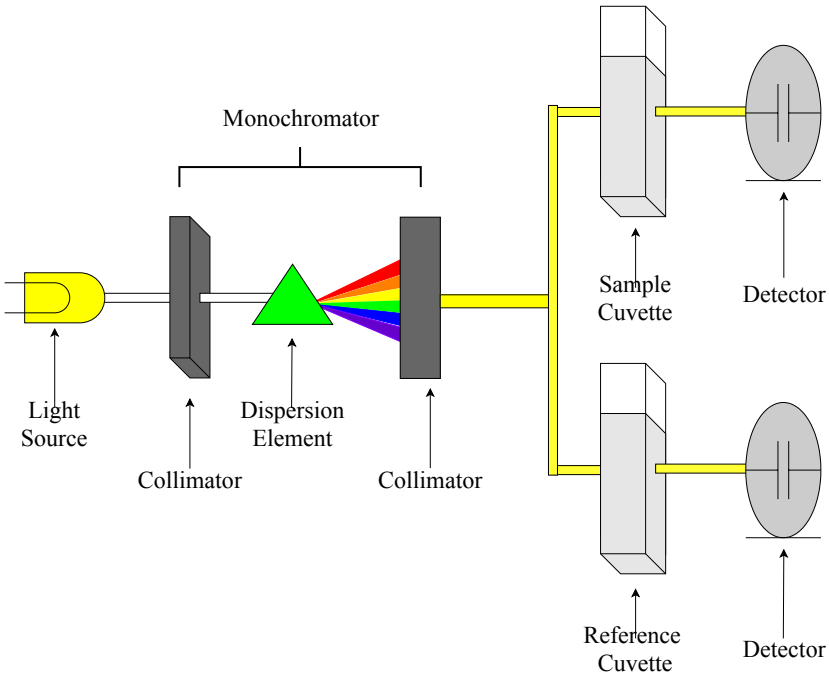

Figure 2.9: Arrangement of a double-beam spectrophotometer. The double beam spectrophotometer consists of a light source, a monochromator, optics that separates the light emitted by the source into two sperate beams, two cuvettes - one contains the reference sample, and the other contains the analyte sample - and two detectors. This setup allows for the measuring of the transmitted light through the reference sample and analytical sample simultaneously.

Nonetheless, three factors must be kept constant to provide accurate results [9]. Firstly, the intensity of both light beams must be identical [9]. Additionally, both detectors must be equally sensitive to radiation [9]. Finally, both cuvettes must be of the same brand and make, and must have the same absorbance characteristics [9].

2.6.3 Comparison of single-beam and double-beam setups

The single-beam setup is less convenient to use than the double-beam setup since the intensity of the light transmitted through the reference and analyte sample must be measured separately. Although the double beam setup eliminates this issue, it does require more components, which means that a double-beam setup is less likely to be compact and portable. Additionally, double-beam setups require that the duplicate components exhibit identical behaviour. Another disadvantage of double-beam spectrophotometers is that the cost to implement them can be high since it requires double the amount of components a single-beam spectrophotometer requires. Therefore, it can be deduced that the most suitable option for this application is to implement a single-beam setup.

2.7 Light Sources

For UV-VIS spectroscopy, it is essential to use a light source that outputs a constant light that is intense enough to allow the detector to detect the transmitted light, within an absorbance value between 0 - 2 [9]. Two types of light sources are commonly used for UV-VIS spectroscopy; tungsten filament lamps and deuterium lamps [9]. Therefore, this chapter aims to obtain Objective 1b by comparing the available types of sources, including tungsten filament lamps, deuterium lamps as well as UV LEDs.

2.7.1 Tungsten lamps

Tungsten lamps are mainly able to radiate visible light, specifically within the interval of 320 - 2500 nm, as observed in Figure 2.10 [9]. Nonetheless, most spectrophotometers implement the use of a tungsten filament lamp [9]. The light intensity of the tungsten filament lamps is drastically low at the lower and upper limits of the shown spectrum, which suggests that they are less suitable for UV spectrophotometry. Tungsten filament lamps operate at a temperature range of approximately 2900 K - 3000 K [9]. As a result of tungsten sublimation, the lifespan of tungsten lamps is not very long [9]. Nonetheless, tungsten filaments are relatively inexpensive [37].

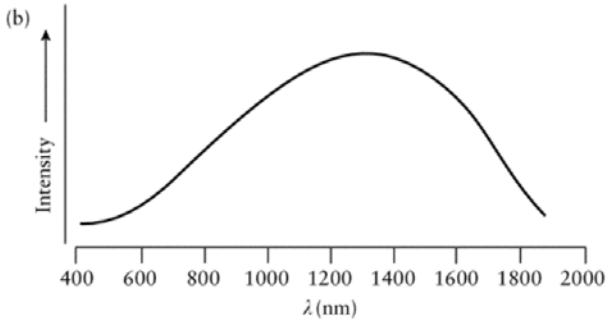

Figure 2.10: Light emission spectrum of conventional tungsten light sources. Tungsten light sources have an emission spectrum that ranges from 400 to 1800 nm.

2.7.2 Deuterium lamps

In most spectrophotometers, tungsten lamps are implemented to emit visible radiation, while deuterium lamps, also known as hydrogen lamps, are used simultaneously with tungsten filament lamps to produce a high-intensity light beam [9]. Hydrogen or deuterium lamps can emit a constant spectrum of UV light at low pressures, usually over a wavelength of 160 - 375 nm [9]. Although their lifespans and prices vary, they perform for longer periods and are more expensive in comparison to tungsten lamps. However, traditional deuterium lamps are not compact and require a power supply, all of which can contribute to the portability, size and weight of a spectrophotometer.

Nonetheless, improvements have been observed with deuterium light sources to make them more transportable and miniature [41]. Heraeus has developed three miniature deuterium light modules, part of the FiberLight D_2 series [41]. The FiberLight D_2 has a wide emission range of 185 to 1000 nm, making it suitable for mobile-based UV-VIS spectroscopy or other handheld instruments [41]. The FiberLight D_2 modules consist of a deuterium lamp, a tungsten lamp, a shutter for the beam opening, and an integrated power supply [41]. The three types of FiberLight D_2 include the Basic, the Compact and the HIghPower, where the Basic and Compact consume 6 W while the HighPower consumes 12 W [41]. The FiberLight D_2 Basic, Compact and HighPower weigh 130 g, 104 g and 230 g respectively [41]. The greatest disadvantage with the FiberLight D_2 light modules is that they are still quite expensive.

2.7.3 UV LEDs

In the past decade, there have been many advances in other UV emitting sources, such as the development of UV LEDs. Sensor Electronic Technology Inc has developed UV LEDs, that can emit light within a range of 240 - 280 nm[38]. These LEDs were designed for sensors, spectroscopy and other

chemical and biological analysis [38]. Besides creating through-hole UV LEDs, with peak wavelengths at 250 - 280 nm, Crystal IS, Inc also created surface-mount UV LEDs, with peak wavelengths as low as 235 nm and as high as 275 nm [39]. Both UV LEDs are referred to as Optan LEDs, can be used for water quality monitoring, oil-in-water monitoring, and other monitoring applications [39]. In addition to designing the FiberLight D_2, Heraeus has also developed the first broadband UV LED, called the FiberLight L_3, that has an emission spectrum of 250 - 490 nm [40]. The FiberLight L_3 is a UV LED module, integrated with a power supply, that consumes less than 1.5 W, making it suitable to be battery operated and implemented in handheld instruments [40]. As it was specifically designed for portable and compact UV spectroscopy applications, it only weighs 110 grams [40].

2.7.4 Comparison of lamps

Even though deuterium lamps are more expensive than tungsten lamps and UV LEDs, they do have one key advantage that makes them suitable for this application. This application aims to detect nitrates and nitrates strongly absorb UV light at 205 nm. Therefore, the wavelength of interest is within the UV range, a range that only deuterium lamps can supply. For this reason, deuterium light sources are the most appropriate for this design. However, instead of choosing a traditional deuterium lamp, the FiberLight D_2 series were chosen since they are less expensive and smaller. Out of the FiberLight D_2 series, the Compact FiberLight D_2 was the most fit light source considering that it is the lightest type of FiberLight D_2.

2.8 UV - visible cuvettes

To hold the analyte sample, an optically transparent cuvette or cell is used [9]. Cuvettes can come in different internal cross-sectional areas, which determines the optical path length [9]. Standard cuvettes have a 1 cm optical path length, with a 1×1 cm internal cross-sectional area [9]. Cuvettes usually have two optically transparent sides, that are opposite to one another, and two optically translucent sides, that are also opposite to one another [9]. The bottom side is also made of optically translucent and there is no top side, however, a lid can be placed on the top to seal the cuvette (an image of cuvettes can be found in Figure 3.1). Since the incident light beam can only pass through the optically transparent sides, these optically transparent sides must remain clean, and free from fingerprints, grease and other things, as it could impact the transmission of the incident light through the cuvette [9]. Therefore, during analysis, the optically transparent sides should be aligned with the light source and detector. Additionally, when handling a cuvette, only the optically translucent sides should be touched [9]. There are three are types of materials that cuvettes

can be made of; optically transparent plastic, optically transparent glass and fused silica or quartz [9]. All three cuvettes will be discussed and analysed in this section.

2.8.0.1 Optically transparent plastic cuvette

Optically transparent plastic cuvettes are most fitting for analysis in the visible spectrum as they are transparent within the range of approximately $480 - 900\,\text{nm}$, varying from one brand to another [9]. Outside of this range, a considerable amount of radiation is absorbed by these cuvettes, making it less fit for ranges outside of the 480 - 900 nm interval [9]. The most notable advantage of plastic cuvettes is that they are the most affordable type of cuvette, with a price fluctuating around R4.00 each [9, 42]. However, it is also the most susceptible to scratches in comparison to the other types of cuvettes, and once scratched, in general, a cuvette is no longer usable [9].

2.8.0.2 Optically transparent glass cuvette

Although optically transparent glass cuvettes are also more suitable for the visible spectrum, it does have a wider optically transparent wavelength range than plastic, of approximately $320 - 900\,\text{nm}$ [9, 42]. However, beyond the range of $320 - 900\,\text{nm}$, glass cuvettes absorb a considerate amount of light, which suggests that glass cuvettes are not adequate for analysis where the wavelength of incident light falls outside of the specified range [9]. Optically transparent glass cuvettes are also more durable than plastic cuvettes since they are less susceptible to scratches [9]. Nonetheless, glass cuvettes can be more expensive than plastic too, as their price can range from R500.00 - R1 600.00, depending on their optical transparency [9, 42].

2.8.0.3 Fused silica or quartz cuvettes

Fused silica cuvettes, commonly known as quartz cuvettes, are capable of being optically transparent within the wavelength range of approximately 190 - 750 nm, depending on the manufacturer, making them most suited for analysis in both the UV and visible spectrum [9]. Similar to glass, quartz is resistant to scratches and more durable [9]. However, the most noticeable drawback of quartz cuvettes is that they are usually more expensive than plastic cuvettes since the price for a quartz cuvette can vary from R1 000.00 to R4 500.00 [9, 42].

2.8.0.4 Comparison of cuvettes

According to current literature, quartz cuvettes are the most reliable option for this application, as it is the only type of cuvette that is reported to be optically transparent to incident light that is emitted at a wavelength of 205

nm - which is the wavelength of concern for this project. Although the literature suggested that at a wavelength of 205 nm, plastic and glass cuvettes will absorb significant quantities of the light, it is unclear what the extent of their absorbance is at 205 nm. Therefore, further evaluations needed to be performed to verify whether plastic or glass cuvettes could be implemented in this application.

2.9 The emergence of smartphone-based technologies

Cellphones have rapidly evolved from simple devices used for communication to devices capable of photography, gaming and conducting sensing and diagnostic measurements and tests [5]. Initially a rare and exclusive device, mobile phones are now used by almost five billion people in the world, ranging from young children to geriatrics, as illustrated in Figure 2.11a [43], including over seven billion mobile phones distributed amongst them [5, 44]. Cellphones are not limited to first-world or developed countries, as seen in Figure 2.11b [5], and they are present and utilised by people in most countries of the world. This is because phones have become dominant, reliable and cost-effective, concerning their software and hardware [5]. Although the minority of these phones are smartphones, there is a steady increase in the number of people who purchase smartphones, especially in African countries [5]. With the emergence of the secondhand market, smartphones have now become more accessible to people who would not be able to afford a full-priced smartphone [5]. Additionally, companies, such as Huawei are manufacturing smartphones that are considered to be entry-level or low-end and are priced below R1 500, which has aided in the ubiquity of smartphones in the recent years [6, 45]. This ubiquitous utilisation of smartphones can be especially observed in the Sub-Saharan countries, reported to be the fastest-growing cellphone region in the world [7]. In 2018, the number of new smartphones sold in South Africa increased by 7%, in comparison, the worldwide sales only grew by 1% [6]. Moreover, almost one-third of South Africa's population has a smartphone, while approximately one-third of the phone users in the Sub-Sahara area are using smartphones [6, 7].

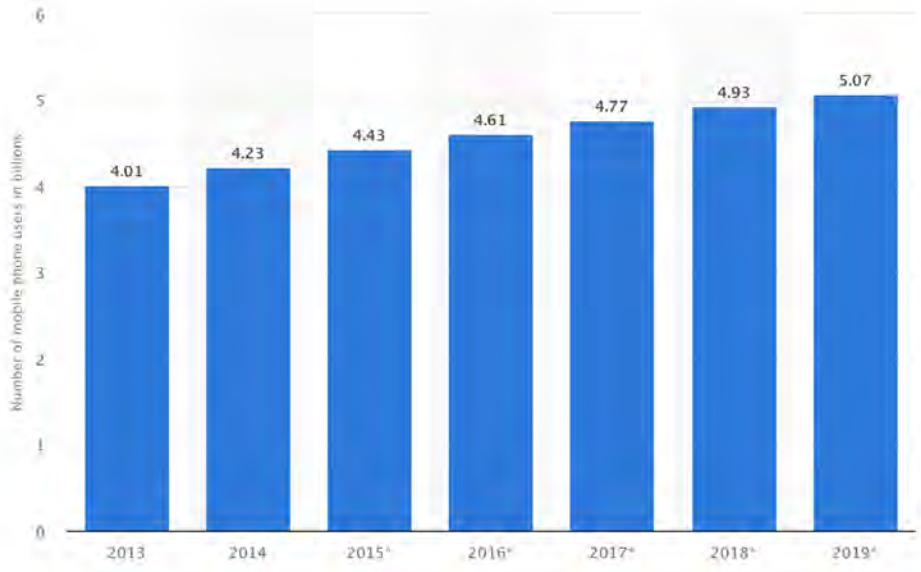

(a) Number of mobile phone users worldwide.

(b) Distribution of mobile users worldwide

Figure 2.11: Worldwide Mobile Phone Users - Retrieved from Ozcan [5]. (a) The number of mobile phone users has steadily increased in the past few years. (b) Mobile phone subscriptions are widely used throughout most of the world

This large scale use of cellphones stimulates the development of improved software and hardware [5]. Improvement in the components and technologies related to mobile phones have allowed for the vast and specialised abilities of today's phones [5]. With the improvement of embedded imaging and sensing technologies, phones are now capable of performing tests and measurements that are usually only achieved by specialised instruments, at a lower cost [5].

2.10 Ultraviolet conversion

Although studies show that (some) CMOS sensors can to some extent detect UV light as low as 200 nm, smartphone CMOS sensors are optimized for visible light detection, and there is an uncertainty of their capabilities and the extent to which they can detect UV light [14, 15]. Consequently, it was necessary to overcome this obstacle by using a component that is able to convert UV light into visible light. Therefore this section will achieve Objective 1d, by discussing the available options that are used to transform UV light into visible light.

2.10.1 Fluorescent materials

UV light can be categorised into three different sections, long-wave, medium-wave and short-wave, also referred to as UVA, UVB, UVC respectively [46, 47]. Each section represents a different wavelength range; long-wave being 315 - 400 nm, medium-wave being 280 - 315 nm and short-wave being 180 - 280 nm [46, 47].

There are many natural and synthesised materials that when induced by UV light, reflect visible light [46]. This phenomenon is commonly known as ultraviolet-induced visible fluorescence [46, 47]. UV induced visible fluorescent materials can fluoresce a wide range of visible light; moreover, they can reflect any colour [46]. However, the wavelength of the emitted UV light, as well as the type of material used, will determine the colour fluoresced [46, 47].

Many materials have been recorded as being UV-induced visible fluorescent. Grant discussed the fluorescence capabilities of the museum objects, mainly arts and artefacts [48]. It was reported that oil paintings with varnish finishes produce visible fluorescence when induced by long-wave UV, ranging from 315 - 400 nm[48]. Likewise, some adhesives, found on repaired ceramics, also experience long-wave UV induced visible fluorescence [48]. While short UV, ranging from 200 - 280 nm can result in the fluorescence of porcelain [48]. Other fluorescent materials or objects included; lead and uranium glass, ivory, bone, modern papers and threads, wood with patina, other coatings and waxes, as well as many gems and minerals [46, 48].

Phosphors and scintillators are other examples of materials that are visibly fluorescent when induced by UV light; they are materials that are activated or doped with ions that contain fluorescent capabilities in the visible region of the electromagnetic spectrum [49]. In the past decades, many have been synthesized. However, one of the most efficient scintillators is europium ion (Eu_2+) doped scintillators, since they fluoresce distinct colours and can be induced by short-wave UV [49].

Sumita Optical Glass, Inc developed a series of europium ion doped scintillators known as Lumilass (fluorescent glass). These fluorescence glasses have been used in a few applications with UV light, as they convert UV light into visible light with a high efficiency [49, 50, 51, 52].

2.10.2 Lumilass - Fluorescent Glass

According to SumitaOptical Glass, the Lumilass is suitable for visible light detection, since it has high sensitivity characteristics [52]. Additionally, it is water resistant, more durable than other fluorescent materials, scintillators and phosphors, and its performance does not deteriorate after long-hours exposure to UV light [50, 52].

There are three types of Lumilass: the Lumilass-G9 (green fluorescent glass), the Lumilass-R7 (red fluorescent glass), and the Lumilass-B (blue fluorescent glass), each with a different peak emission wavelength [52]. Although all Lumilass can efficiently convert a dim UV light of 200 - 400 nm into visible light, each Lumilass is most suitable for a specific region of the UV spectrum [52]. Since nitrates absorb UV light at 205 nm, the goal was to use the Lumilass that could most efficiently convert 205 nm into visible light.

The fluorescent and excitation spectrums of each Lumilass can be observed in Figure 2.12. The fluorescent spectrum specifies the emission of the light fluoresced by the Lumilass, i.e. the plot shows how much light is fluoresced by the Lumilass at the given wavelengths [53]. The peak emission wavelength of the Lumilass-G9, Lumilass-R7 and Lumilass-B can be observed in their fluorescent spectrum shown in Figures 2.12a, 2.12c and 2.12e respectively [53]. By observing these figures, it is apparent that the peak emission wavelength of the Lumilass-G9, Lumilass-R7 and Lumilass-B is at approximately 540 nm, 610 nm and 405 nm, respectively.

The excitation spectrum is a plot of the intensity of the light fluoresced by the Lumilass at its peak emission as a result of the induced light at consecutive wavelengths [53]. More simply, the plot shows how much light is fluoresced by the Lumilass, at the peak emission wavelength, when a light of a particular wavelength is induced onto the Lumilass [53]. By observing the excitation spectrums shown in Figures 2.12b, 2.12d and 2.12f, It can be seen how much light is fluoresced by each Lumilass when it is induced by a light of a wavelength of 205 nm. It appears that the Lumilass-G9 fluoresces the most light out of all the Lumilass when a light of a wavelength of 205 nm induces onto it. Therefore, the Lumilass-G9 seems to be the most suitable for this application.

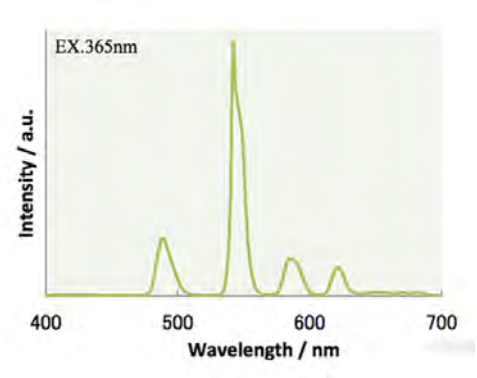

(a) Lumilass-G9 fluorescent spectrum

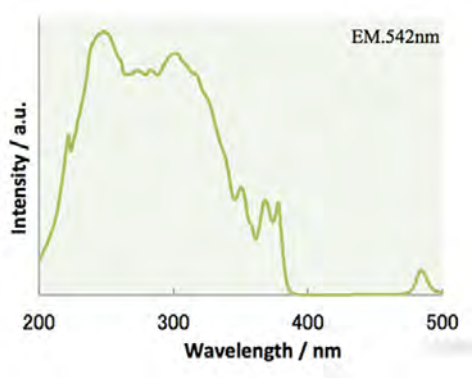

(b) Lumilass-G9 excitation spectrum.

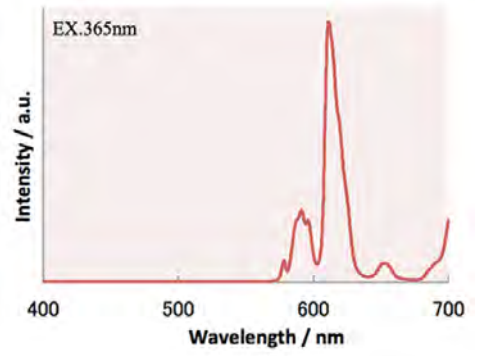

(c) Lumilass-R7 fluorescent spectrum

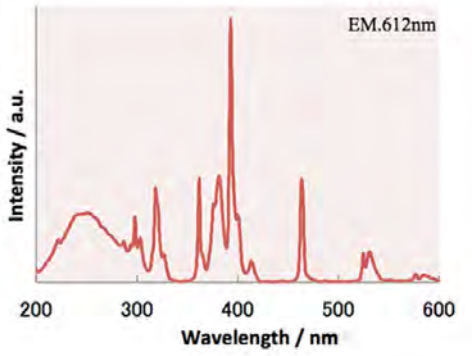

(d) Lumilass-R7 excitation spectrum.

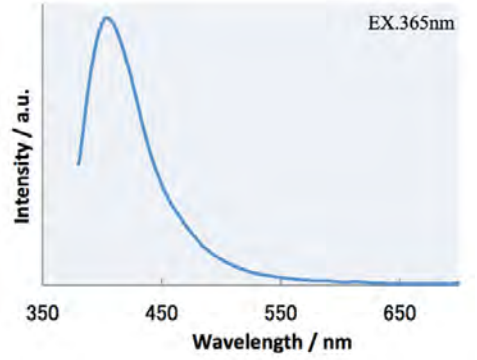

(e) Lumilass-B fluorescent spectrum

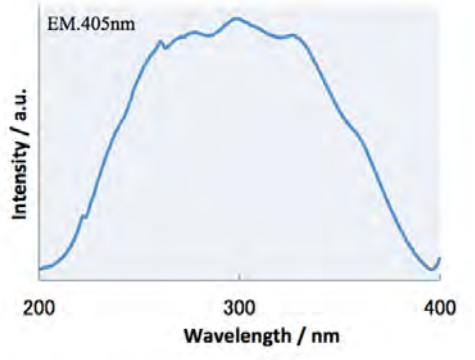

(f) Lumilass-B excitation spectrum.

Figure 2.12: Spectrums of Lumilass-R7, G9 and B - Retrieved from https://www.sumita-opt.co.jp [52]. (a) The Lumilass-G9 readily fluoresces most its light at 540 nm and some light at approximately 490, 590, 610 nm. (b) The Lumilass-G9 predominately fluoresces light when it is induced by light of a wavelength of around 200 - 400 nm and 490 nm. (c) The Lumilass-R7 easily fluoresces most of its light at 610 nm and some light roughly at 590, 650 and 700 nm. (d) The Lumilass-R7 fluoresces light when it is mainly induced by light at a wavelength of approximately 200 - 310 nm, 350 - 410 nm, 460 nm and 540 nm. (e) The Lumilass-B fluoresces light at 405 nm. (f) The Lumilass-B fluoresces light when it is induced by light of a wavelength between 200 to 400 nm.

Shrivastava tested the linearity of Lumilass-G9 and concluded that the intensity of the fluorsced light is directly proportional to the intensity of the UV light emitted on to it [50]. Shrivastava further investigated the behaviour of the Lumilass emissions, and reported that for each point of incident UV light, fluorescent light is emitted in all directions, as observed in Figure 2.13 [50]. Therefore when UV light strikes the Lumilass, the visible fluorescence can be observed from all angles and sides of the Lumilass glass [50].

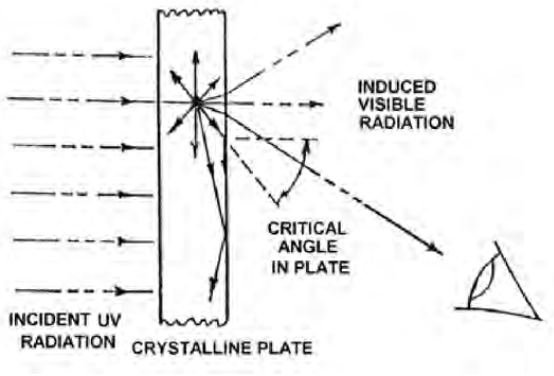

Figure 2.13: Fluorescence of the Lumilass - Retrieved from Shrivastava [50]. When a UV light is an incident on a specific point within the Lumilass, the fluorescence is induced at that point. The fluorescence light diffuses in all directions from that point.

2.11 Related works

In the past decade, many cellphone-based analytical platforms have been increasingly developed and used for analytical sciences for various analysis [54]. Therefore, this section will present and discuss some literature relative to this application. The common subject of the matter is smartphone-based detectors or sensor that are either based on spectrophotometer, colourimetry or electrochemistry. The related literature documents the monitoring of chemicals, such as nitrates, fluoride, sulphur dioxide, apple and other substance.

A smartphone-based device for the detection of fluoride in water samples was implemented by S. Levin et al. [55]. In this paper, the authors developed an affordable, compact and portable field colourimetric analyser, which made use of the smartphone camera as the detector of the coloured solution. Moreover, the authors created a software program that records and analyses the RGB colour of the solution in the picture. The designed smartphone-based meter was able to detect fluoride within in the range of $0 - 2\,\text{ppm}$ of fluoride on field. Overall, it was concluded that the results were on par with the results produced by other more expensive equipment.

Similarly, I. Hussain et al. also developed a low-cost, robust, field-portable smartphone-based photometric sensor for fluoride level detection in drinking water [56]. They used the smartphone ambient light sensor (ALS) as a light detector, and the smartphone LED flashlight as the light source. A smartphone application was designed to analyse the fluoride concentration and was also responsible for sharing the data from any remote location to a central water quality monitoring station. Ultimately, the instrument could reliably detect fluoride in water with a resolution of 1.23×10^{-4}ppm, and the performance corresponded to the performance of commercial instruments.

M. Hossain et al. presented an optical fibre smartphone spectrometer, aimed to be used for various applications - mainly the analysis of agricultural produce [31]. The designed smartphone spectrometer included an endoscopic fibre bundle which allowed for the smartphone camera LED flashlight to be emitted onto the sample, thus eliminating the complications from varying background light and the need for additional components. By using the camera's CMOS sensor and a diffraction grating, the spectrum of the light reflected from the sample was captured. The designed system achieved a minimum spectral resolution of 2.00 nm over a bandwidth of approximately 250 nm. The instrument was tested by measuring the change in the spectra of an apple sample, as its storage time increased [31]. Thereafter, the authors concluded that the results produced were as expected.

Likewise, H. Ding et al. reported a visible smartphone spectrometer with high spectral accuracy for mHealth [30]. The purpose of this application was to increase the precision of the response of CMOS sensors used in smartphone spectrophotometry, through the development of a wavelength calibration and spectral intensity correction method. Subsequently, the designed smartphone spectrometer, integrated with intensity correction, was tested against a standard spectrometer and a smartphone spectrometer that did not have intensity correction. It was detailed that the smartphone spectrometer without intensity correction deviated from the standard spectrophotometer's results, while the smartphone spectrometer with intensity correction produced similar results to the standard spectrophotometer. Nonetheless, the designed tool was able to measure creatinine with a detection limit of 50 μmol/L.

T. Wilkes et al. also developed a low-cost smartphone-based spectrometer, that was designed for UV spectroscopy of sulphur dioxide at 310 nm [15]. This device did not use any optics other than a diffraction grating and, unlike the authors, H. Ding et al. and M. Hossain et al. However, T. Wilkes et al. did not make use of the smartphone camera, but instead, they made use of a modified Raspberry Pi camera module to detect the sulphur dioxide, and ultimately the instrument had a detection resolution of 1 nm. Moreover, the device generally produced similar results to the available pricey equipment [15]. Additionally, T.Wilkes et al. reported that the device had cost approximately \$500 to implement, where the common spectrophotometers can cost around \$10 000.

X. Wang et al. developed an audio jack-based miniaturised mobile phone electrochemical sensing platform [20]. This platform was a low-cost and compact and performed electrochemical measurements of nitrate through the use of an audio jack in the smartphone. Samples were collected in a few microlitres on field, and the geospatial locations were provided through a wireless network. The same researchers managed to design a mobile phone electrochemical sensing platform that was able to detect nitrate concentration in water with a detection limit of 0.2 ppm within 1 minute. Furthermore, the platform performed comparably to other available measuring methods.

Although Wang et al. already designed a low-cost and portable smartphone-based detector for nitrates, it implemented the principles electrochemistry and made use of the audio jack of the phone. Even though all the other authors successfully developed smartphone-based detectors, they are not specific to nitrates. There is still a need for a low-cost and portable detector, that can accommodate all smartphones, and detect nitrates in particular. It should be noted that Hossain et al., Ding et al. and Wilkes et al. all developed mobile-based spectrophotometers that did not cater to short-wave UV light analysis, i.e. UVC light. While Hossain et al. and Ding et al. only focused on visible spectroscopy, Wilkes et al. managed to develop a system cable of detecting as low as 310 nm. However, Wilkes et al. made use of an external camera, which was modified to be able to capture light as low as 310 nm. Hence, there is a gap in the literature for a smartphone-based spectrophotometer that can work within the UVC range, while making use of the embedded mobile's camera.

2.12 Summary

Indeed, high nitrate concentrations found in water can have severe implications for the aquatic ecosystem and humans. The conventionally used methods of detection of nitrates are chromatography, electrochemistry, and spectrophotometry - which is sub categorised into UV spectroscopy and colourimetry. Upon comparison, the spectrophotometric method, particularly UV spectroscopy, was deemed the most suited for the analysis of nitrates samples for this project. Spectrophotometry consists of a light source, a detector, and other optics, to quantify the absorbance of light through a sample. The elaboration of Beer-Lambert's law aided with the understatement of its application in the spectrophotometric analysis. Beer-Lambert's law states that the absorbance of light through a sample is linear to the concentration of the sample; however, under certain circumstances, this law is not held, particularly for higher concentrations. The analysis of different arrangements, lead to the deduction that a single beam spectrophotometric setup was most appropriate to implement a smartphone-based nitrate sensor. Additionally, traditional and alternative light sources for this application were investigated, but the FiberLight D_2 was chosen since it is compact and emits light at 205 nm. The three types of

cuvette used in spectrophotometry are quartz, plastic, and glass. Although it was not concluded which one was to be used for this project, plastic and glass cuvettes appeared to be the least adequate cuvettes to hold the nitrate samples. After a study on the ubiquitous utilisation of smartphones, research was done on the available materials that possess properties that allow them to shift UV light into visible light. The green fluorescence Lumilass glass was considered as the fittest option to perform the conversion of the UV light into visible light, precisely, green light. The discussion of the related works allowed for the discovery of a gap in the current literature, mainly for the development of a smartphone-based sensor that uses UV spectroscopy to detect nitrates in water.

Chapter 3

METHODOLOGY

Firstly, this chapter consists of the documentation of experiments that were performed to confirm the fitness of the three available cuvettes, the absorbance spectrum of nitrates, and the suitability of the chosen scintillator. Thereafter, this chapter describes the method and setup, and the algorithm used in the design of the smartphone-based nitrate sensor. Lastly, this chapter provides the metrics of the smartphone-based nitrate sensor.

3.1 Preparation of known nitrate samples

In the following section, the method used to prepare the nitrate samples is outlined. These nitrate samples were used throughout the process of testing the three types of cuvettes and the prototype of the smartphone-based nitrate sensor.

The aim was to prepare a highly concentrated nitrate solution, precisely a 1 000 ppm NO_3 solution, and from the 1 000 ppm sample, other samples could be prepared by diluting the 1 000 ppm NO_3 solution accordingly.

All samples were mixed by hand and prepared using pipettes and beakers of various volumes. The 1000 ppm sample was prepared by mixing 1.3703 g of sodium nitrate ($NaNO_3$) into a beaker of a volume of 1 L with enough distilled water to form a 1000 ppm nitrate solution. Then, the 1000 ppm nitrate solution was diluted to form a 100 ppm solution and further diluted to form a 10 ppm and a 5 ppm solution. To prepare the 100 ppm sample, 10 mL of the 1000 ppm sample was collected using a 10 mL pipette and added to a 100 mL beaker with enough distilled water to fill the beaker. The 10 ppm sample was prepared by collecting 10 mL of the 100 ppm sample using a 10 mL pipette and adding it to a 100 mL beaker with enough distilled water to fill the beaker. Similarly, the 5 ppm sample was prepared by collecting 5 mL of the 100 ppm sample using a 5 mL pipette and adding it to a 100 mL beaker with enough distilled water to fill the beaker. By diluting the 10 ppm solution appropriately, the 1, 2, 3, 4, 6, 7, 8 and 9 ppm samples were made. The reference or blank sample was

prepared by using distilled water.

3.2 Preliminary evaluation of cuvettes

The first step of designing the smartphone-based nitrate sensor was to determine which cuvette was best suited for this application. For a cuvette to be deemed suitable for this application, it had to be transparent to UV light at 205 nm and not interfere with the absorbance of the UV light by the nitrates. Since the UV light had to first travel through the cuvette, it was essential that as much light as possible was transmitted through the cuvette, so that the nitrates could interact with the UV light, and thus produce significantly measurable and accurate results. As previously mentioned, in spectrophotometry, there are three types of cuvettes used to analyse the concentrations of a solution: plastic, glass and quartz cuvettes - shown in Figure 3.1. Although the literature study suggested that glass and plastic cuvettes were not suitable for this application, it was necessary to verify the suitability of each cuvette, especially since both glass and especially plastic are less expensive than quartz. Hence, it is more likely that one would be able to perform more tests with the smartphone-based nitrate sensor on the field with plastic or glass cuvettes than with quartz cuvettes, as one could easily dispose of them, while with quartz cuvettes one would have to clean them to reuse them. Therefore, two sets of experiments were done to test all three of these cuvettes.

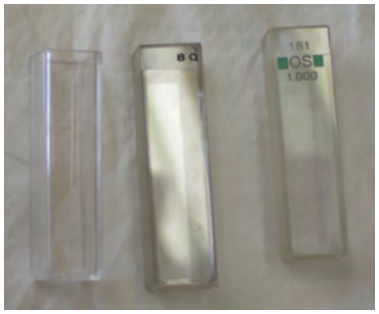

Figure 3.1: Plastic, glass and quartz cuvettes - displayed from left to right

For the first set of the experiments, all three cuvettes were tested individually and kept empty, i.e. each cuvette contained no solution in them. The test consisted of measuring the transmittance and absorbance of each cuvette across the electromagnetic spectrum, using a laboratory spectrophotometer (seen in Appendix D, Figure D.1). The spectrophotometer used was the UV Vis Spectrophotometer (AE-S60), manufactured by A & E Lab, and it could measure both the transmittance and absorbance of any sample. The light emission of the spectrophotometer was set to a wavelength ranging from 195 to 1000 nm, and the absorption spectra of each cuvette were recorded. This

allowed for the absorbance responses to the different parts of the spectrum, of each cuvette, to be observed. Since the λ_{max} of nitrates is at 205 nm, the adequacy of each cuvette was compared at 205 nm.

Figure 3.2 shows that at 205 nm, both glass and plastic cuvettes have a transmittance of less than 10% and an absorbance more significant than 1 unit. Therefore, less than 10% of the light that was incident to the blank cuvette was transmitted. Moreover, the glass and plastic cuvettes absorbed most of the incident light. On the contrary, the quartz cuvette had a transmittance of approximately 90% and an absorbance close to 0 units at 205 nm. Thus, 90% of the light that was incident on the quartz cuvette was transmitted through the cuvette; in other words, very little of the light was absorbed by the quartz cuvette.

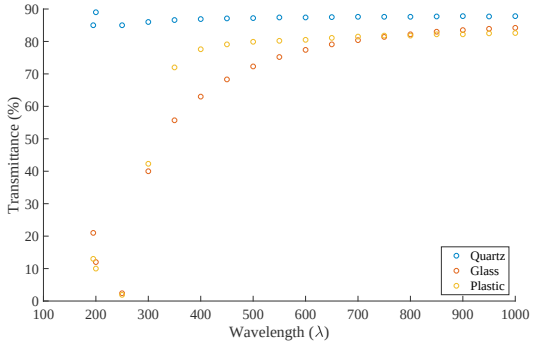

(a) Transmittance of quartz, glass and plastic cuvettes.

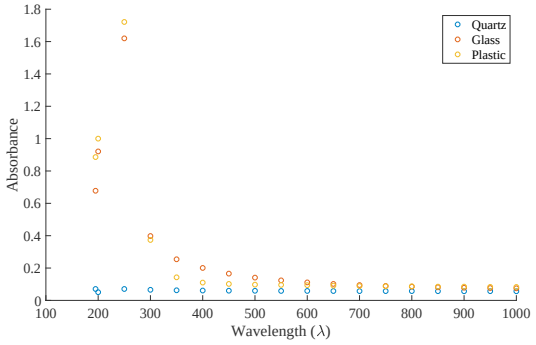

(b) Absorbance of quartz, glass and plastic cuvettes.

Figure 3.2: Transmittance and Absorbance of the quartz, glass and plastic cuvettes. (a) The glass and plastic cuvettes readily allow light to be transmitted at wavelengths beyond 300 nm. The quartz cuvette maintains a stable tendency to allow for the transmittance of all wavelengths. At 205 nm, the glass and plastic cuvettes had a low transmittance, while quartz cuvette has a higher transmittance. (b) The glass and plastic cuvettes readily absorb light at wavelengths below 300 nm. The quartz cuvette maintains a stable absorbance throughout all wavelengths. At 205 nm, the glass and plastic cuvettes had a high absorbance, while quartz cuvette has a lower absorbance.

The results confirmed that, as suggested by the literature study, the quartz cuvette was more suited than the glass and plastic cuvette for the smartphone-based nitrate sensor, as it was the most transparent cuvette and absorbed the least amount of UV light at 205 nm. Therefore, it was probable that smartphone-based nitrate sensor would be more sensitive with the use of the quartz cuvette than with the use of the plastic or glass cuvettes. Even though the plastic and quartz cuvettes would yield less sensitivity, it was still possible that they could display enough sensitivity to allow for the detection of nitrates. Furthermore, the decrease in sensitivity would not outweigh the benefits of plastic and glass, such as being affordable and disposable. On that account, another set of experiments were conducted to investigate the suitability of each cuvette further.

The purpose of the second set of experiments was to identify whether each cuvette, particularly glass and plastic, could conform to Beer Lambert's law and whether it would have been possible to compensate for the UV light absorbed by the plastic and glass cuvettes. For this set of experiments, the cuvettes were filled with a nitrate sample of a specific concentration, that was varied between 0 to 10 ppm.

Firstly, it was essential to prepare the nitrate samples of different concentrations, as specified in Section 3.1. Similar to the first set of experiments, these experiments were performed by using the laboratory spectrophotometer. On this occasion, the light emission was set at 205 nm and kept constant throughout the experiments. Thereafter, the absorbance was measured as each cuvette was filled with the different nitrate samples. Then, the experiment was repeated twice.

Figures 3.3a, 3.3b and 3.3c display the mean of the absorbance measured three times for each nitrate sample, for quartz, glass and plastic, respectively. As observed in Figure 3.3a, the overall absorbance measured with the quartz, complied with Beer-Lambert's law, by behaving substantially linearly, particularly for concentrations below 7 ppm. With Figures 3.3b and 3.3c, the overall absorbance measured with the glass and plastic cuvettes, respectively, clearly did not comply with Beer-Lambert's law. Essentially, the absorbance measured for both glass and plastic cuvettes fluctuated around 0 units throughout, especially for the plastic cuvettes. The results further proved the fitness of quartz cuvettes for the smartphone-based nitrate sensor, since with the quartz cuvette the absorbance was detected with accuracy throughout the varied concentrations. However, for the plastic and glass cuvettes, there was not much of a difference in absorbance between each concentration. More importantly, the distinction between the absorbance measured for each concentration was not consistent or predictable in any form.

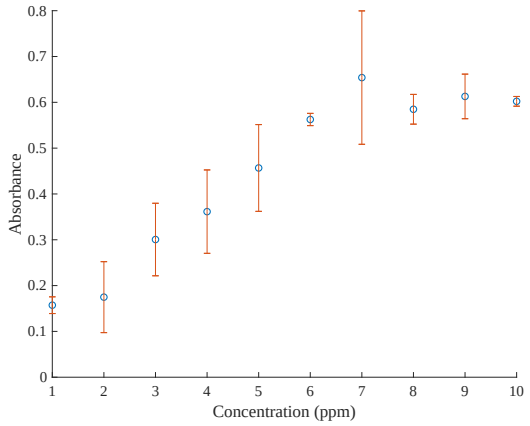

(a) Relationship between measured absorbance for different concentrations - using quartz cuvettes

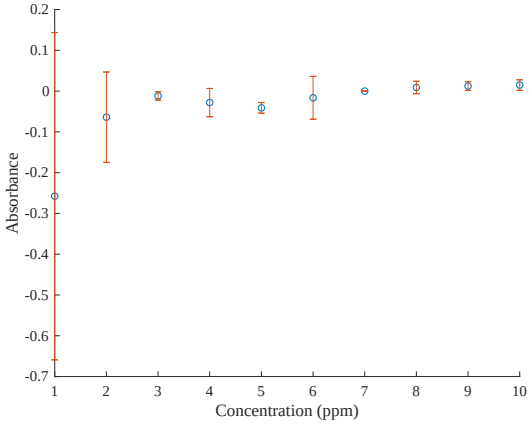

(b) Relationship between measured absorbance for different concentrations - using glass cuvettes

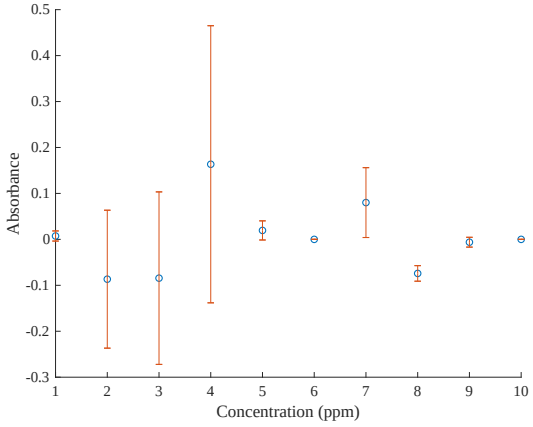

(c) Relationship between measured absorbance for different concentrations - using plastic cuvettes

Figure 3.3: Absorbance measured using quartz, glass and plastic cuvettes. (a) With the quartz cuvette, an evident linear relationship between absorbance and concentration is observed. The absorbance conformed to Beer-Lambert's law. (b) With the glass cuvette, an inconsistent non-linear relationship between the concentration is observed. The absorbance did not conform to Beer-Lambert's law. (c) With the plastic cuvette, the measured absorbance that was relatively constant to the concentration. The absorbance did not conform to Beer-Lambert's law.

Ultimately, it was concluded that the glass and plastic cuvettes could not have been used for the implementation of the smartphone-based nitrate sensor. Furthermore, it was established that the quartz cuvette was to be used for this application.

3.3 Investigation of nitrates peak absorbance

According to the literature study, nitrates have an absorbance peak or λ_{max} at 205 nm. However, it was of interest to further understand the absorption spectra of nitrates, specifically to learn how broad the region of highest absorption for nitrates was. Thus allow for an understanding of how far away from 205 nm could the absorbance of nitrates be measured with accuracy. Understanding this was essential to choose the most fitting components needed to realise the objectives of this thesis. Therefore, an experiment was performed to determine the absorption spectra of nitrates.

To determine the absorption spectra of nitrates, a quartz cuvette was filled with a nitrate sample of a specific concentration. Then using the laboratory spectrophotometer, the absorbance of a nitrate sample was measured at various wavelengths. The wavelengths were varied between 195 to 1000 nm.

As illustrated in Figure 3.4 nitrates had a significant absorbance peak between 195 and 210 nm, and beyond 250 nm, the absorbance was notably low. Nevertheless, the most prominent peak was observed at 205 nm - as predicted by the literature study.

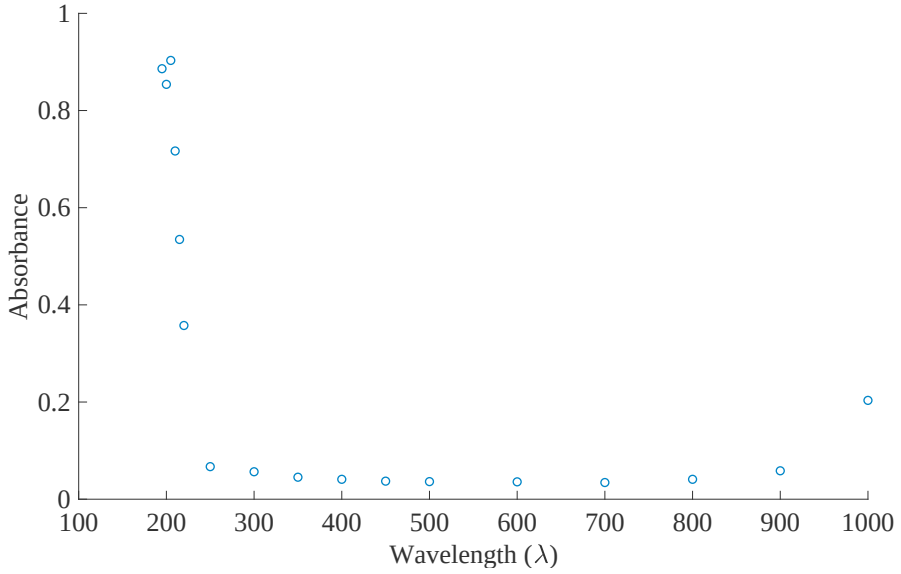

Figure 3.4: Measure absorbance of nitrates at various wavelengths. A peak absorbance is observed at a range of 195 to 210 nm. The λ_{max} of nitrates is equal to 205 nm.

Therefore, the results obtained validated the value of λ_{max}. Additionally, the results illustrated to which extents the absorbance of nitrates could still be detected, mainly from 195 to 210 nm. This investigation further confirmed the requirement of a UV light source, with an emission spectrum that includes 195 to 210 nm, and a UV fluorescence material or scintillator for the actualisation of the smartphone-based nitrate sensor.

3.4 Preliminary evaluations of chosen scintillator

As one of the main components in the design of the smartphone-based nitrate sensor, a scintillator, mainly the Lumilass, was the component that would allow the smartphone camera to identify the presence of nitrates in samples, by detecting the variation in the UV light, indirectly. Therefore, it was necessary to investigate whether the scintillator would be able to realise Objective 2a and convert the UV light into visible green light.

As reported by Sumita Optical Glass Inc [52], if the scintillator is excited by a UV light source, then the scintillator should fluoresce a visible green coloured light, that is distinctly visible to the naked human eye. Using the chosen light source, a UV light with an emission spectrum ranging from 185 to 400 nm, was emitted onto the scintillator, and then it was examined whether the scintillator fluoresced a green light or not. Indeed, the scintillator radiated a distinguishable green light when it was excited by the UV light, as seen in Figure 3.5.

Therefore, this investigation concluded, that the scintillator was working as expected, as it was able to shift the UV light emitted by the light source into visible light, mainly green light.

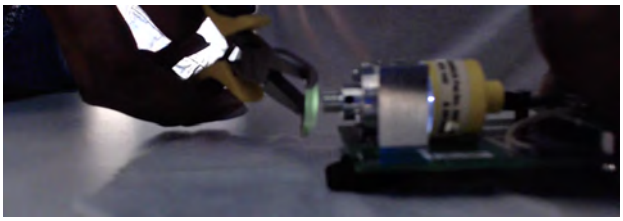

Figure 3.5: A picture of the scintillator being excited by the UV light transmitted by the light source. The scintillator fluoresced a green light when excited by the UV light.

3.5 Method and setup

As previously described, UV-Vis spectroscopy is one of the four main methods of measurement used to quantify the concentration of chemicals, such

as nitrates, in water samples. When compared to the other three methods, UV-Vis spectroscopy is one of the least complicated methods, although it requires optics, it does not require other specialised materials and components like electrochemistry and chromatography require. Additionally, with UV-Vis spectroscopy, there is no need for prerequisite steps or very skilled persons to perform the analysis. The main shortcomings of UV-Vis spectroscopy are its high cost to implement and potential interferences.

Since the purpose of this research was to design a smartphone-based nitrate sensor that implemented spectrophotometry, specifically UV-Vis spectroscopy, the intention was to build a miniaturised version of a traditional single-beam spectrophotometer. However, the smartphone camera was used as the detector, and unlike typical spectrophotometers, this smartphone-based nitrate sensor was supposed to be specific to nitrate detection. As part of one of the objectives (Objective 2b), it was essential to learn whether the smartphone-based nitrate sensor could perform well without the use of specific components commonly implemented in spectrophotometry. Specifically, components that are complicated, expensive, or add to the weight or size of the overall device. Therefore three scenarios were investigated. The first scenario incorporated almost all the typical components used in spectrophotometers. Then for the second scenario, the diffraction grating, was removed, and for the final scenario, a bandpass filter was added. Figure 3.6 illustrates the three scenarios.

In the following sections, the three scenarios are described. Additionally, for each scenario, the method used to determine the intensity of the light captured for each sample is reported.

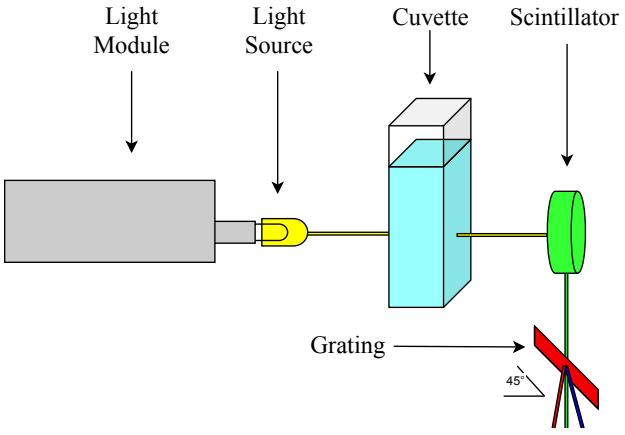

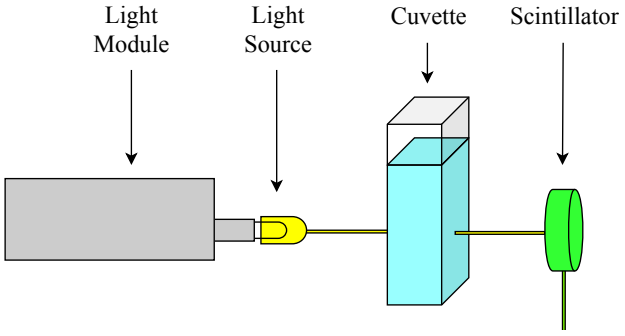

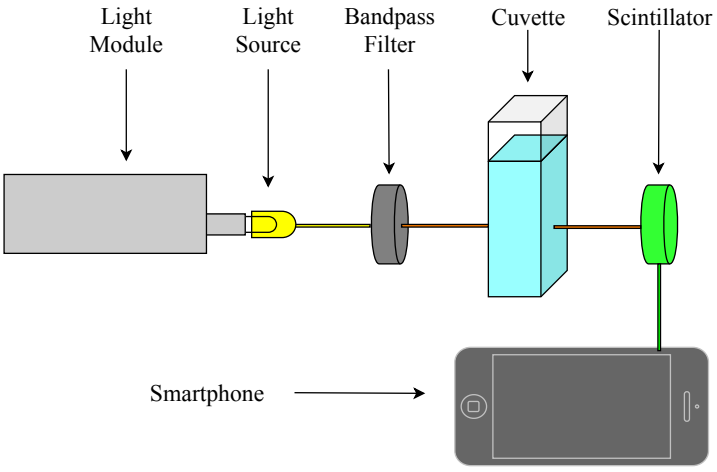

(c) Scenario 3

Figure 3.6: Arrangement of smartphone-based nitrate sensor for scenarios 1, 2 and 3. (a) Scenario 1 includes a light source, a cuvette, a scintillator and a diffraction grating. (b) Scenario 2 includes a light source, a cuvette and a scintillator. (c) Scenario 3 includes a light source, cuvette, a scintillator and a bandpass filter.

3.5.1 Scenario 1 - with the diffraction grating

As outlined previously in Section 3.5, scenario 1 incorporated almost all the typical components used in a spectrophotometer. The typical components used in a spectrophotometer is a light source, a monochromator, a cuvette, and a detector.

For this smartphone-based nitrate sensor, firstly a Compact FiberLight D_2 (Heraeus, Germany) was used as the light source since it was light-weight (104 g), compact and contained both a tungsten and deuterium lamp. The deuterium lamp could emit UV light within the range of 185 to 400 nm, and the tungsten lamp could emit visible light within a range of 400 to 1000 nm. Both lamps were connected to a switch, that allowed each lamp to be switched on independently. The light source required 12 V and 0.6 A.

Secondly, a 100-QS10 quartz cuvette (Hellma, Germany) with a path length of 1 cm, was to be used to contain the samples, since it was proven in Section 3.2 that the fittest cuvette was quartz.

Thirdly, a Lumilass-G9 (green fluorescent glass) (Sumita Optical Glass Inc, Japan) was chosen as the scintillator to shift the UV light into visible light, since it was noted in the literature study that smartphone cameras are not optimised for UV light detection at wavelengths around 205 nm.

It so happens that most deuterium lamps emit some visible light, and when they are switched on, they glow white or pink light [57]. Indeed, it was observed that the deuterium lamp of the light source produced some visible light, and this visible light was detectable by the smartphone camera. A problem arose as the visible light emitted by the deuterium lamp was capable of leaking through the Lumilass. Therefore, when the smartphone camera was placed in line with the light source and the scintillator, the camera could not capture the green light fluoresced by the scintillator, as the leaking light was dominating it. More specifically, the smartphone camera was only detecting the leaking light. Evidence of this situation is illustrated in Appendix E. A solution considered for this issue was to add a narrowband bandpass filter with a central wavelength that corresponded to the peak light emission of the scintillator (540 nm). This solution would prevent the camera from capturing the leaking light by blocking all the wavelengths around 540 nm. Authors Shrivastava et al. and Zakaria et al. implemented this strategy [50, 51]. Both authors were investigating the behaviour of lasers through the use of a scintillator, specifically the Lumilass-G9. However, this approach was disregarded as it would have increased the overall cost, complexity and size of the smartphone-based nitrate sensor. A simple and cost-effective solution was to change the alignment of the smartphone camera. Instead of placing the smartphone camera directly in line with the light source and the scintillator, the smartphone camera was placed at a 90°angle with the front face of the scintillator. Therefore, the camera would inevitably only capture the fluoresced green light, since little to no leaking light was protruding to the sides of the scintillator. Placing the

detecting medium perpendicular to the fluorescence material is a technique used in fluorescence spectrophotometry, as a means of cancelling out leaking light [58, 59].

Since this application was specific to nitrates, there would be no need to switch and select between different λ_{max}. Therefore, the use of a complete monochromator was not necessary. However, a diffraction grating was still added, between the scintillator and the smartphone camera, to allow for the separation the light emitted by the scintillator into its colour components. By separating the light fluoresced by the scintillator into its colour components, the smartphone camera would be able to capture the spectrum of the light. The diffraction grating was made of a small 2×2 cm piece of a DVD recordable (DVDR) since it is the most inexpensive alternative to a commercial grating and still performs reasonably well [15, 60]. The DVDR was separated into its two layers, in which only the bottom layer was used, and the top layer was discarded. Then the grating (DVDR bottom layer) was strategically placed at a 45 °angle from the output light of the scintillator, to permit the light bands to lay orthogonal to the grating [60]. Additionally, the grating was also placed as close as possible to the smartphone camera, to enable a large enough angle of view [60]. However, the grating was kept as far away as practicable from the scintillator, so that the rays travelled as parallel as possible to one another [61]. Therefore, the distance between the scintillator and the grating was 15 cm.

Lastly, an iPhone Xs Max (Apple Inc) with a 12 MP camera of a fixed aperture of f/1.8 was employed [62]. Since the objective of this project was to design a smartphone-based nitrate sensor, the embedded camera was used as the detector responsible for detecting the transmitted UV light through the nitrate samples.

Each component, except the diffraction grating, was placed less than 2 mm away from one another, allowing the device to be compact to the upmost. Additionally, the short distance also ensured that the intensity of light transmitted between each component was not significantly lost. Figure 3.6a shows an overview of the component placement and alignment.

Finally, a holder was utilised to align all the components together. The holder created a dark and airtight environment, without any gaps, that prevented outside light from entering and interfering with the measurements. All components were placed in a suitcase to allow for easy manoeuvring of the smartphone-based nitrate sensor.

3.5.1.1 Calibration: the relative power spectral distribution of a captured spectrum

An image can only provide information in terms of pixels; however, to analyse an image of a spectrum, it is necessary to transpose the pixel information into a relative spectral power distribution. A relative spectral power distri-

bution illustrates the relationship between the intensity of a light beam and the wavelength. The use of a diffraction grating enables each light component always to be reflected at a fixed position relative to the camera, granted that all components remain in the same alignment [63]. Therefore, the position of where a specific light component falls onto the camera sensor can be related to the respective wavelength of that same light component [30, 60, 64, 65]. To relate pixel position to wavelength, the software must be calibrated. Firstly, the camera should capture the spectrum of a light source that has a distinct peak emission wavelength at the red, green and blue part of the electromagnetic spectrum [60, 64, 65]. The wavelength of the distinct peak emission at the red, green and blue part of the electromagnetic spectrum must be known [60, 64]. Once the spectrum has been captured, the position of the red, green and blue peak pixel intensities of the captured spectrum should be determined [60, 64, 65]. Then the position of peak pixel intensities must be mapped to the respective known wavelengths of the distinct peak emissions, and the relationship between the pixel position and wavelength can be determined [60, 64, 65]. Therefore, this process calibrates the software to convert from pixel position to wavelength. Alternatively, three separate light sources, with a narrow peak emission intensity at the red, green and blue part of the electromagnetic spectrum, respectively, can be used for the calibration process [65].

For this application, three different light sources were used for the calibration, a red, blue and green LED with a peak emission at 630, 535 and 470 nm, respectively. The light source was temporarily replaced with each one of the three LEDs, and for each LED the respective spectrum was captured by the smartphone camera, as shown in Figures 3.7a, 3.7c and 3.7e. Then, for each captured spectrum, a cross-sectional line was drawn across the image, making sure that the line was kept constant and that it intersected the spectrum. In Figures 3.7a, 3.7c and 3.7e, the cross-sectional line can be seen drawn in red. Next, the pixel intensity across the cross-sectional line was determined. Once the pixel intensity was plotted against the pixel position, as illustrated in Figures, 3.7b, 3.7d and 3.7f, the pixel position of the peak pixel intensity was found and stored. The pixel positions for the peak pixel intensity of the red, green and blue spectrum was approximately 2500, 2160 and 2000 each.

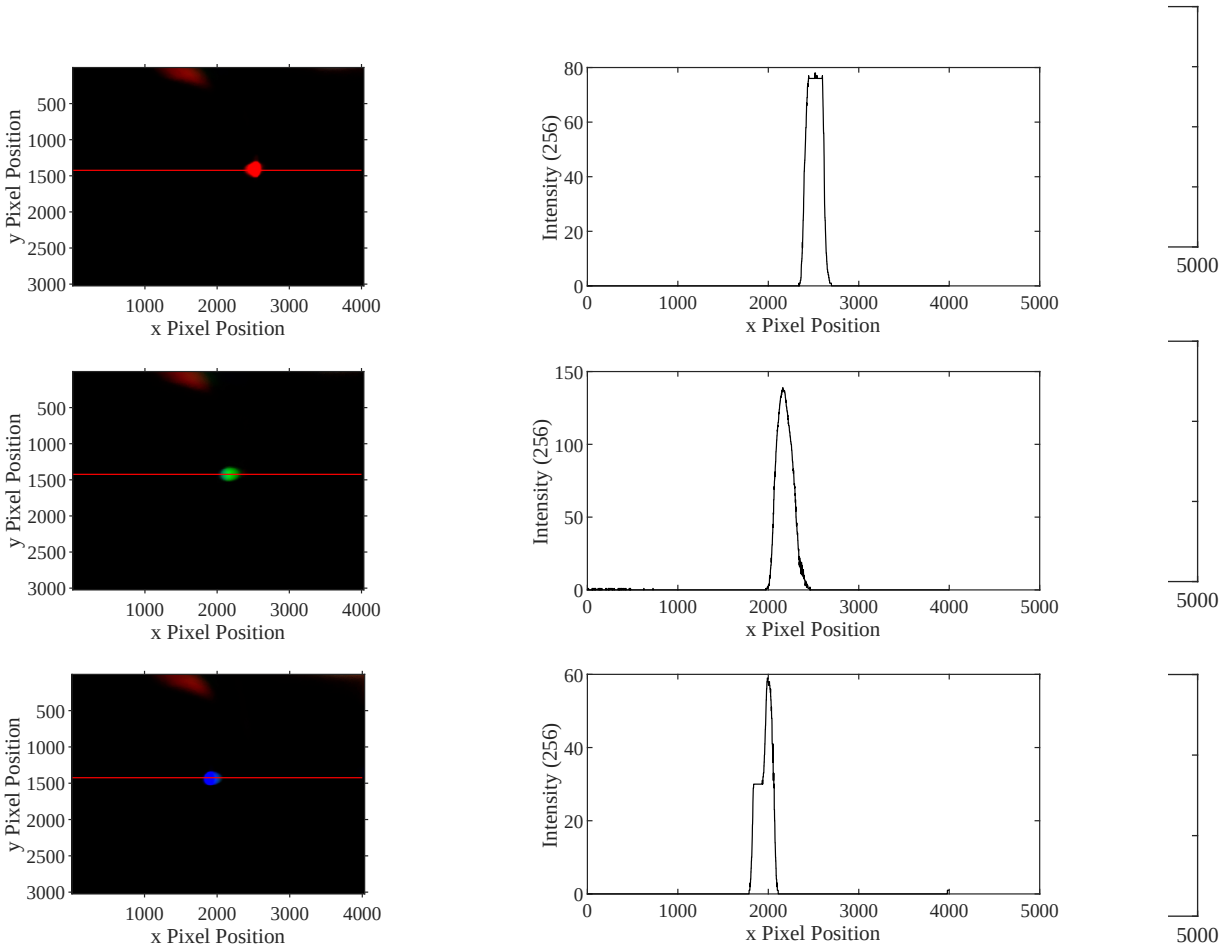

(e) Spectrum of the blue LED

(f) Intensity profile for the spectrum of the blue LED

Figure 3.7: Calibration: Spectrums of red, green and blue LEDs and their respective pixel intensity profiles. (a) The spectrum of the red LED shows that the red LED has one colour component. (b) By plotting the pixel intensity across the red line on the red LED spectrum, a distinctive peak at a pixel position approximately 2500 is observed. (c) The spectrum of the green LED shows that the green LED has one colour component too. (d) By plotting the pixel intensity across the red line on the green LED spectrum. (e) The spectrum of the blue LED shows that the blue LED also has one colour component. (f) By plotting the pixel intensity across the red line on the blue LED spectrum, a distinctive peak at a pixel position approximately 2000 is observed.

Thereafter, the pixel position of the peak pixel intensity for each LED was plotted against the known respective peak emission wavelength, as depicted in

Figure 3.8. From this, it was possible to derive a relationship between pixel position and wavelength through the use of linear regression. Therefore the line of best fit, as observed in Figure 3.8, was described as in Equation 3.5.1.

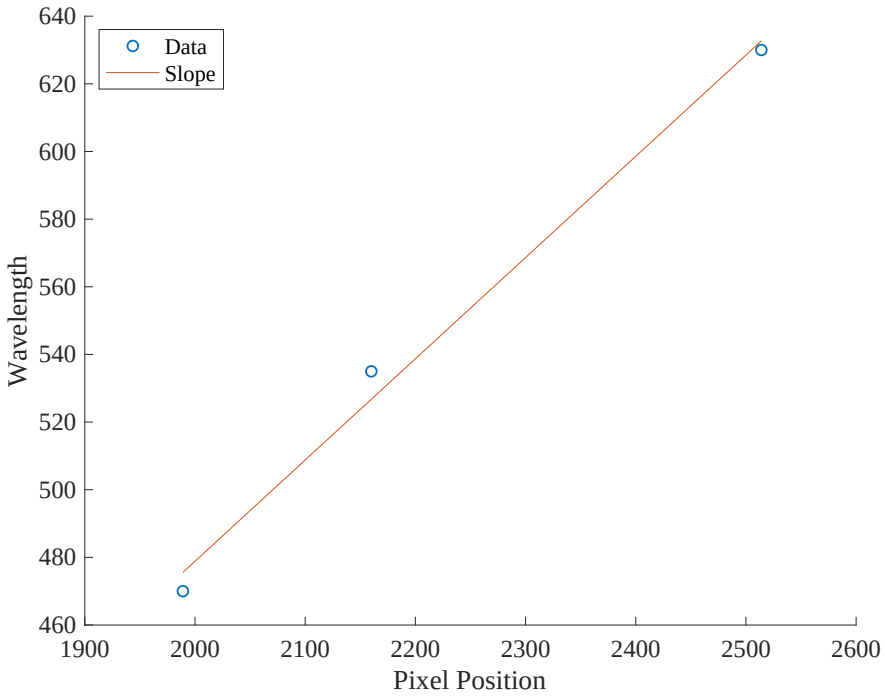

Figure 3.8: Linearisation of pixel position and wavelength

Figure 3.9: Calibration: Linearisation. The position of the peak pixel intensity determined for the image captured of the red, green and blue LED light is mapped to their respective peak wavelengths. The relationship between pixel position and wavelength is derived by performing linear regression.

$$\lambda = 0.2993x - 119.7016 \tag{3.5.1}$$

Where λ is the wavelength, the x is the pixel position. With Equation 3.5.1, the smartphone-based nitrate sensor could now transpose all pixel positions on the cross-sectional line into wavelength and thus determine the relative spectral power distribution of the captured light spectrum. However, Equation 3.5.1 was only held, if the alignment of the components and the cross-sectional line remain constant. In Figure 3.10a, the captured spectrum of the green fluorescence light produced by the scintillator is observed, while Figure 3.10c shows the respective relative spectral power distribution. The determined relative spectral power distribution resembles the spectrum depicted in Figure 2.12a (page 34), with a distinctive peak at around 540 nm. Therefore, this

suggested that the smal
determine the relative s
Nonetheless, this furthe
specifically the scintillat
based nitrate sensor was
Objective 2b.

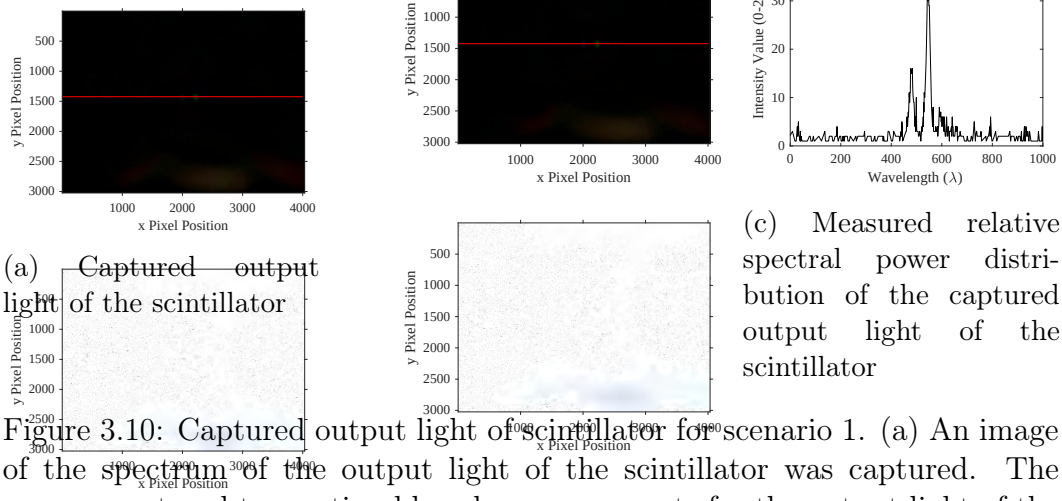

(a) Captured output light of the scintillator

(c) Measured relative spectral power distribution of the captured output light of the scintillator

Figure 3.10: Captured output light of scintillator for scenario 1. (a) An image of the spectrum of the output light of the scintillator was captured. The camera captured two noticeable colour components for the output light of the scintillator. The image shown in (b) is the negative version of the image of the spectrum of the output light of the scintillator. (c) In the relative spectral power distribution of the output light of scintillator, there is a pronounced peak at approximately 540 nm, and the intensity distribution resembles intensity described by the manufactures of the scintillator.

3.5.2 Scenario 2 - without diffraction grating

Before scenario 2 was tested, it was evident that there were a few shortcomings to the design of the smartphone-based nitrate sensor. Since scenario 1 had a diffraction grating, and the diffraction grating was kept 15 cm from the scintillator, it added to the weight and size of the smartphone-based nitrate sensor. Additionally, the diffraction grating added to the complexity, as all components need to remain constant to the diffraction grating, and the grating had to be placed at a specific angle relative to the light emitted onto it. Furthermore, the use of a diffraction grating meant that the smartphone-based nitrate sensor would need to be regularly calibrated to relate wavelength and pixel position. The calibration process could be tedious since the light source had to be temporarily replaced with a red, green and blue LED sources. Moreover, determining the relative spectral power distribution of a captured spectrum complicated the algorithm used for the smartphone-based nitrate sensor.

In light of these reasons, it was decided that the diffraction grating would be removed in scenario 2. As such, the setup for scenario 2 consisted of the light source, the quartz cuvette, the scintillator and the smartphone. Additionally, the alignment was also kept the same; yet, the smartphone camera was placed closer to the scintillator. In Figure 3.6c, the full setup for scenario 2 can be observed.

Without the diffraction grating, the camera captured the concentrated green light, fluoresced by the scintillator, instead of the spectrum of the green light, as seen in Figure 3.11b. Therefore, there was no need to profile the intensity across the cross-sectional line and determine the relative spectral power distribution for this scenario. Alternatively, the intensity of each pixel of the image of the captured light was taking into consideration. Figure 3.11c illustrates the three-dimensional representation of the pixel intensity distribution of the captured light.

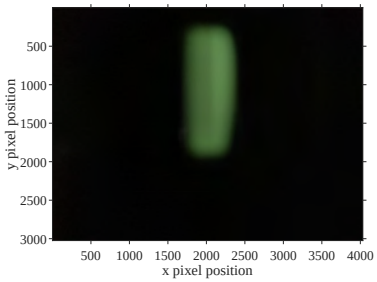

(a) Captured output light of the scintillator

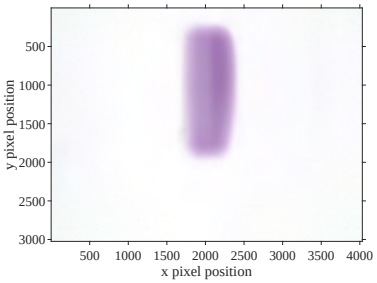

(b) Negative version of captured output light of the scintillator

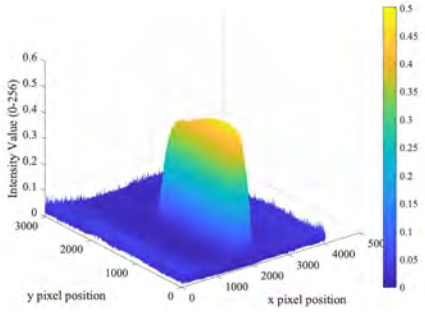

(c) 3D Intensity distribution of the Captured output light of the scintillator

Figure 3.11: Captured output light of scintillator for scenario 2. (a) The output light captured is concentrated about the x pixel position of 2000. The image shown in (b) is the negative version of the output light captured is concentrated about the x pixel position of 2000. (c) The 3D intensity distribution is the representation of the pixel intensity of each pixel square for the image shown in (a).

It was hypothesised that the smartphone-based sensor would still perform

well without a diffraction grating since the overall intensity of the captured light would still be proportional to the concentration.

3.5.3 Scenario 3 - with the bandpass filter

In scenario 1, it was concluded that a monochromator was not required. The reason being that there was no need to switch between various wavelengths since this application focused only on the detection of nitrate. Therefore, the only wavelength of interest was 205 nm. However, as the light source is a polychromatic source, and it emits a UV light with a broadband of 185 to 400 nm, the smartphone-based nitrate sensor was susceptible to some of the issues mentioned in Section 2.5.1. Such issues included the potential interferences caused by other chemicals that could be present in the nitrate sample that might have absorbance peaks within other parts of the UV spectrum. Another issue considered in Section 2.5.1 is that the use of polychromatic sources can cause the relationship between the concentration and the absorbance to be non-linear. Additionally, if the excitation spectrum of the scintillator, in Figure 2.12a (page 34), is considered, the excitation intensity is relatively low at approximately 205 nm. In comparison, at around 250 to 310 nm, the excitation spectrum is particularly high. This indicated that out of all the green light that was fluoresced by the scintillator, the light emitted at 205 nm induced only a small portion of it. This further suggested that the change between the signals measured for different concentrations, would not be too significant. The problem with small signals is that it is likely that the difference between them is not quantifiable or accurately determined, especially if there is substantial noise on both signals.

In light of the above, for scenario 3, the smartphone-based nitrate sensor remained the same as in scenario 2, where the light source, the quartz cuvette, the scintillator and the smartphone were still present. However, a narrow band bandpass filter (Edmund Optics, United States) was added to the smartphone-based nitrate sensor, in between the light source and cuvette, as illustrated in Figure 3.6c. The bandpass had a centre wavelength at 200 nm and a bandwidth of 10 nm. Thus, the bandpass filter would allow the wavelength of interest of 205 nm, to be emitted, while blocking the unwanted emissions, specifically below 195 nm and above 205 nm.

Similar to the previous scenario, the smartphone camera captured the concentrated green light fluoresced by the scintillator - shown in Figure 3.11b. Therefore, the intensity of each pixel in the image of the captured green light was taken into consideration. The speculation was that the smartphone-based sensor would still perform equally as well as it did with and without the diffraction grating, considering that the overall intensity of the captured light would still be proportional to the concentration.

3.6 Configuring camera settings and denoising

To capture the green light fluoresced by the scintillator with the smartphone camera, it was first necessary to identify the best camera settings, that would allow the camera to capture as much light as possible. However, it was crucial not to saturate the camera and to produce the least amount of noise.

In photography, the exposure of an image is controlled by the aperture and the shutter speed [66]. The aperture stipulates where the light that passes through can fall on the camera lens. While the shutter speed specifies how long the camera sensor stays open or close for, to allow incoming light to pass through the camera lens [66]. On the other hand, the sensitivity of an image is controlled by the ISO speed, which determines how sensitive the camera is to incoming light [66]. All of which help make an image darker or brighter [66]. Hence, this next section will describe the process of finding the most appropriate sensitivity and exposure settings to permit the smartphone camera to capture the green light fluoresced by the scintillator. Additionally, a strategy used to decrease the noise captured by the camera is also discussed. These settings were used in all three scenarios; however, the settings were configured during the design of scenario 1.

3.6.1 Determining best exposure

Unfortunately, the smartphone that was used did not have a variable aperture, as the aperture was fixed at f/1.8. Therefore no improvements could be made to the exposure in terms of the aperture settings. Nevertheless, the shutter speed and ISO of the smartphone could be altered. While the white balance and focus settings were kept at their mid-range of 5000 and 0.5, respectively, the shutter speed was decreased to its minimum of 1 second. Once the shutter speed was decreased, the smartphone camera was able to capture a brighter and clearer spectrum of the green fluorescence light, where all the present colour components were more noticeable. This can be observed in Figure 3.12a. If Figure 3.12c (page 57) is compared to Figure 3.10c, it is clear that the magnitude of the overall intensities has increased. Furthermore, it is more apparent that the green light fluoresced by the scintillator produced the expected spectral distribution shown in Figure 2.12a, page 57. Once again confirming that Objective 2a had been fulfilled.

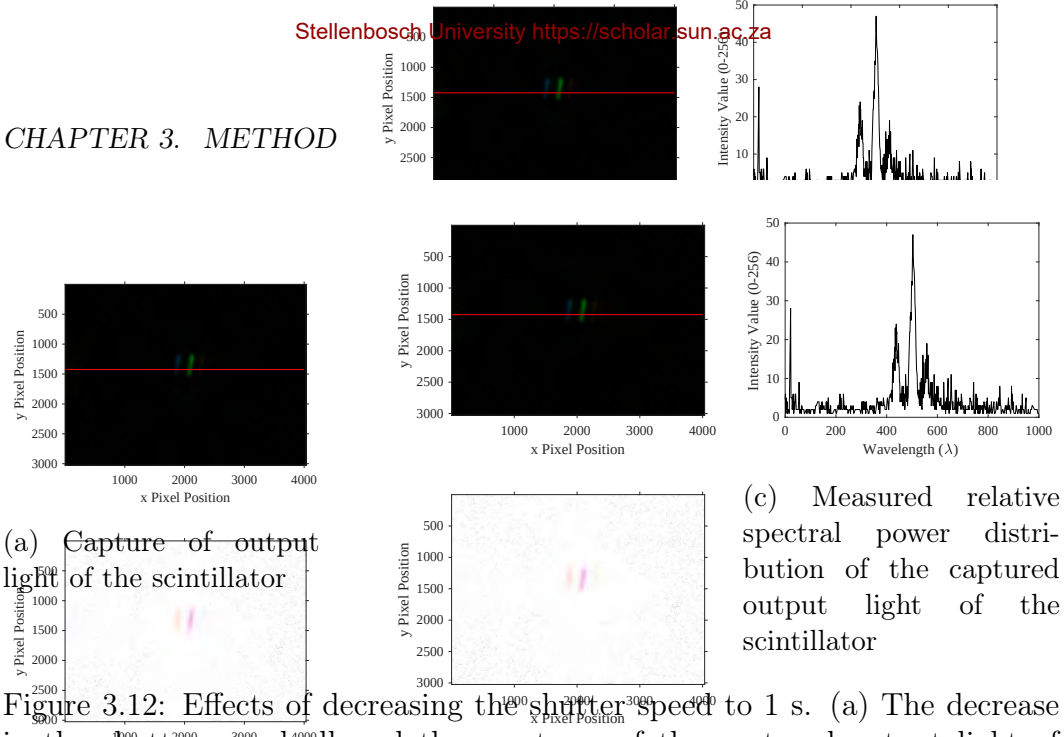

(a) Capture of output light of the scintillator

(c) Measured relative spectral power distribution of the captured output light of the scintillator

Figure 3.12: Effects of decreasing the shutter speed to 1 s. (a) The decrease in the shutter speed allowed the spectrum of the captured output light of the scintillator to be more apparent. (b) The decrease in the shutter speed allowed the negative image of the spectrum of the captured output light of the scintillator to be more apparent. (c) There is a noticeable increase in the overall intensity of the relative spectral power distribution of the output light of scintillator.

3.6.2 Determining best ISO

To find the most suitable ISO, all the camera settings remained the same (with a shutter speed of 1 second), while various ISO settings were tested. The aim was to select an ISO speed that would deliver the highest intensity while keeping the noise at a minimum. Therefore, the ISO speeds that were tested were 24, 500, 1000, 1500, 2000 and 2300. It is apparent from Figure 3.13a, that with an ISO of 24 the smartphone camera captured nothing and that the software could not make out a relative spectral power distribution at all, therefore an ISO of 24 was immediately discarded. If Figures 3.13f and 3.13r, are compared, the least amount of noise was observed when the ISO was set to 500, and the most significant amount of noise was observed when the ISO was set to 2300. However, with both ISOs, the measured light intensity was one of the lowest. Looking at Figures 3.13i, 3.13l and 3.13o, the noise seemed to be roughly the same, but the intensity achieved with ISO 1000 and ISO 2000 was weak in comparison to the intensity measured with ISO 1500. Thus, the best option was to use an ISO of 1500. However, further work needed to be done to further reduce the noise.

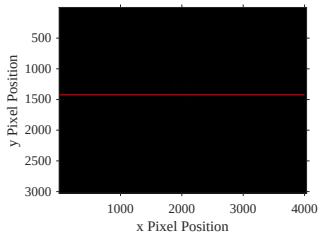

(a) Image Capture of Output Light of the scintillator at an ISO of 24

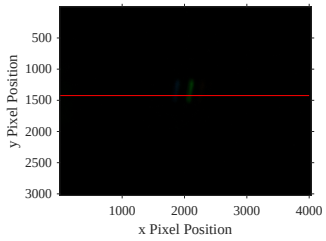

(d) Image Capture of Output Light of the scintillator at an ISO of 500

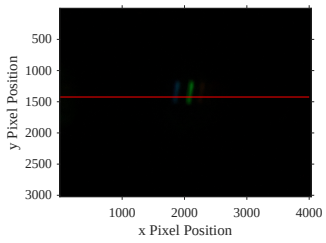

(g) Image Capture of Output Light of the scintillator at an ISO of 1000

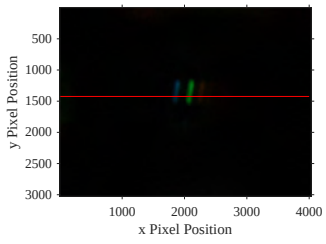

(j) Image Capture of Output Light of the scintillator at an ISO of 1500

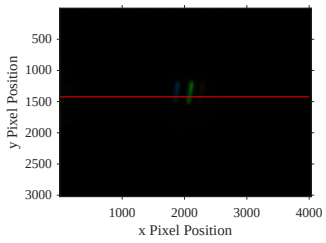

(m) Image Capture of Output Light of the scintillator at an ISO of 2000

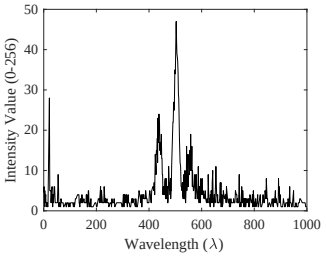

(i) Spectrum of Output Light of the scintillator at

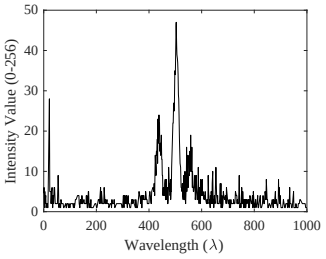

(o) Spectrum of Output Light of the scintillator at an ISO of 2000

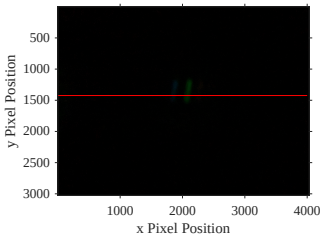

(p) Image Capture of Output Light of the scintillator at an ISO of 2300

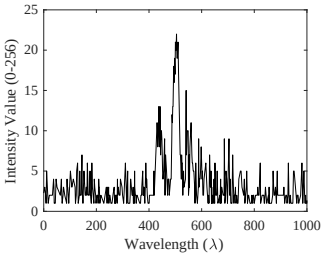

(r) Spectrum of Output Light of the scintillator at an ISO of 2300

Figure 3.13: Comparison between ISO speeds. (a)-(c) With an ISO of 24, nothing is captured. (d)-(f) With an ISO of 500, some light and noise are captured. (g)-(i) With an ISO of 1000, the light intensity is increased, but so is the noised. (j)-(l) With an ISO of 1500, the light intensity is the highest, but noise is observed. (m)-(o) With an ISO of 2000, the light intensity is decreased, but the noise seems to have remained the same. (p)-(r) With an ISO of 2300, the light intensity decreased further, and the noise seems to have increased or remained the same.

3.6.3 Stacking

A digital image processing technique referred to as image stacking, was used to decrease the noise captured by the camera. This process involves the taking of multiple pictures instead of just one, then adding all the images together and finally dividing the summation of the images by the number of the images [67]. Therefore, the output image is the average of the images taken. Since noise occurs randomly, if the average of multiple images is taken, then the noise is reduced. Subsequently, a reduction in the noise should be observed on the output stacked image.

To determine the number of images that should be stacked, multiple pictures of the output light were captured. At first, the images of the captured output light were stacked 5 times as shown in Figure 3.14d. Figures 3.14a and 3.14c display a single image of the captured light and its relative spectral power distribution, respectively. If Figures 3.14c and 3.14f are compared, less noise is observed by the output of the 5 stacked images. However, it was evident that there was still some noise present, therefore, the images were then stacked 10 times - illustrated in Figure 3.14g. When 10 images were stacked the noise was further diminished. The diminished noised can be noticed by comparing Figures 3.14i and 3.14f. Nonetheless, another attempt was made to further decrease the noise, and this was done by stacking 15 images, where the output is given in Figure 3.14j. By examining Figures 3.14l and 3.14i, only some minor noise reduction was noted when 15 images were stacked. Since there was only a minor difference between the noise level achieved with 10 stacked images and

15 stacked images, it wa
than 15 images. Theref
captured output light we

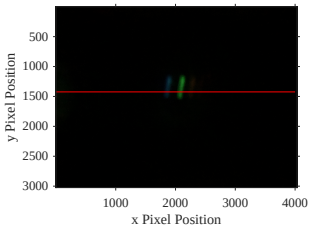

(a) Capture of output light of the scintillator

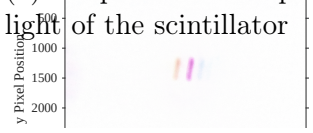

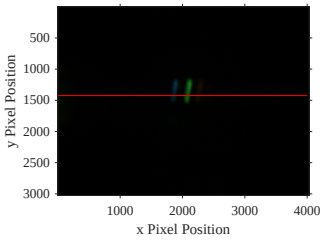

(d) 5 stacked images of capture of output light of the scintillator

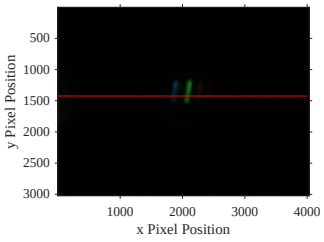

(g) 10 stacked images of capture of output light of the scintillator

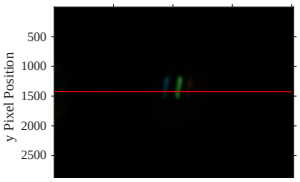

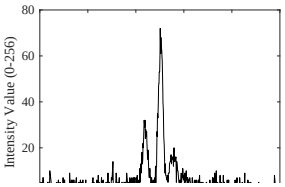

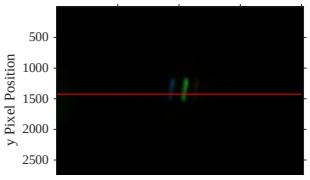

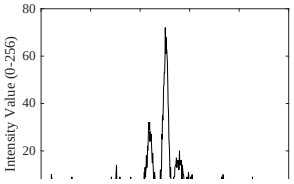

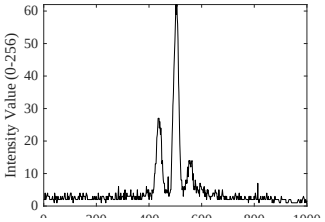

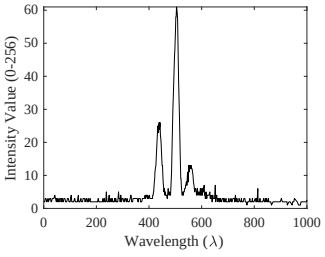

(i) Measured relative spectral power distribution of the 10 stacked images of capture of output light of the scintillator

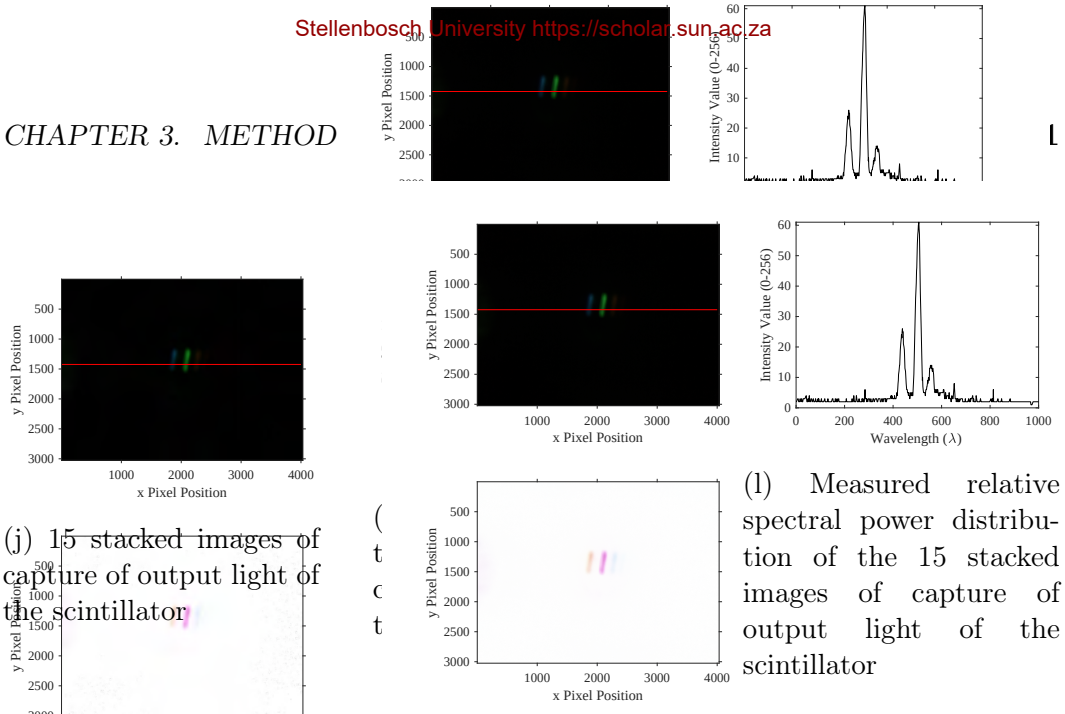

(j) 15 stacked images of capture of output light of the scintillator

(l) Measured relative spectral power distribution of the 15 stacked images of capture of output light of the scintillator

Figure 3.14: Effect of stacking images. By stacking more than 5 images, the noise of the captured output light is decreased. Similarly, there was an additional decrease in the noise when the images were stacked 10 times. The least amount of noise was achieved by stacking 15 images.

3.7 Detection method and algorithm

The smartphone-based nitrate sensor made use of an algorithm that analysed the output light emitted by the scintillator. The first part of the algorithm focussed on determining the absorbance of a nitrate sample of a known concentration. The second part of the algorithm calibrated the absorbance against the concentration. Lastly, the last part was concerned with estimating the concentration of nitrate samples of unknown concentrations. Therefore, this section describes the algorithm as mentioned above. A description of the software used and a diagrams of the algorithm can be found in Appendix C.

3.7.1 Algorithm for determining the absorbance of a sample

For each nitrate sample and the one reference sample, 15 images of the output green light were taken, saved and uploaded onto the software. Each image had a resolution of 4032×3024 pixels. Then, for each sample, the 15 images were stacked into one. Subsequently, the intensity of the captured light was quantified by analysing the output stacked image. For each scenario, the light intensity was quantified differently. For scenario 1, the light intensity was equivalent to the integral of the intensity of the relative power spectral distribution. While, for scenarios 2 and 3, the light intensity was equivalent to the integral of the pixel intensity of the whole image. Thereafter, the transmittance of each nitrate sample was determined by dividing the calculated light intensity of each nitrate sample by the calculated light intensity of the

reference sample and multiplying it by 100. Following that, the absorbance of each nitrate sample was calculated by substituting the transmittance into Equation 2.4.2 (page 19). Finally, the calculated absorbance for each sample was plotted against the respective concentration.

3.7.2 Calibration algorithm

This part of the algorithm imported the absorbance measured for three sets of nitrate samples of known concentrations and determined the mean and the standard deviation of the three sets of absorbances measured for each concentration. Then the mean and standard deviation of each concentration was plotted, and the line of best fit was defined. Subsequently an absorbance or calibration equation, with the same format as Equation 2.5.1 (page 20), was determined. Since the path length of the cuvette was 1 cm, then the calibration equation was reduced to the format given in Equation 3.7.1.

$$A = \epsilon C \tag{3.7.1}$$

3.7.3 Algorithm to find concentration of unknown sample

For the estimation of the concentration of unknown samples, the algorithm performed similarly to the first part of the algorithm. The algorithm read in a set of 15 images for the unknown sample and the reference sample. All 15 images were stacked into one image, for the unknown and reference sample. Thereafter, the light intensity for each output stacked image of the captured green light was quantified. For scenario 1, the light intensity was quantified by finding the integral of the pixel intensity of the relative power spectral distribution. Alternatively, for scenario 2 and 3, the light intensity was quantified by finding the integral of the pixel intensity of the whole image. Subsequently, the transmittance was calculated by dividing the calculated light intensity of the unknown sample by the calculated light intensity of the reference sample and multiplying it by 100. Using Equation 2.4.2, the absorbance could be calculated and by using the absorbance or calibration equation, Equation 3.7.1, the concentration of the unknown sample could be calculated.

3.8 Metrics

This section summarises the metrics used to asses the performance and results of the smartphone-based nitrate detector.

For the three scenarios of the smartphone-based nitrate detector, it was essential to evaluate whether each scenario was producing valid results. Therefore, for each scenario, the mean of the absorbance measured for the three

sets of nitrate samples, of different known concentrations, was plotted. Then the relationship of the absorbance and concentration was evaluated against Beer-Lambert's law. If the absorbance were to be linear to the concentration - as stated by Beer-Lambert's law, at least for lower concentrations, then the scenario of the smartphone-based nitrate detector would have performed as expected.

The next step was to determine which scenario performed the best and whether the diffraction grating and the bandpass filter was necessary or not. For each scenario and the laboratory spectrophotometer, the mean and the standard error of the absorbance measured for the three sets of nitrate samples of different concentrations was compared with one another. If the three scenario designs produced results that were similar to the results produced with the laboratory spectrophotometer (provided in Figure 3.3a, page 43), then all three scenario designs would have performed well. Alternatively, if only one or two of the scenario designs obtained results that were similar to the results achieved with the spectrophotometer, then only those or that scenario design(s) would be considered as working adequately. Should the scenario design, that uses a specific component yield results that are more comparable to the results achieved with the laboratory spectrophotometer, in comparison to the results achieved by the other two scenario designs, then the specific component would be considered as necessary.

Finally, it was fundamental to determine the validity of the smartphone-based nitrate sensor. This validation consisted of determining the concentration of nitrate samples of unknown concentrations, with the smartphone-based nitrate sensor. Therefore, the mean and standard error between the concentration measured with the chosen scenario design and laboratory spectrophotometer was to be compared to one another. The smartphone-based nitrate detector would perform appropriately if the margin between the concentration measured with the smartphone-based nitrate sensor and the laboratory were not significantly different from one another.

Chapter 4

RESULTS

This chapter reports the results obtained from the tests performed on the smartphone-based nitrate sensor. The first set of tests involved the analyses of the three design scenarios of the smartphone-based nitrate sensor. The concluding test was conducted to validate the performance of the final smartphone-based nitrate sensor. Therefore, this chapter examines the realisation of objectives 2b, 2c and 3. Additionally, this chapter reports the overall achievements of the smartphone-based nitrate sensor.

4.1 Testing all three scenarios

Section 3.5 described three design scenarios of the smartphone-based nitrate sensor. All scenarios consisted of the same foundation components, which included the light source, the quartz cuvette, the scintillator and the smartphone camera. Scenario 1 differed from scenario 2 and 3, as it had a diffraction grating. Scenario 2 had no diffraction grating, and scenario 3 had a bandpass filter. The following section provides the results achieved with each scenario and a comparison of the three scenarios. Lastly, the following section concludes which scenario operated optimally, better yet, whether the diffraction grating or the bandpass filter was necessary for the smartphone-based nitrate sensor to function well.

4.1.1 Testing scenario 1 - with the diffraction grating

Firstly, three sets of nitrate samples were prepared according to the method used in Section 3.1. Each set of samples prepared included a reference, a 1 ppm, a 2 ppm, a 3 ppm, a 4 ppm, a 5 ppm and a 10 ppm. By using the algorithm described in Section 3.7.1, the absorbance of each prepared nitrate sample was determined. Figure 4.1 illustrates the mean of the calculated absorbance for the three sets of samples. If Figure 4.1 is analysed, it is evident that an almost linear relationship between the absorbance and the concen-

tration is observed, especially for the lower concentrations. Additionally, the R-square value of the line of best for the absorbance was 0.897, which further indicates the linearity of this plot. Therefore, the measured absorbance of the samples adhered to Beer-Lambert's law for the most part. The 10 ppm sample, however, deviated slightly from the linear trend; this suggested that the 10 ppm sample did not follow Beer-Lambert's law. Nonetheless, these results implied that the smartphone-based nitrate detector was capable of detecting nitrates in a sample of various concentrations when all primary components and the diffraction grating were included.

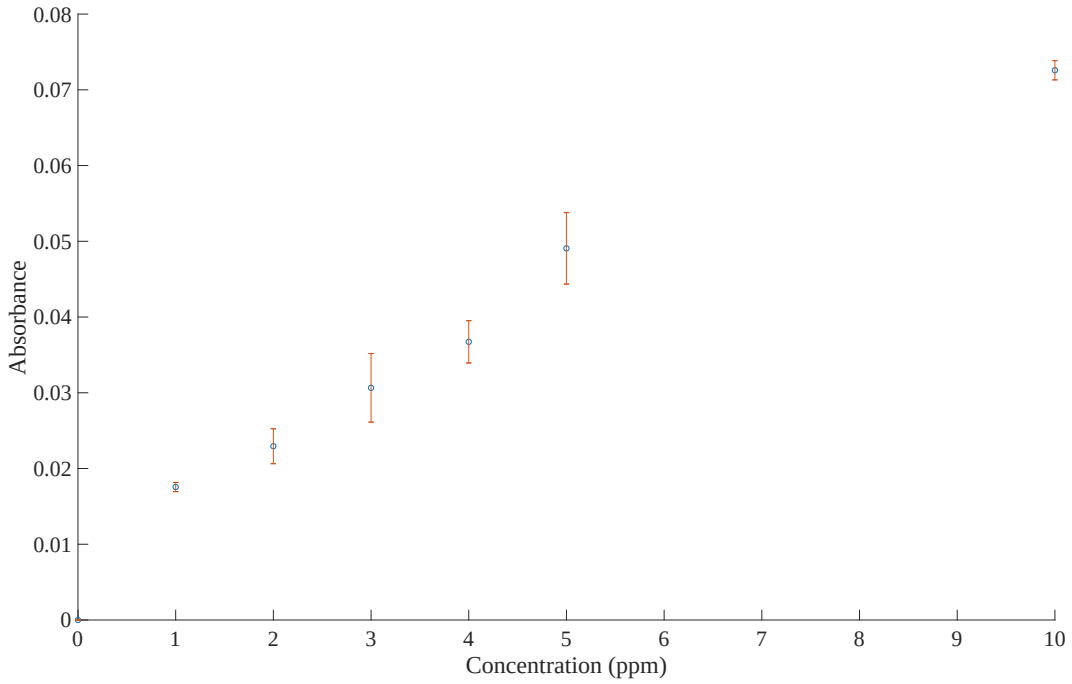

Figure 4.1: Mean of measured absorbance curve for scenario 1 - with the diffraction grating. The relationship between the absorbances and the concentration is approximately proportional, as the R-squared value was 0.897.

4.1.2 Testing scenario 2 - without the diffraction grating

Similar to scenario 1, three sets of nitrate samples were also prepared according to the method used in Section 3.1. Likewise, each set consisted of a reference, a 1 ppm, a 2 ppm, a 3 ppm, a 4 ppm, a 5 ppm and a 10 ppm sample. Then, the absorbance of each prepared sample was calculated through the use of the algorithm, described in Section 3.7.1. The R-square for the relationship between the absorbance and concentration was 0.689, suggesting that the relationship was roughly linear and that scenario 2 obeyed Beer-Lambert's law to an extent. This is observed in Figure 4.2, which shows the mean absorbance for the three sets of samples. As expected, the 10 ppm samples also diverged

from Beer-Lambert's law in the same way it did with the first scenario, since it was not within the linear region. Furthermore, the results indicated that the smartphone-based nitrate sensor was still capable of determining the presence of nitrates in a water sample, even without the use of a diffraction grating.

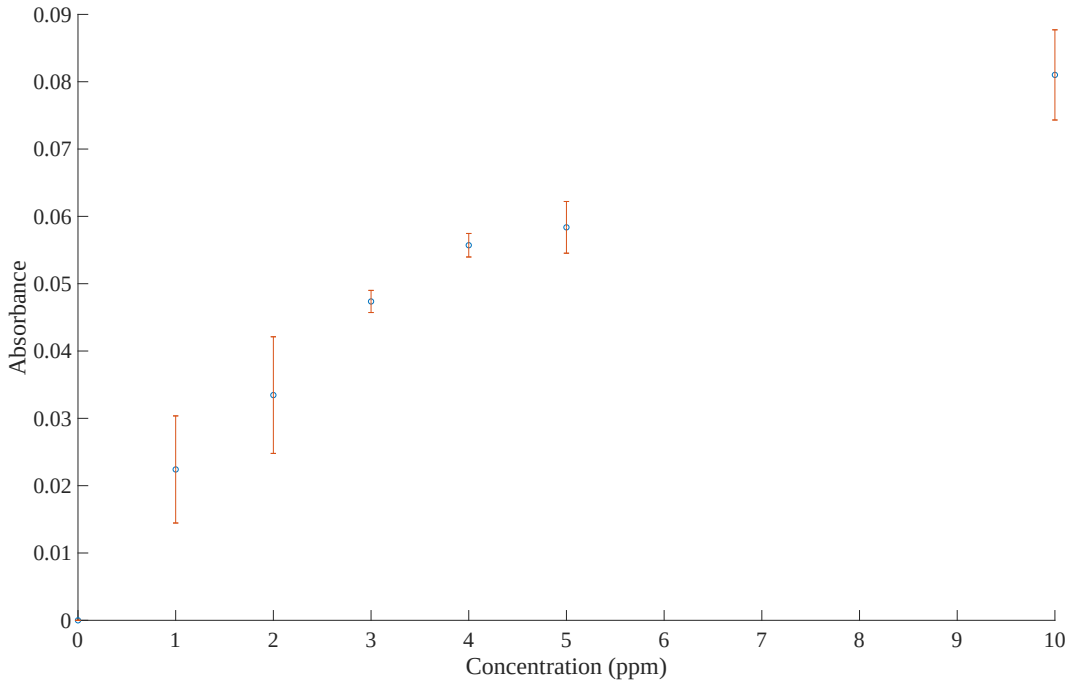

Figure 4.2: Mean of measured absorbance curve for scenario 2 - without the diffraction grating. The overall absorbance was not far from being precisely linear to the concentration, as the R-squared value was 0.689.

4.1.3 Testing scenario 3 - with the bandpass filter

For scenario 3, the same procedure was followed as with scenario 1 and 2. Therefore, three sets of a reference, a 1 ppm, a 2 ppm, a 3 ppm, a 4 ppm, a 5 ppm and a 10 ppm nitrate sample were prepared, using the method described in Section 3.1. For each sample, the absorbance was calculated by using the algorithm, detailed in Section 3.7.1. By observing the mean of the absorbance of the three sets of samples, plotted in Figure 4.3, it is apparent that the absorbance is proportional to the concentration and thus conforms to Beer-Lambert's law. With the exception of the 10 ppm sample, which seems to be out of the linear range of the plot. Additionally, the linearity of the absorbance and concentration is further confirmed by the R-square, which was 0.951. Once again, the smartphone-based nitrate detector was still able to identify the different concentrations of the known nitrates samples distinctly, even though the diffraction grating had been removed, and a bandpass filter had been added.

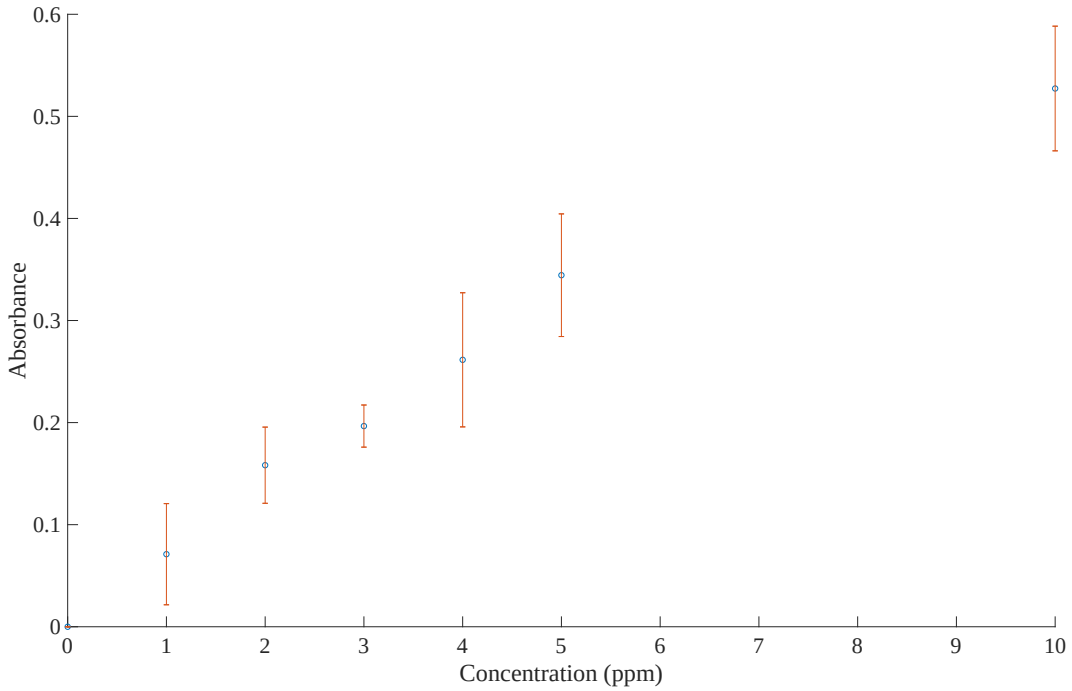

Figure 4.3: Mean of measured Absorbance Curve for scenario 3 - with the bandpass filter. A linear relationship is observed between the absorbances and the concentration, as the R-squared value was 0.951.

4.1.4 Discussion

This section compares the performance of the smartphone-based nitrate sensor for each scenario; mainly scenario 1, which included a diffraction grating, scenario 2, which did not include a diffraction grating, and scenario 3, which included a bandpass filter.

According to Beer-Lambert's law, the absorbance can be described as the concentration of a sample multiplied by the molar absorptivity (the gradient of the absorbance curve) and the path length, known as Equation 2.5.1. To compare the results achieved with the different scenarios, the calibration algorithm, described in Section 3.7.2, was implemented to obtain the absorbance equation of the results reported in Sections 4.1.1, 4.1.2 and 4.1.3 for scenarios 1, 2 and 3, respectively. For each scenario, two absorbance equations were determined, one using all the plots (0 - 10 ppm) and one excluding the 10 ppm plot.

When the results produced by scenario 1 and 2 were compared against one another, the relationship between the absorbance and concentration was quite similar for both scenarios, as observed in Figure 4.4. Taking into consideration only samples 0 to 5 ppm, the molar absorptivity of scenario 1 and 2 was 0.0100 and 0.0136, respectively. When sample 10 ppm was included, then the molar absorptivity of scenario 1 and 2 was 0.0082 and 0.0100, respectively. The

molar absorptivity of scenario 2 was slightly higher than that of scenario 1. This could have been attributed to the fact that with scenario 1, the green fluorescence light emitted by the scintillator was placed further away from the smartphone camera than with scenario 2. In scenario 1, the diffraction grating was placed in between the smartphone camera and the scintillator, and it was kept at a distance of 15 cm from the scintillator. Therefore, the overall light intensity captured with scenario 1, was lower than the overall light intensity captured with scenario 2. Although the molar absorptivity of scenario 2 was larger than that of scenario 1, the molar absorptivities of both scenarios were not too distant from one another. This suggested that the smartphone-based nitrate sensor was capable of performing similarly for both scenarios. Thus proving that the diffraction grating could indeed be discarded for this application, without compromising the functionality of the sensor. The purpose of a diffraction grating in spectrophotometers is to split light into different components, and thus allow the monochromator to distinguish between the different light components, so that the correct wavelength of the incident light may be selected. Therefore, the diffraction grating did not make much of a difference because it simply splits light into its various beams. If the overall intensity of all the beams is measured then it should still be similar to the intensity of the same light when it is condensed (not diffracted).

For scenario 1 and 2, the difference between the absorbance for every two concentrations was not statistically significant. Similarly, the range between the magnitude of the lowest and highest absorbance measured with scenario 1 and 2 was not particularly significant either. This is apparent if the absorbance curves for scenario 1 and 2 are compared to the absorbance curves of the laboratory spectrophotometer, shown in Figure 4.4. The measured change in the absorbance from 0 to 10 ppm was 0.0726 and 0.0810 for scenario 1 and 2, respectively. On the contrary, for the results obtained with the laboratory spectrophotometer, the change in the absorbance from 0 to 10 ppm was 0.602. This low variance between the absorbance measured with 0 and 10 ppm implied that the difference between the intensity of light measured for each nitrate sample was minute, for scenario 1 and 2. Furthermore, it implied that scenarios 1 and 2 had a fairly low measurement sensitivity.

The results recorded with scenario 3 conformed to Beer-Lambert's law, as it did with scenario 1 and 2. However, by looking at Figure 4.4, it is apparent that absorbance determined with scenario 3 was not comparable to the absorbance determined with scenario 1 and 2, concerning the molar absorptivity and overall absorbance magnitude. When samples 0 to 5 ppm were taken into consideration, the molar absorptivity of scenario 3 was 0.0681, and when sample 10 ppm was also included, then the molar absorptivity was 0.0582. Therefore, the molar absorptivities obtained with scenario 3 were more substantially greater than the molar absorptivities obtained with scenario 1 and 2.

Additionally, for scenario 3, the measured change in absorbance from 0 to

10 ppm and the variance between the absorbance of every two concentrations were much more apparent. More specifically, the difference in absorbance from 0 to 10 ppm was 0.527, for scenario 3. This difference was much closer to the difference measured with the laboratory spectrophotometer. The fact that scenario 3 had a significantly higher molar absorptivity and variance between the lowest and highest absorbance, in comparison to scenario 1 and 2, suggested that with the addition of the bandpass filter, the variation between the intensity of light measured for each concentration was greater, moreover, the measurement sensitivity of scenario was higher. Therefore, scenario 3 functioned the best, in contrast to scenario 1 and 2.

The absorbance curve determined with the laboratory spectrophotometer produced a molar absorptivity of 0.0934 for samples 0 - 5 ppm and 0.0720 for samples 0 - 10 ppm. Scenario 3 had the molar absorptivity that was most approximate to the molar absorptivity achieved with the laboratory spectrophotometer, varying by 27% and 19% for the samples of 0 - 5 ppm and 0 - 10 ppm, respectively. In contrast, the molar absorptivity for scenario 1 and 2, varied by over 85% for both samples of 0 - 5 ppm and 0 - 10 ppm. Once again, this variance suggested that scenario 3 delivered the most reliable results out of all three scenarios.

Scenario 3 was the only scenario that measured a mean absorbance that had standard deviation bars that intersected with the mean absorbance measured with the laboratory spectrophotometer, specifically for samples 0, 2, 4 and 5 ppm. Therefore, it could be considered that the difference between the overall mean absorbance measured with scenario 3 and the laboratory spectrophotometer was small. However, the mean of the absorbances measured with scenario 1 and 2 was considerably different from the mean of the absorbances measured with the laboratory spectrophotometer, where the standard deviation bars were far from overlapping with one another.

A possible reason for the disparity between the results achieved with scenario 3 and the other two scenarios could be due to a reason mentioned in Section 3.5.3. It was speculated that for the green fluorescence light generated by scintillator, only a small part was as a result of the light emitted at 205 nm. If the excitation spectrum of the scintillator (Figure 2.12a on page 34) is observed, the excitation intensity is considerably low for wavelengths around 205 nm. While at about 250 to 310 nm, the excitation intensity is rather high. It was thus indicating that the majority of the light emitted by the scintillator was as a result of the incident light that had a wavelength range of 250 - 310 nm. Since the light at 205 nm excited such a minute fragment of the green fluorescence light, whenever there was a change in the light intensity at 205 nm, the change in resultant the green fluorescence light was not too significant. Consequently, with scenario 1 and 2, the absorbance of the nitrates was not as measurable as the absorbance determined with the laboratory spectrophotometer. However, since scenario 3 made use of a bandpass filter, it ensured that the majority of the green light that was fluoresced by the

scintillator was induced by the incident light of a wavelength of 195 to 205 nm. This could be a reason why the absorbance of the nitrates, measured with scenario 3, correlated more to the absorbance measured with the laboratory spectrophotometer.

With the addition of the bandpass filter, the light source was only emitting a narrow wavelength range of 195 to 205 nm. Contrarily for scenario 1 and 2, the light source was emitting a wide wavelength range of 185 to 400 nm. As mentioned in Section 2.5.1, the use of polychromatic source can cause the analyte to experience different molar absorptivity towards the different wavelengths of an incident polychromatic light and thus influence the measured absorbance. If Figure 3.4, in Section 3.3 (page 44), is observed, the absorbance of nitrates can be perceived for a wide range of wavelengths. It is clear that the nitrates absorbed the most light at approximately 195 to 210 nm. Contrarily, for wavelengths between 250 to 400 nm, the nitrates absorbed a minute amount of light. If the overall absorbance of nitrates is measured for all wavelengths between 185 to 400 nm, then it can be expected, that the magnitude of the absorbance will be small. The reason being that nitrates only have a high absorbance at approximately 195 to 210 nm, which accounts for a fraction of the region of between 185 to 400 nm. Scenario 3, eliminated 95 % of the spectrum that was being emitted, by adding a bandpass filter that was centred about λ_{max} for nitrates. Therefore, in scenario 3, the absorbance was being measured in a small region were nitrates experience a UV absorbance of similar magnitude. Consequently, the addition of the bandpass filter could have lessened the effects that occur with the use of a polychromatic source. Hence, this is another potential reason why scenario 1 and 2 did not do as well as scenario 3.

The laboratory spectrophotometer makes use of a monochromator that permits only one or a very narrowband of wavelengths to be emitted onto the analyte. Therefore, the laboratory spectrophotometer was not prone to the effects of the use of a polychromatic light source. On the contrary, scenarios 1, 2 and 3 were all emitting more than one wavelength onto the analyte. This could be why the molar absorptivity of the three scenarios differed from that of the laboratory spectrophotometer. However, since scenario 3 was emitting a smaller range of wavelengths, in comparison to scenario 1 and 2, the effects of the use of a polychromatic source could have still been present, but it was not as pronounced as for scenarios 1 and 2. This could be why the molar absorptivity of scenario 3, differs the least from the molar absorptivity of the laboratory spectrophotometer.

Furthermore, it is also possible that the measured magnitude of the light intensity of the reference sample for the three scenarios was more significant than that of the laboratory spectrophotometer. This could be why the molar absorptivity for all three scenarios was less than that of the laboratory spectrophotometer. Another factor that could have influenced the results is that the laboratory spectrophotometer directly detects the UV light that is

transmitted through the cuvette. While, in all three scenarios, the smartphone camera was indirectly detecting the UV light that was first transmitted through the cuvette and then converted into green light.

Finally, this investigation proved that all three scenarios were able to sense nitrate samples while conforming to Beer-Lambert's law. The investigation also established that the diffracting grating, used in scenario 1, was dispensable since, in scenario 2, without the diffraction grating the smartphone-based nitrate sensor still operated almost equally. However, the diffraction grating would have been useful if the UV spectrum was being directly analysed without the scintillator and more than one chemical was to be analysed. The reason being that the diffraction grating would allow one to know at which wavelengths was light being absorbed, and whether the wavelengths corresponded to λ_{max} of the various analytes. In this case, the diffraction grating provided the spectrum of the fluoresced light and helped confirmed that the scintillator was shifting the UV light into green light, with a relative spectral power distribution that was similar to the one described by the manufacturer. Nonetheless, the results attained with scenario 1 and 2 had an unusually low molar absorptivity. Such a low molar absorptivity suggested that scenario 1 and 2 had a low measurability and sensitivity, which could be problematic. Especially in a situation where the concentration of nitrate samples differ by less than one ppm, then absorbance may be inaccurate or unquantifiable. Nonetheless adding a bandpass filter with a narrow band about λ_{max} helped enhance the performance of the smartphone-based nitrate sensor, as seen with scenario 3. Even though the bandpass filter came at an expense, it improved the measurability and sensitivity of the smartphone-based nitrate sensor while limiting the size and weight of the overall system. By analysing the results, it was evident that scenario 3 was the closest to working on par with the laboratory spectrophotometer. Therefore, scenario 3 had proven to be the most suitable for this application. Moreover, the bandpass filter proved to be indispensable. Hence, the final prototype was built by implementing the components and design of scenario 3 (as illustrated in Appendix B). For the remainder of the thesis, only scenario 3 was taken into consideration.

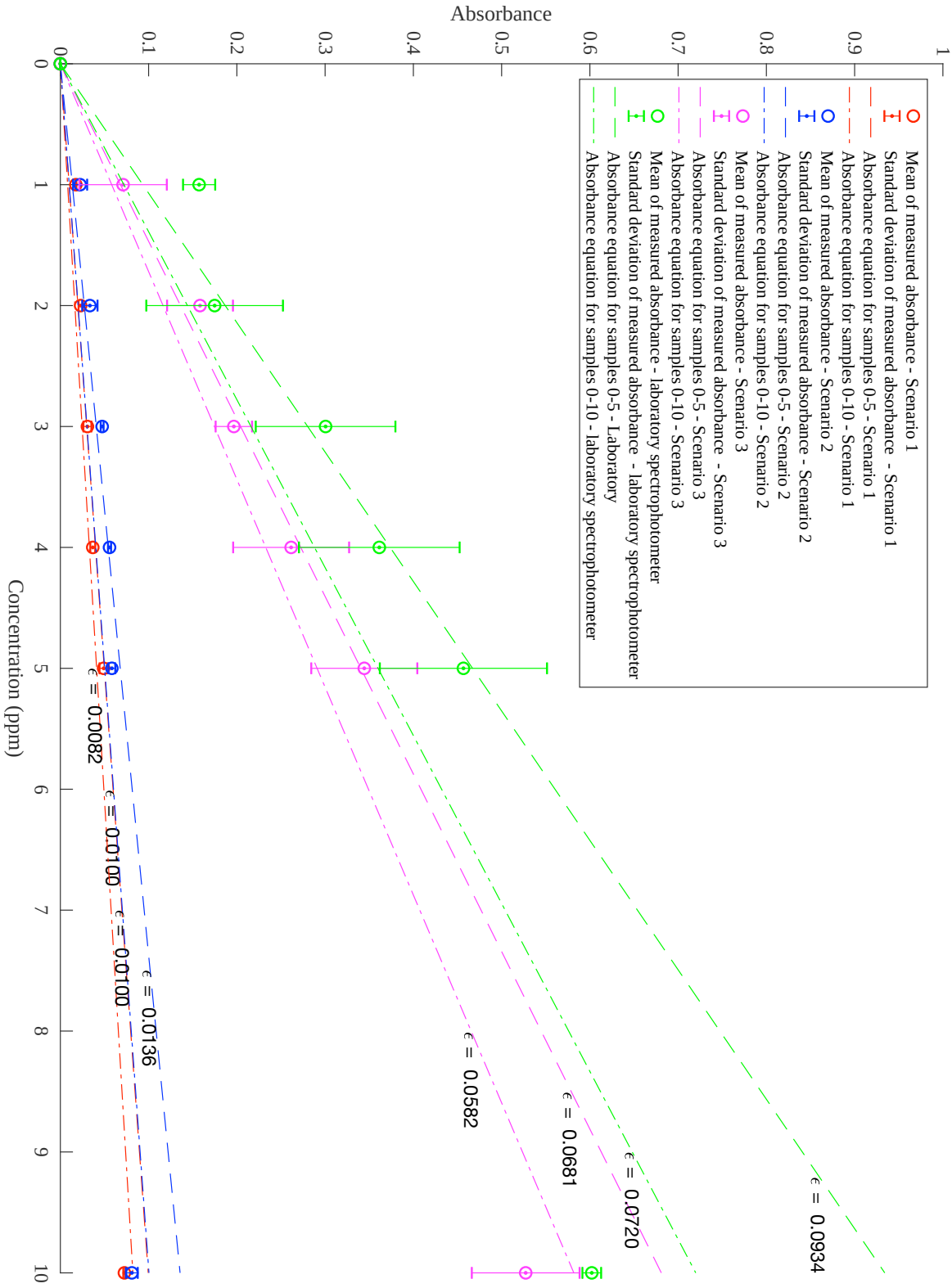

Figure 4.4: Comparison of the three scenarios and the laboratory spectrophotometer. The mean absorbances measured and the measured ϵ of each scenario and the laboratory spectrophotometer can be observed. There is a clear distinction between the performance of the laboratory spectrophotometer and scenario 1 and 2. The distinction between the performance of laboratory spectrophotometer and scenario 3 is much smaller.

4.2 Validation of smartphone-based nitrate sensor

This section validates the performance of the smartphone-based nitrate sensor by using nitrate samples of unknown concentration. More specifically, this section verifies the ability of the smartphone-based nitrate sensor to sense the concentration of a nitrate sample, by comparing its results against the results achieved with a laboratory spectrophotometer.

Before performing the validation, it was necessary to calibrate both the smartphone-based nitrate sensor and the laboratory spectrophotometer. The smartphone-based nitrate sensor was calibrated by finding the absorbance equation of the absorbance plot measured in Section 4.1.3, shown in Figure 4.3 (page 66), using the algorithm described in Section 3.7.3. However, the only samples that were taken into consideration were 1 to 5 ppm, since sample 10 ppm was out of the linear region. The laboratory spectrophotometer was calibrated by finding the absorbance equation of the absorbance curve achieved in Section 3.2, shown in Figure 3.3a (page 43), using a similar procedure followed in the algorithm described in Section 3.7.3. Again, the only samples taken into consideration were 1 to 5 ppm. Equations 4.2.1 and 4.2.2 give the absorbance equation determined for the smartphone-based nitrate sensor and the laboratory spectrophotometer, respectively.

$$A = 0.0681C \tag{4.2.1}$$

$$A = 0.0934C \tag{4.2.2}$$

The approach for this validation was to determine the ability of the smartphone-based nitrate sensor to determine the nitrate concentration of a nitrate sample of unknown concentration. To serve as the nitrate sample of unknown concentration, an environmental sample that had a high likelihood of containing nitrates, was to be used. For this application, effluent water was chosen as the environmental sample. Effluent water is found in wastewater treatment plants, as it is produced during one of the treatment processes. During the treatment of wastewater, the wastewater undergoes a process, called nitrification, which breaks down the ammonia present in the wastewater into nitrates and nitrites [68]. The water that is produced in this process is referred to as effluent water [68]. The nitrate concentration of effluent water can vary sporadically, as it is influenced by the source, geographic area, seasons, weather conditions and other factors of the plant [69]. It was reported that the range of nitrate concentration in the effluent water found in three Eastern Cape wastewater treatment plants was 0.24 to 26.5 ppm [69]. In June 2005 the nitrate concentration of the effluent water found in 22 wastewater treatment facilities in the Western Cape varied from 16.0 to 83.2 ppm [70]. The local

municipal Wastewater Treatment Plant (WWTP) recorded a nitrate concentration that ranged from 11.1 to 29.7 ppm for the month of July 2019 [71]. The effluent sample used to validate the smartphone-based nitrate sensor was collected on the 10^{th} July 2019 from the local municipal WWTP. The municipal WWTP recorded that the effluent water had a nitrate concentration of 18.2 and 21.3 ppm on the 8^{th} and 15^{th} July, respectively [71]. Since the collection day was on the 10^{th} July 2019, it was estimated that nitrate concentration measured with both devices would be closest to the concentration measured on the 8^{th} July 2019. However, considering that significant variances could occur within two days, it was supposed that potentially both devices could measure a nitrate concentration that would lie between or close to the range of 18.2 and 21.3 ppm.

Before the smartphone-based nitrate sensor was tested with the effluent water, it was necessary to test the effluent water with the laboratory spectrophotometer. Subsequently, the results measured with the laboratory spectrophotometer would be compared to the results measured with the smartphone-based nitrate sensor. Additionally, by first testing the effluent water with the laboratory spectrophotometer, it would be known whether the concentration of nitrates in the collected effluent water was detectable or not. Moreover, it would confirm whether the concentration was not too low or too high for the laboratory spectrophotometer to sense. If the laboratory spectrophotometer was not able of detecting the concentration of the nitrates in the effluent water, then chances were that the smartphone-based nitrate sensor would not be able to do so either.

When the effluent sample was tested with the laboratory spectrophotometer, the concentration of the effluent sample was found to be too high. Therefore the effluent sample had to be diluted. Consequently, the effluent water sample was diluted to produce three different samples. The first diluted sample had a composition of 2 parts effluent water to 8 parts distilled water (1:5). The second and third diluted samples had a composition of 1:10 and 1:20, respectively.

The three diluted samples were then analysed using the laboratory spectrophotometer. Once again, distilled water was used as the reference sample. For each diluted sample, the absorbance was determined. Then, by using Equation 4.2.2, the concentration of each diluted sample was calculated. Subsequently, another set of three diluted samples with the same composition of 1:5, 1:10 and 1:20, respectively, was also prepared from the effluent water. Then the exact process of determining the concentration, with the laboratory spectrophotometer, was followed. The measured concentrations of the first and second set of diluted samples can be found in Tables 4.1 and 4.2, respectively.

Thereafter, the two sets of the three diluted samples were also analysed with the smartphone-based nitrate sensor, using the algorithm described in Section 3.7.3. Where the absorbance of each diluted sample was calculated and then by using Equation 4.2.1, the concentration of each diluted sample

was measured. The measured concentrations of the first and second set of diluted samples can be found in Tables 4.1 and 4.2, respectively.

Once the concentrations of the diluted sample were determined, the total initial concentration of the effluent sample was estimated. From each diluted sample, the initial concentration of the effluent sample was calculated by dividing the concentration of the diluted sample by the dilution ratio. The initial concentration of the effluent sample calculated with each diluted sample can be observed in Tables 4.1 and 4.2, for the first and second set of samples, respectively.

For simplicity, the smartphone-based nitrate sensor and the laboratory spectrophotometer will be referred to as the SNS and LS, respectively, for the remainder of this section.

For the first set of samples, the results reported in Table 4.1, show that for specific diluted samples, the concentrations obtained with the SNS and the LS were not very comparable. In general, the concentrations measured with the SNS were lower than the concentrations measured with the LS. The difference between the concentrations measured with the SNS and LS for the 1:5 and 1:10 sample was 20% and 18%, each. While for the 1:20 sample, the SNS measured a concentration that had a variance of 42% less in comparison to the LS. A relationship was observed in the change of the concentration between every two samples. The SNS and LS measured a change of 49% and 47%, individually, between the 1:5 and 1:10 sample. While, the SNS and LS measured a change between the 1:10 and 1:20 sample of 38% and 51%, individually.

Sample	1:5	1:10	1:20
Laboratory Spectrophotometer			
Concentration of Diluted Samples (ppm)	5.371	2.565	1.319
Concentration of Initial effluent sample based on diluted sample (ppm)	26.855	25.650	26.380
Smartphone-based nitrate sensor			
Concentration of Diluted Samples (ppm)	4.256	2.117	0.8116
Concentration of Initial effluent sample based on diluted sample (ppm)	21.280	21.17	16.240

Table 4.1: Concentration measured with first set of diluted samples of the effluent water sample

Unlike the first set, the concentrations of the diluted samples obtained with the SNS and LS were more comparable. The concentrations measured with the SNS were lower than the concentrations measured with the LS, likewise with the first set. The variation between the concentrations measured with the SNS

and the LS were particularly close for the 1:5 and 1:10 samples, as it differed by 4% and 10%, respectively. Contrarily, for sample 1:20, the SNS measured a concentration that was 39% less than that of the LS. A trend was observed in the change of the measured concentration between two samples, for the SNS and LS. The measured change between the 1:5 and 1:10 sample was 51% and 54% for the SNS and LS, respectively. As for the 1:10 and 1:20 sample, the measured change was 35% and 55% for the SNS and LS, respectively.

Sample	1:5	1:10	1:20
Laboratory Spectrophotometer			
Concentration of Diluted Samples (ppm)	4.214	2.298	1.276
Concentration of Initial effluent sample based on diluted sample (ppm)	21.070	22.980	25.520
Smartphone-based nitrate sensor			
Concentration of Diluted Samples (ppm)	4.031	2.077	0.745
Concentration of Initial effluent sample based on diluted sample (ppm)	20.155	20.770	14.900

Table 4.2: Concentration measured with second set of diluted samples of the effluent water sample

4.2.1 Discussion

These results indicated that SNS was relatively on par with the LS, in sensing the 1:5 and 1:10 diluted samples, especially for the second set. However, when compared to the LS, the SNS was not as successful in measuring the 1:20 diluted samples. Since the 1:20 diluted sample only contained 5 ppm of the effluent water, it was probable that the nitrate concentration was too small for the SNS to sense it correctly. As suggested in Section 2.5.1, lower concentrations can deviate from Beer-Lambert's law, because the difference between the signals measured for a reference and a lower concentration sample can be so small, that inaccuracies may occur. This could explain why the SNS and LS measured significantly different concentrations, for the 1:20 diluted samples.

It was expected to observe a change of 50% between each dilution since the 1:5 sample is 50% more concentrated than 1:10 sample, and 1:10 sample is 50% more concentrated than 1:20 sample. For both sets, the LS measured a change of approximately 50% between each diluted sample. Nevertheless, for both sets, the SNS only measured a change of approximately 50% between the 1:5 and 1:10 sample. The SNS overestimated the change between the 1:10

and 1:20 samples. The deviation in the ratio difference between the 1:10 and 1:20 samples, further implied that the SNS had inaccurately measured the concentration of both sets of 1:20 samples.

By analysing the concentration of the initial effluent sample calculated with both sets of the 1:20 sample, it was further suggested that the SNS was not able to sense the concentration of the 1:20 samples accurately. The reason being that the concentration of the initial effluent sample calculated with the 1:20 sample diverged from initial concentration calculated with the other two diluted samples by over 23% and 26% for the first and second set of samples respectively.

Since various evidence alluded to the invalidity of the measurement of the 1:20 samples for the SNS, it was decided that the 1:20 samples would be ignored from the calculation of the mean concentration of the initial effluent sample. Figure 4.5 displays the mean concentration of the initial effluent sample for each set of sample, calculated without the inclusion of the 1:20 samples. As observed in Figure 4.5, the standard deviation of the mean concentration of the initial effluent sample determined with the first set of samples did not overlap. However, for the second set of samples, the standard deviation of the mean concentration of the initial effluent sample did overlap. Moreover, the SNS measured a mean concentration of the initial effluent sample for both samples that were significantly approximate to that of the LS. More specifically, the variation between the mean concentration of the initial effluent sample determined with the SNS and LS was 19% and 7% for the first and second set of samples, respectively.

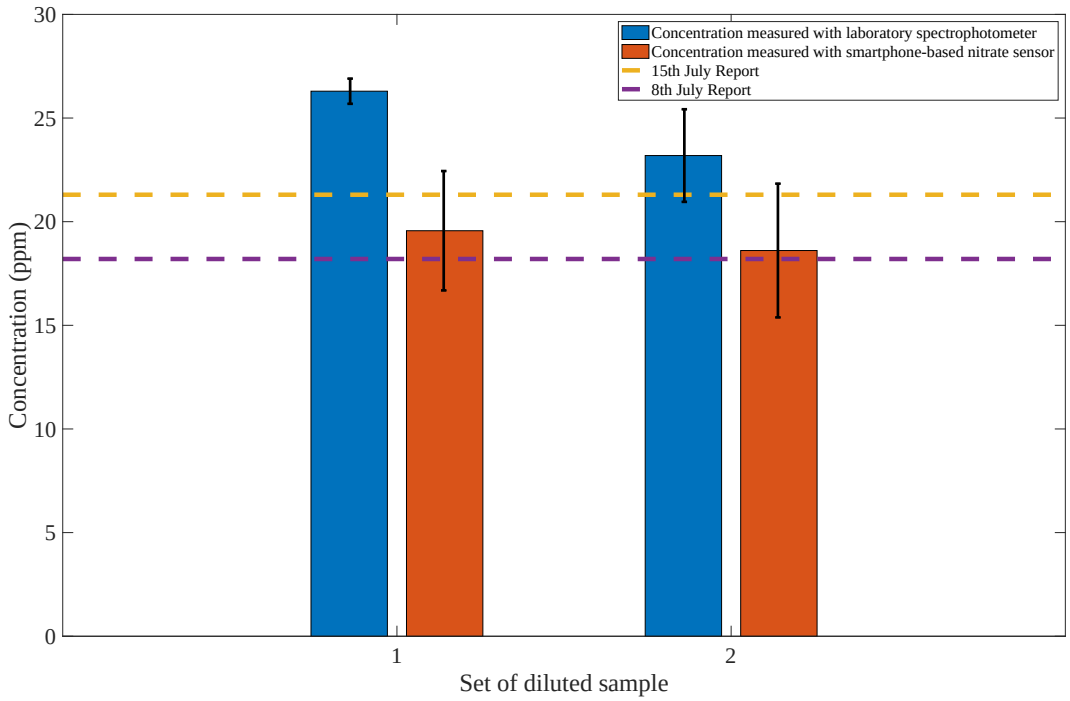

Figure 4.5: Average concentration of initial effluent water sample. For both the LS and SNS, the average concentration of the initial effluent water sample (collected on the 10th July) was calculated for the first and second set of diluted samples. A slight variance between the average concentration of the initial effluent water measured with the SNS and LS is observed for the first set of diluted samples. A less significant variance between the average concentration of the initial effluent water measured with the SNS and LS is observed for the second set of diluted samples. The average concentration of the initial effluent water measured with the SNS lies between the concentrations reported on the 8th and 15th July. The average concentration of the initial effluent water measured with the LS is slightly higher than both the concentrations reported on the 8th and 15th July.

In general, the concentration measured with SNS was slightly lower than the concentration measured with the LS, for all diluted samples. A possible reason for this difference could be due to the issues associated with polychromatic sources. For the SNS setup, even though the bandpass filter was restricting the number of wavelengths emitting onto the sample, there was still a small range of wavelengths interacting with the sample. Contrarily, for the LS, only one or a very narrow band of wavelengths was emitting onto the sample. As mentioned in Section 2.5.1, emitting various wavelengths onto a sample can affect the ability of the absorbance of the sample to follow Beer-Lambert's law. Therefore, it is possible that the functionality of the SNS was being affected by this issue. Alternatively, It could otherwise be that the SNS might have

measured an intensity for the reference sample that was considerably higher than the intensity measured with the LS.

It was predicted that nitrate concentration of the initial effluent sample measured with SNS and LS would have fallen within or around the range reported by the municipal WWTP for the 8th and 15th July 2019. The mean concentration measured with the SNS was within the concentration interval reported by the municipal WWTP. Additionally, It is apparent that the SNS measured a concentration that was closest to the mean concentration reported on the 8th by the municipal WWTP.

Conclusively, the results achieved with the SNS were similar to the results of the LS, especially for the second set of samples. The SNS performed well in sensing the more highly concentrated diluted samples. Though for the least concentrated, diluted sample, the SNS was not able to determine the concentration with accuracy. However, such low levels of nitrates in water do not pose any adverse health threats to the aquatic system and humans. Therefore, it was not a grave problem that the SNS could not precisely measure low concentrations. For this same reason, the 1:20 sample was not considered when calculating the mean concentration of the initial effluent sample. The SNS was relatively on par with the LS in terms of measuring the mean concentration of the initial effluent sample. This was especially true for the second set of samples, where the difference between the mean determined with the SNS and LS was minor. Additionally, the mean concentration of the initial effluent sample measured with the SNS was similar to the concentration reported by the municipal WWTP. Therefore, these results implied that the performance of the SNS was satisfactory.

4.3 Achievements of the smartphone-based nitrate sensor

This section reports the overall quantitative achievements of the smartphone-based nitrate sensor, in terms of its accuracy, sensitivity, resolution and detection range. Additionally, this section compares the achievements of the smartphone-based nitrate sensor with the related works reviewed in Section 2.11.

The accuracy of the smartphone-based nitrate sensor was determined by finding the relative error between the concentrations of an unknown sample measured with the smartphone-based nitrate sensor and the laboratory spectrophotometer. As observed in the previous section, the smartphone-based nitrate sensor had a relative error of 7% to 19% (reported in Table 4.3).

The sensitivity of the smartphone-based nitrate sensor was measured by determining the relationship between the input (concentration) and the output signal (measured intensity). As noted in Table 4.3, the sensitivity was

1.402×10^7(pixel intensity units)/ppm.

The resolution was calculated by finding the standard deviation of the measured intensities for 3 reference samples and dividing it by the sensitivity. Consequently, the resolution was found to be 0.2014 ppm, as shown in Table 4.3.

Table 4.3 shows that the detection range achieved with the smartphone-based nitrate sensor was 1 - 5 ppm. Nonetheless, samples of higher concentrations can be measured with the smartphone-based nitrate sensor by diluting the sample, as it was observed in the previous section the smartphone-based nitrate was able to detect up to 21 ppm.

Parameter	Quantity	Units of measurement
Accuracy	7 - 19	Relative Error (%)
Sensitivity	1.402×10^7	Pixel Intensity per Concentration (P.U/ppm)
Resolution	0.2014	Concentration (ppm)
Detection range	1 - 5	Concentration (ppm)

Table 4.3: Quantitive achievements of the smartphone-based nitrate sensor

4.3.1 Comparison of the smartphone-based nitrate sensor with related works

This section provides a comparison between the performance of the smartphone-based nitrate sensor and the current literature discussed in Section 2.11. Table 4.4 outlines the achievements of the current related literature and the smartphone-based nitrate sensor, in terms of their resolution, detection range, sensitivity, ease of use and costs. However, most of the authors did not mention or specify the quantity for all achievements. The overall costs of the smartphone-based nitrate sensor can be found in Appendix F.

Author	Resolution	Detection range	Sensitivity	Ease of use	Cost(R)
[55]	Not mentioned	0 - 2 ppm	Not mentioned	Easy	7600
[56]	1.23×10^{-4}ppm	0 - 0.1 ppm	0.86 A.U/ ppm	Easy	3000
[31]	1 nm	Not mentioned	Not mentioned	Easy	Low
[30]	Not mentioned	Not mentioned	0.305 nm/pixel	Easy	Low
[15]	1 nm	Not mentioned	Good	Easy	7600
[20]	2 nm	6 - 309 ppm	Not mentioned	Medium	Low
This	0.2014 ppm	0 - 5 ppm	1.402×10^7P.U/ppm	Easy	11500

Table 4.4: Achievements of the related literature and the smartphone-based device

Authors [55] and [56] developed a smartphone-based fluoride sensor based on colourimetry, and author [20] developed a smartphone-based nitrate sensor based on electrochemistry. Authors [31], [30] and [15] implemented general-purpose smartphone-based spectrophotometers; as such, these authors were

mainly interested in assessing the spectral performance of their devices rather than the device's concentration detection abilities. For this reason, the resolution, detection level and sensitivity stated by these authors were not compared to that of the smartphone-based nitrate sensor.

The resolution of the smartphone-based nitrate sensor was relatively high but not as high as the resolution reported by [56]. However, the purpose of the smartphone-based nitrate sensor was not to detect minute concentrations; therefore, it was not essential to have a very high resolution. The detection range of the smartphone-based nitrate sensor was overlapped with the detection range reported by [55] and [56], however, the upper limit of the detection range was higher than that reported by [55] and [56]. In comparison to [20], the detection range of the smartphone-based nitrate was not similar; yet, the smartphone-based nitrate sensor could sense lower concentrations while the device described by [20] could not. Although the detection range of provided by [20] included very high concentrations, it was proven that through dilutions, the smartphone-based nitrate sensor was also able to measure higher concentrations. The sensitivity of the smartphone-based nitrate sensor was almost half as much as the sensitivity recorded by [56], but since the purpose of the smartphone-based nitrate sensor was not to detect minute concentrations; the achieved sensitivity was enough for this application. The ease of use of the smartphone-based nitrate sensor was comparable to most of the devices discussed in the literature. The smartphone-based nitrate sensor was adaptable to most smartphones, like most devices reported. Nevertheless, the device designed by [20] was only adaptable to phones that have an auxiliary port. All the smartphone-based devices were easily portable and user-friendly. In terms of costs, the smartphone-based nitrate sensor was more costly than the applications whose costs were stated. Nonetheless, relative to a typical UV-Vis spectrophotometer, the smartphone-based nitrate sensor was affordable. Additionally, the potential for a smartphone-based device to perform UV analysis of nitrates, at 205 nm, outweighed the costs of the smartphone-based nitrate sensor.

4.4 Summary

In this chapter, the three design scenarios of the smartphone-based nitrate sensor were compared. Mainly, the necessity of the diffraction grating and the bandpass filter were assessed. Upon the comparison of all three scenarios is was concluded that the bandpass filter was necessary, as it allowed the smartphone-based nitrate sensor to produce results that were most similar to the laboratory spectrophotometer. Therefore, the final prototype of the smartphone-based nitrate sensor utilised a bandpass filter. Thereafter, this chapter reported the validation of the performance of the final prototype of the smartphone-based nitrate sensor. The validation was achieved by comparing

the concentration of an unknown sample with the smartphone-based nitrate sensor and the laboratory spectrophotometer. From the unknown sample, two sets of diluted samples were prepared, as the concentration of the initial unknown sample was too high to be detected. The results showed that the smartphone-based nitrate sensor was able to measure the concentration of the unknown sample reasonably well, with an accuracy of 19% and 7%, for the first and second set of samples, respectively, in comparison to the laboratory spectrophotometer. Finally, the overall achievements of the smartphone-based nitrate sensor were discussed and analysed against the current literature. The smartphone-based nitrate sensor attained a sensitivity of 1.402×10^7P.U/ppm, a resolution of 0.2014 ppm, and a detection limit of $1 - 5$ ppm.

Chapter 5

CONCLUSION

When water is contaminated with high concentrations of nitrates, it can place in danger the aquatic environment, aquatic life and ultimately, humans who consume it. Such gangers include eutrophication and anoxia, which are conditions that severely deteriorate the aquatic environment and create a propitious site for disease-causing bacterias. In humans, high concentrations of nitrates can induce many health concerns, such as cancer and methaemoglobinaemia ("blue baby syndrome"). Methaemoglobinaemia is a condition that inhibits the circulation of oxygen in one's body and leads to lifetime complications or eventually becomes fatal. Fetuses, infants, and adults with particular predispositions are the most vulnerable to methaemoglobinaemia. The latter might not be of huge consequence in developed countries, but in least developed countries and areas, nitrate contamination is more prevalent and causes significant health concerns. Residents of rural areas, especially the ones reliant on agriculture, are in jeopardy of the health complications that the consumption of high nitrates concentrations can generate. The reasons are that, firstly, agricultural activities worsen water quality and contribute to nitrate contamination. Secondly, in rural areas, water treatment and sanitation facilities are rudimentary or non-existent. Lastly, the detection of nitrates requires intricate equipment, which is not usually accessible to individuals or communities in rural areas.

In light of the above, this research aimed to develop a smartphone-based sensor that could measure nitrate concentrations in water through the use of spectrophotometric analysis. Spectrophotometry is a conventional method used to detect nitrate levels in water samples. Spectrophotometry operates based on Beer-Lambert's law that states that the absorbance of light through a sample is proportional to the concentration of the sample. Hence, spectrophotometry quantifies the amount of light, of a fixed wavelength, that a chemical absorbs. Through this quantification, the concentration of the chemical is estimated. To best determine the nitrate concentration of a sample, the absorbance of the sample is measured using UV light, typically at 205 nm.

A challenge arose with the implementation of a smartphone-based sensor that could detect UV light (specifically at 205 nm). The cause of the challenge

was that smartphone cameras are not intended for UV light, particular not at wavelengths as low as 205 nm. Therefore, to implement the smartphone-based nitrate sensor, it was necessary to address these constraints.

Ultimately, the purpose of this research was to develop a "lab-in-a-suitcase" water quality sensor, specific to nitrate sensing that implemented the principles of spectrophotometry (UV spectroscopy) and to use a smartphone camera as a detector while overcoming the UV light detection limitations of a smartphone camera. Additionally, the instrument was to be inexpensive and portable in comparison to its traditional counterparts.

5.1 Objective fulfilment

This research addressed the problem statement and fulfilled the purpose of the project by establishing and addressing three main objectives related to the problem statement. Figure A.1 on page 99, illustrates a complete layout of the thesis, as well as where the objectives accomplished. This section discusses the fulfilment of the three objectives stated in Section 1.2.

1. Objective 1: Assess the suitability of spectrophotometry as the means of measuring nitrates for this smartphone-based nitrate sensor.

   To arrive at Objective 1, it was necessary to meet four sub-objectives:

   a) Assess spectrophotometry against other chemical analytical methods, commonly used to detect nitrates - based on the literature.

   b) Assess and choose appropriate light source - based on the literature.

   c) Assess and choose appropriate sample holder - based on experiments.

   d) Assess methods of shifting UV light into visible light.

   Objective 1(a), in Section 2.3, was successfully achieved by reviewing the most common chemical analytical methods that are used to identify nitrates in water. These methods were chromatography, electrochemistry and spectrophotometry - categorised into colourimetry and UV-VIS spectroscopy. Although spectrophotometry had its limitations, it was the least complex and most feasible to implement, making it the most suited for this application.

   A literature investigation was performed, in Section 2.7, to realise Objective 1(b) and learn which light sources were typically used for spectrophotometry. The light sources that were commonly implemented included tungsten and deuterium. However, these sources were not appropriate for this application, since they are costly, extensive and coud not be easily manoeuvred. Consequently, other compact sources such as UV LEDs

were reviewed. Nonetheless, most compact light sources did not emit at a wavelength of 205 nm - the wavelength required to detect nitrates. The ideal option was a compact deuterium light module, namely the Compact FiberLight D_2 considering that it was the only compact source that was found to emit at a wavelength of 205 nm.

Further, Objective 1(c) was successfully attained by studying the three main types of cuvettes used in spectrophotometry: glass, plastic and quartz. Firstly, in Section 2.8, a literature review was performed on the available types of cuvettes and their suitability for UV analysis. It was learnt that the recommended cuvette for UV analysis was quartz as it did not absorb much UV light, that is to say, quartz was transparent to UV light. By being transparent to UV light at 205 nm, quartz cuvettes allow for the absorbance of nitrates to be detected without interferences. However, it was speculated that opacity of the glass or plastic cuvettes towards UV light could be compensated for and that the detection of nitrate, at 205 nm, could be made possible to some extent. To verify this speculation, in Section 3.2, two experiments were performed with the three types of cuvettes. Both experiments were completed using a laboratory spectrophotometer to analyse how well each cuvette absorbed UV light at 205 nm. The first experiment consisted of measuring the amount of light each empty cuvette absorbed throughout the electromagnetic spectrum. The second experiment involved measuring the absorbance of a few nitrate samples of varying concentrations, using each cuvette. Eventually, the results of the experiments verified that the quartz cuvette was the most appropriate cuvette for this application since it was the only cuvette that allowed for accurate nitrate detection.

Regarding Objective 1(d), the aim of this project included the use of a smartphone camera as the detector. With spectrophotometry, the concentration of a nitrate sample is analysed by detecting how much UV light, usually at 205 nm, is absorbed by the nitrate sample. However, smartphone cameras are not meant for UV light detection, especially not at such a low wavelength of 205 nm. Therefore, it was required to perform a spectral shifting of the UV light into visible light. In the literature review (Section 2.10), it was discovered that the UV light could be transformed into visible through the use of certain fluorescence materials. These materials varied from porcelain to synthesised phosphors and scintillators; however, Lumilass was the scintillator that was readily available and that had been designed explicitly for converting UV into visible light, specifically green light. In this way, Objective 1(d) was fulfilled.

2. Objective 2: Design and build a prototype of the smartphone-based nitrate sensor that uses spectrophotometry to detect nitrates.

It was necessary to reach four sub-objectives to achieve Objective 2:

a) Preform a spectral shift of UV light into visible light.

b) Evaluate the necessity of typical components used in spectrophotometers.

c) Implement an algorithm to determine the concentration of nitrates in a water sample, based on the information captured by the smartphone.

d) Calibrate the smartphone-based nitrate detector, using known nitrate samples.

In Section 3.4, Objective 2(a) was accomplished. The scintillator was tested to confirm the findings of the literature review which stated that scintillator could successfully perform a spectral shift of the UV light emitted by a light source into green light. The test consisted of emitting the UV light onto the scintillator and observing whether scintillator would fluoresce a green light. Indeed, the test proved that scintillator was able to convert the UV light emitted onto it into green light.

Concerning Objective 2(b), typically spectrophotometry makes use of sophisticated and expensive components, that also add up to the size of the spectrophotometer. Therefore, it was investigated whether commonly used components in spectrophotometers were required for the smartphone-based nitrate sensor to function optimally. To test this, three scenarios of the smartphone-based nitrate sensor were designed, as illustrated in Section 3.5. Each scenario consisted of a smartphone, a scintillator, a quartz cuvette and a light source as the fundamental components. Though, for scenario 1, a diffraction grating was added, while in scenario 2 the diffraction grating was removed. Lastly, in scenario 3, a bandpass filter was added. All three scenarios of the smartphone-based nitrate sensor were evaluated against one another and the laboratory spectrophotometer, as explained in Section 4.2 and thus Objective 2(b) was met. The results revealed that the smartphone-based nitrate sensor could still perform adequately without the diffraction grating, considering that the results achieved with and without the diffraction grating were fairly similar. The diffraction did not have much of an effect on the performance because its sole purpose is to split into its separate beams. Even though the light was split into its beams, the overall intensity of all the light beams should still be equivalent to the intensity of the same light when it is concentrated, i.e. not diffracted. Nonetheless, the smartphone-based nitrate sensor produced the most reliable results when the bandpass filter was attached. The results achieved with the use of the bandpass filter were the most comparable to the results measured with the laboratory spectrophotometer. Additionally, the inclusion of

the bandpass filter allowed the smartphone-based nitrate sensor to have a high measurement sensitivity. Therefore, it was inferred that although the diffraction grating was redundant, the bandpass filter was indispensable since it did increase to the functionality of the smartphone-based nitrate sensor.

Objective 2(c) was carried through as reported in Section 3.7, where an algorithm was developed to determine the concentration of a nitrate sample. The algorithm was responsible for analysing the image of the captured output light fluoresced by the scintillator. Through this analysis, the algorithm calculated the absorbance of the light emitted onto the nitrate sample. After saving enough data, the algorithm was able to calibrate the absorbance versus the concentration of nitrates. Through the calibration, the algorithm could estimate the concentration of a nitrate sample. The implementation of the algorithm, as explained in Section 4.1, was used to measure the absorbance of nitrate samples of known concentrations. Additionally, in Section 4.2, the algorithm was used to calibrate the smartphone-based nitrate sensor and furthermore to determine the concentration of an unknown sample. Ultimately, the algorithm performed successfully.

Objective 2(d) was actualised and gets mentioned in Section 4.2, as the smartphone-based nitrate sensor was calibrated using the calibration algorithm described in Section 3.7.2. The calibration process defined a relationship between the measured absorbance and concentration of nitrates for the smartphone-based nitrate sensor.

3. Objective 3: Assess the validity of the designed smartphone-based nitrate sensor.

   The final requirement needed to obtain the primary intent of this project was to verify whether the performance of the smartphone-based nitrate sensor was adequate. Section 4.2 described the testing of the ability of the smartphone-based nitrate sensor to determine the nitrate concentration of an environmental sample. The test involved measuring the nitrate concentration of the environmental sample with the smartphone-based nitrate sensor and the laboratory spectrophotometer. Thereafter, the nitrate concentration measured with the smartphone-based nitrate sensor and laboratory spectrophotometer was compared to one another. The assessment proved that the smartphone-based nitrate sensor could determine the nitrate concentration of the environmental sample sufficiently. Hence, view Section 4.2 to see Objective 3 realised.

5.2 Overall evaluation

The section above proved that all three objectives set for this research project were successfully met and therefore, it was deduced that the smartphone-based nitrate sensor has the potential to measure the concentration of nitrate samples accurately. This is despite a slight variation noticed in the results which were possibly due to a difference in the components and methodology used between the smartphone-based nitrate sensor and laboratory spectrophotometer.

The smartphone-based nitrate sensor functioned ideally under controlled conditions. The controlled conditions included measuring the absorbance of prepared nitrate samples of different concentrations, with the smartphone-based nitrate sensor. The smartphone-based nitrate-sensor was able to measure the absorbance for each nitrate sample adequately, as the overall absorbance and respective concentrations were linear to one another. Therefore, the smartphone-based nitrate sensor produced results that obeyed Beer-Lambert's law. When compared to the absorbance measured with the laboratory spectrophotometer, the smartphone-based nitrate sensor performed comparably well. Even though the calibration equation of the smartphone-based nitrate sensor and the laboratory spectrophotometer were not identical, statistical similarities were still observed. These similarities suggested that the performance of the smartphone-based nitrate was pleasing.

Under uncontrolled conditions, the smartphone-based nitrate sensor did work sufficiently well in comparison to the laboratory spectrophotometer. The uncontrolled conditions included the testing of the ability of the smartphone-based nitrate sensor to sense the nitrate concentration of an environmental sample against that of the laboratory spectrophotometer. The environmental sample used was collected from the municipal Wastewater Treatment Plant. The smartphone-based nitrate sensor was able to sense the concentrations of the diluted samples with accuracy in comparison with the laboratory spectrophotometer. However, the sensor did not measure the concentrations of the lowest concentrated diluted samples with as much accuracy as the laboratory spectrophotometer. Since lower concentrations of nitrates in water do not pose threats to the aquatic and human health, it was not a concern that the smartphone-based nitrate sensor could not sense low concentrations correctly. Nevertheless, the smartphone-based nitrate sensor measured the nitrate concentration of the environmental sample with high accuracy in comparison to the laboratory spectrophotometer. Therefore, the results suggested that smartphone-based nitrate sensor was able to sense the nitrate concentration of an environmental sample comparably to the laboratory spectrophotometer. Moreover, the nitrate concentration measured with the smartphone-based nitrate sensor was approximate to the nitrate concentrations of the environmental sample reported by the municipal Wastewater Treatment Plant. Thus, further indicating that the smartphone-based nitrate sensor was able to satisfy its requirements of detecting the concentrations of environmental samples with

accuracy.

Although the prototype was only tested with an iPhone Xs, which is a high-end phone, the smartphone-based nitrate sensor should be employable with other smartphones that more affordable, such as the Google Pixel 3A and the Motorola Moto G7. These three smartphones are more or less half the price of the iPhone Xs but have very similar camera capabilities. An example of a lower-end phone that could be used is the Huawei Y5, which is a fraction of the iPhone Xs' price, yet it has a camera sensor with the same size and aperture as the iPhone Xs, but the pixel size is likely lower than that of the iPhone Xs. The lower pixel size would probably influence the noise of the light intensity, which would implicate that a greater number of images would have to be stacked.

Ultimately, this thesis satisfactorily answered the problem statement posed at the beginning of the thesis. The statement problem was accomplished by designing a smartphone-based nitrate sensor that was more affordable than other traditional equipment to a rural community. The smartphone-based nitrate sensor was designed so that it could be usable and portable beyond the confines of a laboratory. The smartphone-based nitrate sensor eliminated the use of some components typically implemented in spectrophotometry, which made the smartphone-based nitrate sensor less complicated. These characteristics make the smartphone-based nitrate sensor preferable to a laboratory spectrophotometer since the latter are usually benchtop-operatable, and consist of sophisticated components that make them very expensive. Additionally, most spectrophotometers measure the transmittance and absorbance of a sample, thereafter the calibration and the calculation of the concentration of the sample have to be manually done. However, a further advantage of the smartphone-based nitrate sensor is that the algorithm performs the calibration and calculation of the concentration. Moreover, although colourimetry is a method which can be implemented inexpensively for nitrate analysis, the smartphone-based nitrate sensor is still more convenient to use since it does not require prerequisites steps to be performed on the sample. Over and above that, in contrast to the related works, the smartphone-based nitrate sensor can perform UV analysis at 205 nm, while the other applications focused on visible or UV analysis at 310 nm. Most importantly, the smartphone-based nitrate sensor is successfully capable of detecting and sensing the concentration of nitrates in a water sample.

5.3 Recommendation

The smartphone-based nitrate sensor could have provided better results, if a bandpass filter with a more narrow bandwidth, centring at 205 nm, were used. It would eliminate the inaccuracies and constraints that are caused by using a polychromatic light source.

Additional work could be done to implement a fourth design scenario, which would include the smartphone, the scintillator, the quartz cuvette, the light source, the bandpass filter and the diffraction grating, to further investigate the necessity of the diffraction grating and bandpass filter.

5.4 Further works

The use of a quartz cuvette influenced the cost of implementation of the smartphone-based nitrate sensor. However, there were no other available alternatives to quartz cuvettes that could be used for this application. It was considered that an alternative holder could be developed, one where the transparent sides are made of quartz, while the bottom and the translucent sides are made of plastic.

The Compact FiberLight D_2 was the most critical factor to the cost and size of the smartphone-based sensor. Nonetheless, it was the best option for this project, since all the other compact UV light sources that are much lighter and inexpensive, such as UV LEDs cannot emit at wavelengths as deep as 205 nm. However, in the next few years, more advances will probably be presented in UV LED technologies, that will enable UV LEDs to emit at wavelengths as low as 205 nm.

Bibliography

[1] All-About-Water-Filters.com, "Lack of clean water in africa: Understanding the reasons behind the water crisis." [Online]. Available: http://all-about-water-filters.com/lack-of-clean-water-in-africa/#tab-con-1

[2] G. T. Howard S.Peavy, Donald R. Rowe, *Environmental Engineering*. McGraw-Hill Book Company, 1985.

[3] MicahGallant, "Nitrates and their effect on water quality – a quick study." [Online]. Available: http://www.wheatleyriver.ca/media/nitrates-and-their-effect-on-water-quality-a-quick-study/

[4] W. H. Organisation, "Water-related diseases water-related diseases water-related diseases water-related diseases water-related diseases water-related diseases." [Online]. Available: http://www.who.int/water_sanitation_health/diseases-risks/diseases/methaemoglob/en/

[5] A. Ozcan, "Mobile phones democratize and cultivate next-generation imaging, diagnostics and measurement tools," *Lab Chip*, vol. 14, no. 17, pp. 3187–3194, 2014. [Online]. Available: http://xlink.rsc.org/?DOI=C4LC00010B

[6] B. I. SA. (2019, February) More than 13 million new smartphones were sold in south africa last year – and almost two-thirds cost less than r1,500. [Online]. Available: https://www.businessinsider.co.za/more-than-13-million-new-smartphones-were-sold-in-south-africa-last-year-and-almost-two-thirds-c

[7] D. Radcliffe. (2018, Octiber) Mobile in sub-saharan africa: Can world's fastest-growing mobile region keep it up? [Online]. Available: https://www.zdnet.com/article/mobile-in-sub-saharan-africa-can-worlds-fastest-growing-mobile-region-keep-it-up/

[8] M. Sohail and S. B. Adeloju, "Nitrate biosensors and biological methods for nitrate determination," *Talanta*, vol. 153, pp. 83–98, 2016. [Online]. Available: http://dx.doi.org/10.1016/j.talanta.2016.03.002

[9] S. Higson, *Analytical Chemistry*. Oxford University Press Inc., 2004.

[10] F. J. N. T. A. Skoog, Douglas A.; Holler, *Principles of Instrumental Analysis*, 5th ed. Brooks Cole, 1998.

[11] C. A. D. Thomas Wenzel, "Beer's law," June 2019. [Online]. Available: https://chem.libretexts.org/Bookshelves/Analytical_Chemistry/Supplemental_Modules_(Analytical_Chemistry)/Analytical_Sciences_Digital_Library/Active_Learning/In_Class_Activities/Molecular_and_Atomic_Spectroscopy/03_Text%3A_Molecular_and_Atomic_Spectroscopy/1%3A_General_Background_on_Molecular_Spectroscopy/1.2%3A_BeerâĂŹs_Law

[12] A. Drolc and J. Vrtovšek, "Nitrate and nitrite nitrogen determination in waste water using on-line UV spectrometric method," *Bioresource Technology*, vol. 101, no. 11, pp. 4228–4233, 2010. [Online]. Available: http://dx.doi.org/10.1016/j.biortech.2010.01.015

[13] R. J. Karlsson, M., Karlbergb, Bo, Olssona, "Determination of nitrate in municipal waste water by UV spectroscopy," *Analytica Chimica Acta*, vol. 312, no. 1, pp. 107–113, 1995.

[14] D. Igoe, A. Parisi, and B. Carter, "Characterization of a smartphone camera's response to ultraviolet a radiation," *Photochemistry and Photobiology*, vol. 89, no. 1, pp. 215–218, 2013.

[15] T. C. Wilkes, A. J. S. McGonigle, J. R. Willmott, T. D. Pering, and J. M. Cook, "Low-cost 3d printed 1âĂĽâĂĽnm resolution smartphone sensor-based spectrometer: instrument design and application in ultraviolet spectroscopy," *Optics Letters*, vol. 42, no. 21, p. 4323, 2017. [Online]. Available: https://www.osapublishing.org/abstract.cfm?URI=ol-42-21-4323

[16] "Blue baby syndrome," April 2018. [Online]. Available: http://www.bhia.org/articles/childrens-health/bluebabysyndrome.html

[17] Q. H. Wang, L. J. Yu, Y. Liu, L. Lin, R. gang Lu, J. ping Zhu, L. He, and Z. L. Lu, "Methods for the detection and determination of nitrite and nitrate: A review," *Talanta*, vol. 165, no. October 2016, pp. 709–720, 2017.

[18] D. of Water Affairs and Forestry, "South african water quality guidelines," 1996.

[19] K. Academy, "Principles of chromatography principles of chromatography principles of chromatography principles of chromatography principles of chromatography principles of chromatography." [Online]. Available: https://www.khanacademy.org/test-prep/mcat/chemical-processes/separations-purifications/a/principles-of-chromatography

[20] X. Wang, M. R. Gartia, J. Jiang, T. W. Chang, J. Qian, Y. Liu, X. Liu, and G. L. Liu, "Audio jack based miniaturized mobile phone electrochemical sensing platform," *Sensors and Actuators, B: Chemical*, vol. 209, pp. 677–685, 2015. [Online]. Available: http://dx.doi.org/10.1016/j.snb.2014.12.017

[21] J. P. Ingles, "Cow dung sniffer," 2017.

[22] N. Aeronautics and S. Administration. (2013, MARCH) The electromagnetic spectrum. [Online]. Available: https://imagine.gsfc.nasa.gov/science/toolbox/emspectrum1.html

[23] B. Arnold, "The working principle of colorimeters," June 2015. [Online]. Available: https://www.azosensors.com/article.aspx?ArticleID=324

[24] T. Technetium. Smartphone "spectrophotometer".

[25] N. Gayathri and N. Balasubramanian, "Original articles Spectrophotometric determination of nitrogen dioxide , nitrite and nitrate with Neutral Red Original articles," pp. 174–181, 1999.

[26] N. V. TKACHENKO. (2006) Monochromators. [Online]. Available: https://www.sciencedirect.com/topics/physics-and-astronomy/monochromators

[27] W. Soutter. (2012, August) What is a monochromator? [Online]. Available: https://www.azooptics.com/Article.aspx?ArticleID=380

[28] AZoOptics. (2013, June) What is a collimator? what is a collimator? what is a collimator? what is a collimator? what is a collimator? [Online]. Available: https://www.azooptics.com/Article.aspx?ArticleID=541

[29] ——. (2013, June) What is a diffraction grating? what is a diffraction grating? what is a diffraction grating? [Online]. Available: https://www.azooptics.com/Article.aspx?ArticleID=542

[30] H. Ding, C. Chen, S. Qi, C. Han, and C. Yue, "Smartphone-based spectrometer with high spectral accuracy for mhealth application," *Sensors and Actuators A: Physical*, vol. 274, pp. 94–100, 2018.

[31] M. A. Hossain, J. Canning, K. Cook, and A. Jamalipour, "Optical fiber smartphone spectrometer," *Optics Letters*, vol. 41, no. 10, p. 2237, 2016. [Online]. Available: https://www.osapublishing.org/abstract.cfm?URI=ol-41-10-2237

[32] P. E. J. Paul R Haddad, *Ion chromatography : principles and applications*. Elsevier, 1990.

[33] "Definition of solvent," 2017. [Online]. Available: https://www.chemicool.com/definition/solvent.html

[34] Simulab. Study notes: Deviations from beer's law. [Online]. Available: http://simulab.ltt.com.au/5/Laboratory/StudyNotes/snDeviatFromBeerLaw.htm

[35] M. W. Davidson. Refractive index (index of refraction). [Online]. Available: https://www.microscopyu.com/microscopy-basics/refractive-index-index-of-refraction

[36] Spectrophotometry. [Online]. Available: https://www.cefns.nau.edu/capstone/projects/CENE/2014/NitrateDetectionMethods/Web%20Pages/page%207.html

[37] Shimadzu, "Light sources for spectrophotometers." [Online]. Available: https://www.shimadzu.com/an/uv/support/fundamentals/lightsources.html

[38] I. Sensor Electronic Technology, *UVTOP® Specification TUD59H1B*, Sensor Electronic Technology, Inc, 2017.

[39] I. Crystal IS. (2019) Optan uvc led products. Crystal IS, Inc.

[40] H. Holding. (2019, April) Heraeus noblelight introduces the first broadband uv led light source module for analytical measurement. Heraeus Holding. [Online]. Available: https://www.heraeus.com/en/hng/press/heraeus_noblelight_introduces_the_first_broadband_uv_led_light_source_module_for_analytical_measurement.html

[41] ——, *FiberLight D2® Portfolio*, Heraeus Holding.

[42] (2019). [Online]. Available: https://www.sigmaaldrich.com/catalog/search?interface=All&N=0+104902938&mode=partialmax&focus=product&lang=en&region=ZA

[43] Statista, "Number of mobile phone users worldwide from 2015 to 2020 (in billions)." [Online]. Available: https://www.statista.com/statistics/274774/forecast-of-mobile-phone-users-worldwide/

[44] S. Davis, "Is your child ready for a cell phone?" [Online]. Available: https://www.webmd.com/parenting/features/children-and-cell-phones#1

[45] Y. Kazeem. (2017, July) Mobile subscriptions are still growing faster in sub saharan africa than anywhere else. [Online]. Available: https://qz.com/africa/1027935/ethiopia-tanzania-dr-congo-and-nigeria-are-leading-mobile-subscriber-growth-in-africa/

[46] D. Measday, "A summary of ultra-violet fluorescent materials relevant to Conservation," *The Australian Institute for the Conservation of Cultural Material*, pp. 1–13, 2017. [Online]. Available: https://aiccm.org.au/national-news/summary-ultra-violet-fluorescent-materials-relevant-conservation

[47] M. S. Grant, "The Use Of Ultraviolet Induced Visible-Fluorescence In The Examination Of Museum Objects , Part I," *Museum*, vol. 1/10, no. 1, p. 4, 2000.

[48] ——, "The Use Of Ultraviolet Induced Visible-Fluorescence In The Examination Of Museum Objects , Part II," *Museum*, vol. 1/10, no. 1, p. 4, 2000.

[49] Y. Fujimoto and T. Yanagida, "Basic optical and radiation response properties of Lumilass-B fluorescent glass," *Japanese Journal of Applied Physics*, vol. 53, no. 8, pp. 4–8, 2014.

[50] B. B. Shrivastava, N. S. Benerji, P. Bhatnagar, H. S. Vora, and U. Nundy, "Development of automated ultraviolet laser beam profiling system using fluorometric technique," *International Conference in Photonics*, pp. 4–9, 2004.

[51] R. Zakaria and P. E. Dyer, "Beam characterization and spatial coherence measurement of F 2 laser using Lumilass glass fluorescence," *Optics Communications*, vol. 285, no. 24, pp. 4844–4849, 2012. [Online]. Available: http://dx.doi.org/10.1016/j.optcom.2012.08.004

[52] I. SUMITA OPTICAL GLASS. Uv to visible light converter fluorescent glasses. [Online]. Available: https://www.sumita-opt.co.jp/en/products/lumilass.html

[53] M. W. D. Mortimer Abramowitz. Overview of fluorescence excitation and emission fundamentals. [Online]. Available: https://www.olympus-lifescience.com/en/microscope-resource/primer/lightandcolor/fluoroexcitation/

[54] S. K. Vashist, O. Mudanyali, E. M. Schneider, R. Zengerle, and A. Ozcan, "Cellphone-based devices for bioanalytical sciences Multiplex Platforms in Diagnostics and Bioanalytics," *Analytical and Bioanalytical Chemistry*, vol. 406, no. 14, pp. 3263–3277, 2014.

[55] S. Levin, S. Krishnan, S. Rajkumar, N. Halery, and P. Balkunde, "Monitoring of fluoride in water samples using a smartphone," *Science of the Total Environment*, vol. 551-552, pp. 101–107, 2016. [Online]. Available: http://dx.doi.org/10.1016/j.scitotenv.2016.01.156

[56] I. Hussain, K. U. Ahamad, and P. Nath, "Low-Cost, Robust, and Field Portable Smartphone Platform Photometric Sensor for Fluoride Level Detection in Drinking Water," *Analytical Chemistry*, vol. 89, no. 1, pp. 767–775, 2017.

[57] A. Skorucak. Is there any way to see ultra violet light, or make it? is there any way to see ultra violet light, or make it? [Online]. Available: https://www.physlink.com/education/askexperts/ae225.cfm

[58] H. Yu, Y. Tan, and B. T. Cunningham, "Smartphone fluorescence spectroscopy," *Analytical Chemistry*, vol. 86, no. 17, pp. 8805–8813, 2014.

[59] W. Zhao and K. Sakurai, "CCD camera as feasible large-area-size X-ray detector for X-ray fluorescence spectroscopy and imaging," *Review of Scientific Instruments*, vol. 88, no. 6, 2017.

[60] E. Widiatmoko and M. Budiman, "A simple spectrophotometer using common materials and a digital," 2011.

[61] OpenStax. (2019, August) 4.1: Single-slit diffraction. [Online]. Available: https://phys.libretexts.org/Bookshelves/University_Physics/Book%3A_University_Physics_(OpenStax)/Map%3A_University_Physics_III_-_Optics_and_Modern_Physics_(OpenStax)/4%3A_Diffraction/4.1%3A_Single-Slit_Diffraction

[62] A. Inc, 2018. [Online]. Available: https://www.apple.com/za/iphone-xs/specs/

[63] Warren, "Spectrometry," September 2018. [Online]. Available: https://publiclab.org/wiki/spectrometry#Whats+spectrometry

[64] "convert rgb pixel to wavelength," February 2017. [Online]. Available: https://stackoverflow.com/questions/35481345/convert-rgb-pixel-to-wavelength

[65] (2006, October) Mapping pixels to wavelength. [Online]. Available: https://forums.ni.com/t5/LabVIEW/Mapping-pixels-to-wavelength/td-p/430770?profile.language=en

[66] C. in Colour. Camera exposure. [Online]. Available: https://www.cambridgeincolour.com/tutorials/camera-exposure.htm

[67] D. BUCKLEY. (2018, January) How to stack star photos to reduce noise in photoshop. [Online]. Available: https://www.naturettl.com/stack-star-photos-reduce-noise-photoshop/

[68] B. B. W. T. Plant, "'what is the process of producing effluent water'," July 2019.

[69] M. A. Agoro, O. O. Okoh, M. A. Adefisoye, and A. I. Okoh, "Physicochemical Properties of Wastewater in Three Typical South African Sewage Works," vol. 27, no. 2, pp. 491–499, 2018.

[70] U. C. P. L. Ninham Shand (Pty), "Overview of water re-use potential from wastewater treatment plant," Department of Water Affairs and Forestry, Tech. Rep., 2007.

[71] A. Mogolegeng, "Stellenbosch effluent nitrate results," Stellenbosch Wastewater Treatment Plant, Tech. Rep., 2019.

Appendices

Appendix A

Dissertation overview diagram

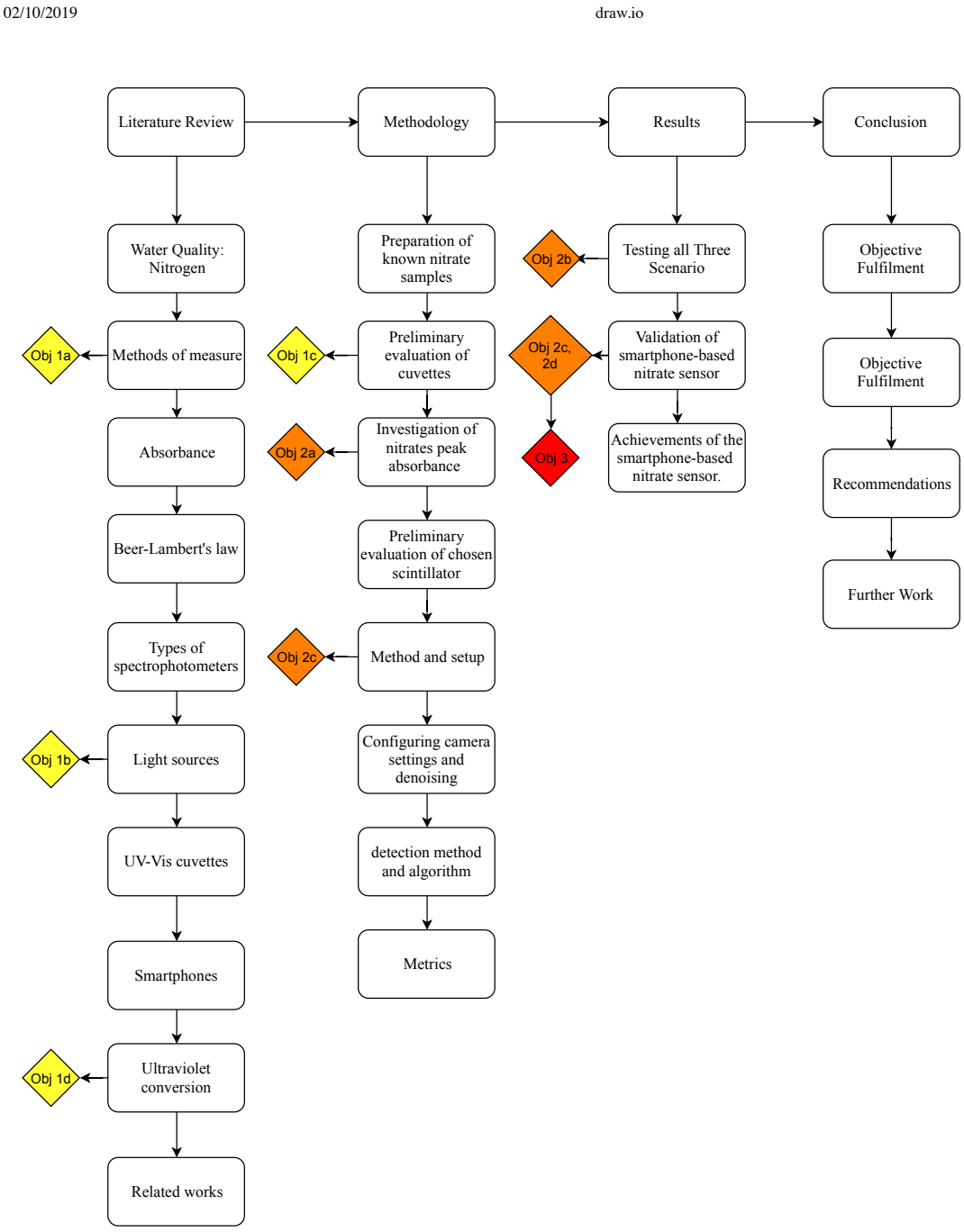

Figure A.1: Layout of thesis. Flow diagram of thesis layout and indication of where objectives were fulfilled in thesis

Appendix B

Final prototype

(a) "Lab-in-a-suitcase"

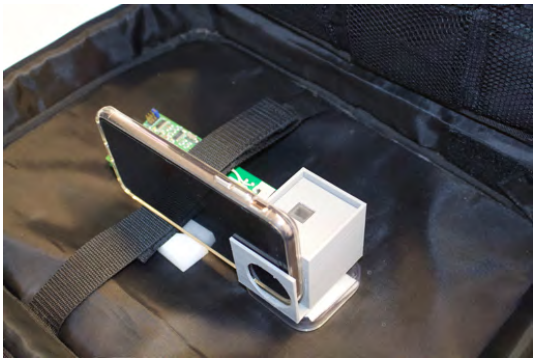

(b) Close up of the "Lab-in-a-suitcase"

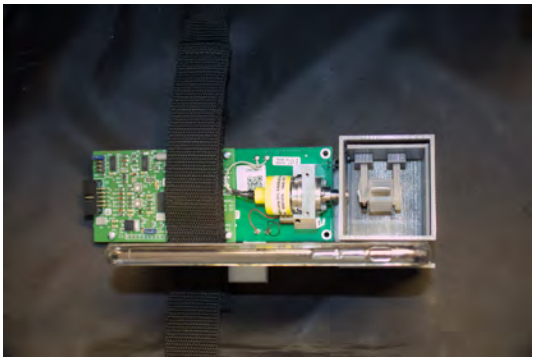

(c) Close up of Components. The components shown are the smartphone, the FibreLight module, the bandpass filter, the quartz cuvette and the Lumilass

Figure B.1: Photograph showing the final smartphone-based nitrate sensor

Appendix C

Software Design

Initially, MATLAB was used to stack the images and analyse the output of the stacked images. It was also used to determine the absorbance, calibration equation and concentration. Therefore, all the results that were achieved and discussed in this thesis were obtained using MATLAB. Nevertheless, for the final chosen design of the smartphone-based nitrate sensor, an IOS application was designed with a user interface, shown in Figures C.1. The application was written in Swift language and was designed to take images with the shutter speed and ISO adjusted to 1 s and 1500, respectively. The application was designed so that the user could select the option to capture the output light of a reference sample or an analyte sample and the camera would automatically take 15 photos, instead of just one. Then the application would stack the 15 images to produce one image. Thereafter, the software could analyse the output image to determine the intensity of the light. The application needed further development to find the calibration equation of a set of absorbances and to determine the concentration of unknown samples. The application was designed, but the accuracy of the application was not tested against that of the software that was generated with MATLAB. The application was only usable with iPhones and would need to be rewritten in JAVA to accommodate for Android phones. However, MATLAB can be used both with IOS and Android phones.

Figure C.1: Screenshots of user interface

C.1 Absorbance determination algorithm flow diagram

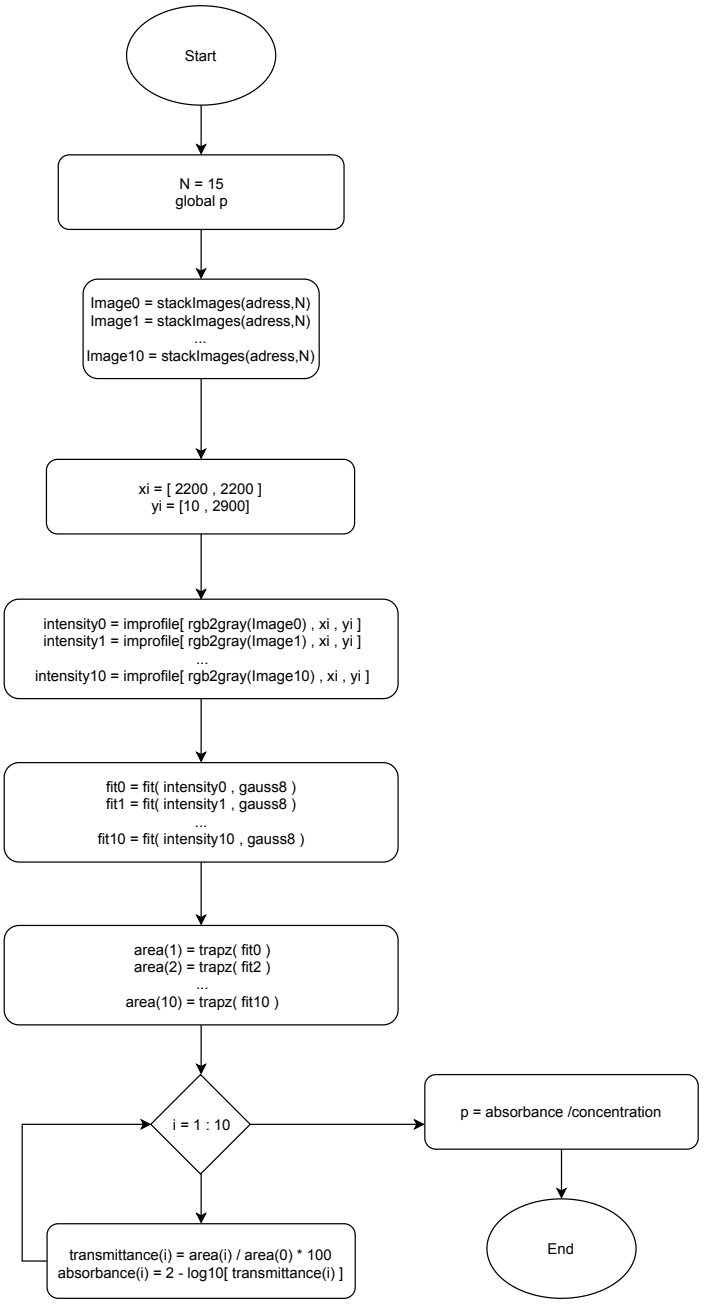

Figure C.2: Flow diagram of the absorbance determination algorithm

C.2 Concentration Detection algorithm

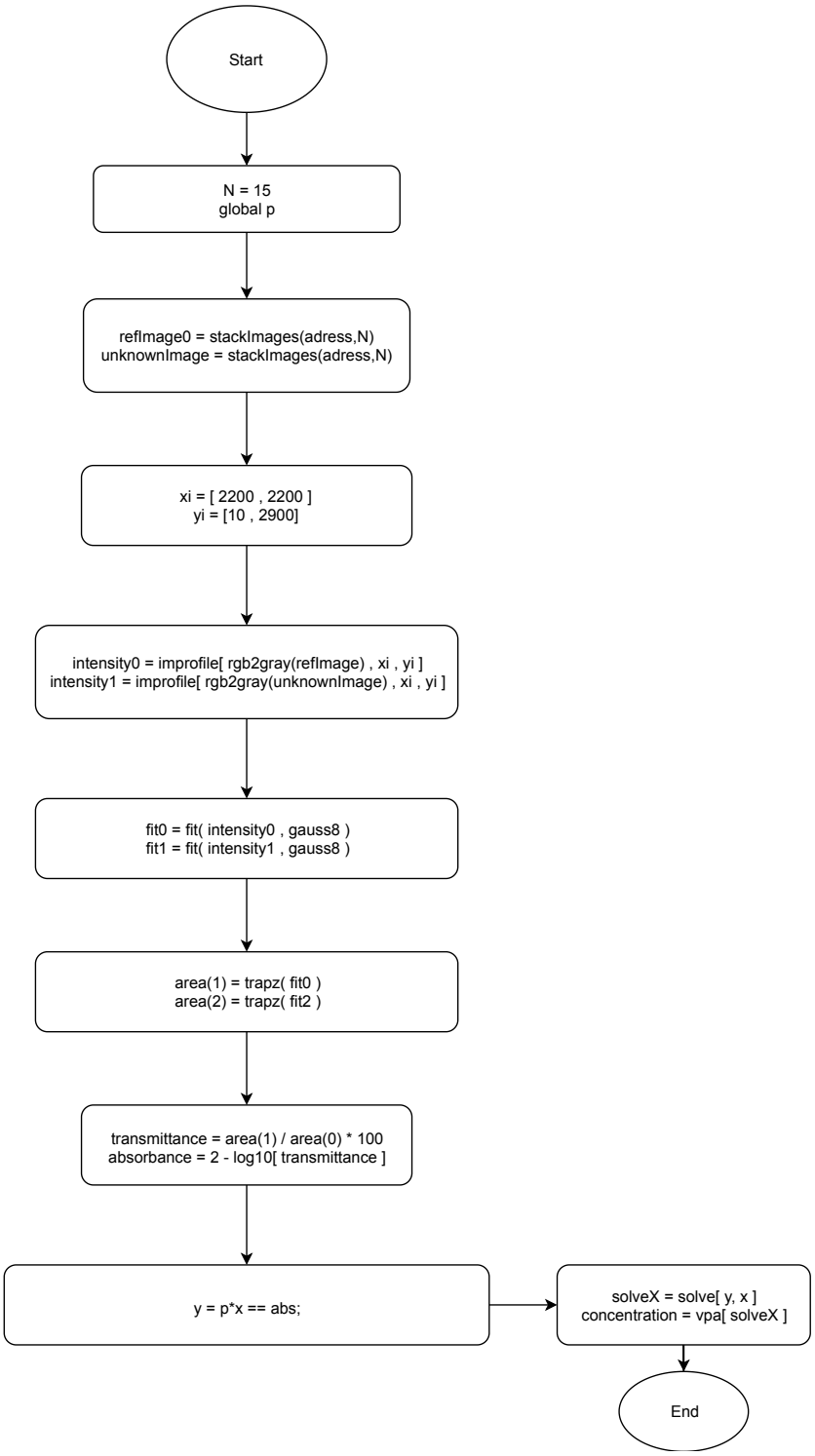

Figure C.3: Flow diagram of the concentration detection algorithm

Appendix D

Photograph of spectrophotometer

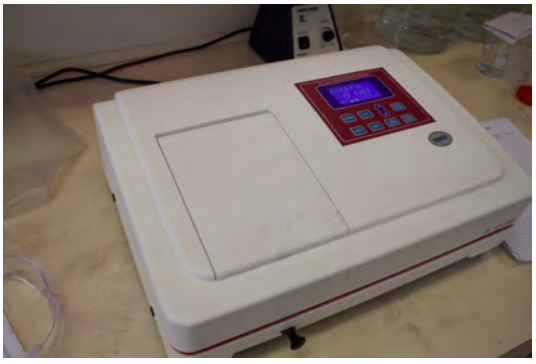

Figure D.1: Photograph of the lUV Vis Spectrophotometer (AE-S60).The opening allows for the cuvette with a sample to be inserted, and the lid prevents background light from interfering with the measurements. The interface allows the user to select the λ_{max}, to select the option to zero the absorbance or transmittance with a reference sample, to view the measured transmittance or absorbance.

Appendix E

Smartphone camera capturing visible light emitted by the deuterium lamp of the light source

Figure E.1a displays the captured spectrum of the UV light beam emitted by the chosen light source, FiberLight D_2, alone, and Figure E.1b shows the captured spectrum of the light captured when the scintillator was placed in front of the UV light beam emitted by the light source.

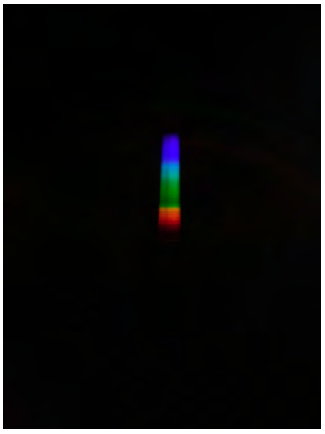

(a) Output light of deuterium lamp

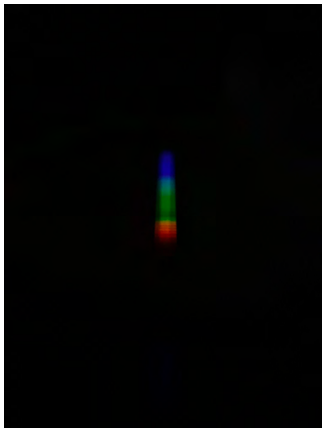

(b) Output light of deuterium lamp with scintillator placed in front of the beam's pathway

Figure E.1: Output light of deuterium lamp. (a) The output light of deuterium light was captured with the smartphone directly, and some white light was captured. (b) The output light of the deuterium was captured when the scintillator was places in front of the beam's pathway, a dimmer white light was captured.

Appendix F

Overall cost of the smartphone-based nitrate sensor

The Table F.1 below breaks down the price of each component. The prices are subject to currency and tax change since most components were sourced from outside of South Africa.

Component	Approximate Price (R)
Light source (FiberLight D_2)	8 000
Narrow band Bandpass filter	1100
Quartz Cuvette	1200
Scintillator (Lumilass)	1100
Structure	100
Total	**11 500**

Table F.1: Overall cost of the smartphone-based nitrate sensor